EXTERNALLY INDUCED AGGLOMERATION DURING CHEMICAL MECHANICAL POLISHING OF METALS AND DIELECTRICS

By

FENG-CHI CHANG

A DISSERTATION PRESENTED TO THE GRADUATE SCHOOL
OF THE UNIVERSITY OF FLORIDA IN PARTIAL FULFILLMENT
OF THE REQUIREMENTS FOR THE DEGREE OF
DOCTOR OF PHILOSOPHY

UNIVERSITY OF FLORIDA

2008

To my family

ACKNOWLEDGMENTS

First I am deeply appreciative of my advisor, Dr. Rajiv Singh, for his research advice, support, and encouragement. His creative thinking and enthusiastic attitude for fundamental material research are deeply impressed on my mind. I would also like to thank my committee, Dr. Stephen Pearton, Dr. David Norton, Dr. Wolfgang Sigmund, and Dr. Fen Ren, for their advice and support. I am also very thankful to Dr. Brij Moudgil for his many insightful comments in particle science and CMP research.

I am extremely grateful to Levitronix LLC for their financial and experimental support, and the industrial partners of the Particle Engineering Research Center (PERC) for financial support throughout my graduate program.

Many thanks are given to all of my friends and colleagues for their friendship and helpful discussion. I would like to thank my past and present group members, Siddharth Tanawade, Purushottam Kumar, Sejin Kim, Jaeseok Lee, Sushant Gupta, Taekon Kim, Yoonjae Moon, Aniruddh Khanna, and Myoung Hwan, for their contributions to this research with valuable discussions and friendship, and my good friends, Jiahau Yan, Tienyu Chang, Yu-Ping Huang, for their friendship and memorable time in Gainesville.

I would like to thank Gary Scheiffele and Gill Brubaker in PERC for their dedication and experimental support throughout my research. I would also like to thank Kyoung-Ho Bu for his helpful research support and discussion.

I would like to express my gratitude to family members: my parents, Cheng-Tsung Chang and Li-Yu Li, and my brothers, Feng-Shih Chang and Chung-Hao Chang, for their love, encouragement, and great anticipation for me. Finally, I would like to thank my cutest wife, Jia-Yuan Chang, for her love and optimistic attitude to encourage and accompany me go through my graduate studies.

TABLE OF CONTENTS

page

LIST OF TABLES

LIST OF FIGURES

Abstract of Dissertation Presented to the Graduate School
of the University of Florida in Partial Fulfillment of the
Requirements for the Degree of Doctor of Philosophy

EXTERNALLY INDUCED AGGLOMERATION DURING CHEMICAL MECHANICAL POLISHING OF METALS AND DIELECTRICS

By

Feng-Chi Chang

December 2008

Chair: Rajiv K. Singh
Major: Materials Science and Engineering

With the miniaturization of semiconductor devices, chemical mechanical planarization (CMP) is now commonly employed for both the front and back end processing of such devices due to its unique global planarization capability. Highly stable slurry plays an important role in minimizing the process-induced particle agglomeration and ensuring a superior polishing performance. However, abrasive particles can be agglomerated during the slurry formulation and handling processes. The presence of oversize particles in the slurry is one of the main causes of defectivity during CMP of metals and dielectrics.

We investigated the stress effects on slurry agglomeration and particle-induced defectivity during CMP of metals and dielectrics. Our results indicate that the agglomeration of the slurries was found to depend both on the external shear stress and the interparticle forces acting on the slurries. The magnetically levitated centrifugal pump caused low shear flow and insignificant increase in agglomerated particles during the handling process as compared to the positive displacement pump. In addition, the interparticle forces were determined by the colloidal probe technique. An increase of repulsive interparticle force corresponded to a considerable decrease in agglomerated particles during the handling process. The addition of chemicals (e.g., salt, pH, and surfactant) into ceria and silica slurries can influence the slurry stability and the polishing

performance. A positive correlation was established between the roughness/defect density and the degree of agglomeration.

Slurry stability is qualitatively assessed through interparticle force and/or zeta potential measurements. However, these types of measurements do not fully describe agglomeration phenomena in CMP slurries. Therefore, we developed a novel experimental/theoretical approach for quantifying the degree of agglomeration in CMP slurries. This method involves subjecting the slurry to high shear forces and measuring particle agglomeration characteristics in their tail distribution. By modeling changes in tail distribution using Smoluchowski's slow aggregation theory, the agglomeration index can be used to quantify the degree of agglomeration caused by external shear stress and internal slurry chemistry. Our modeled and experimental results revealed that the shear stress in a positive displacement pump was 100 times greater than that in a magnetically levitated centrifugal pump. In addition, our numerous polishing experiments revealed that slurries with higher agglomeration index values ($AI > 1.8$) contained more agglomerated particles during the handling process and caused more surface defectivity during polishing. Our novel method can be applied to determine slurry stability, and thus further minimize particle-induced defectivity during CMP of metals and dielectrics.

CHAPTER 1
INTRODUCTION

Chemical Mechanical Polishing

Chemical mechanical polishing (CMP) was first introduced by IBM in the 1980s to fabricate multilevel interconnect structure in silicon integrated circuits (IC) [Zan04]. Multilevel metallization (MLM) is established by depositing the interlayer dielectrics (ILD), the tungsten as the inlaid metal, and the metal interconnect as the planar interconnect. To improve the device speed, the semiconductor industry had replaced SiO_2 ILD and Al interconnects with low k dielectrics and Cu interconnects, respectively. Currently, the nine layers of Cu interconnect with low k ILD have developed for semiconductor manufacturing at 45nm technology node [Mis07]. With the shrinking of feature size in devices, the semiconductor industry has reported many challenges. For example, to fabricate miniature and dense interconnects, a low step height of the surface topography is an important requirement to accomplish the high resolution photolithography. To meet challenges such as this, CMP has become an unavoidable solution for the processing of MLM structure due to its unique global planarization capability. Advantages of the CMP process in semiconductor manufacturing include the ability to

- Achieve better global planarization
- Planarize a large variety of materials (*e.g.*, Cu, W, Al, Ta, TaN, SiC, SiO_2, and Si_3N_4)
- Reduce prior step defects
- Achieve multilevel metallization
- Improve metal step coverage
- Provide higher photolithography
- Replace reactive ion etching (RIE) and plasma etching with etching metals and alloys.

Typically, CMP is a complicated process to control and understand because there are more than 20 input variables (e.g., particle types, chemicals in the slurries, physical conditions, and pad characteristics) necessary to achieve corresponding output parameters (e.g. removal rate and planarization), as shown in Table1-1 [Sin02]. The CMP system comprises the polishing pad,

carrier head, and slurry distribution system, as shown in Figure 1-1. During the polishing process, CMP slurry is supplied from the slurry distribution system and the wafer is pressed against the polishing pad. The material removal rate is controlled by adjusting the rotation speed of the platen and down pressure of the carrier head. Typically, the angular velocity of the carrier and platen keep the same direction.

Slurry Handling

CMP slurry is a synergistic combination of particles and chemicals, and is perhaps the most critical consumable product in the semiconductor industry as it controls the uniqueness and technical performance of the CMP process. Abrasive particles in slurries typically provide the mechanical component of the polishing process. To reduce/minimize process dependent defectivity is to ensure that the particle size distribution, especially in the oversize tail region, is as small as possible and does not increase with time during the slurry delivery and polishing process. The slurry distribution system is comprised of daytanks, chemical blending vessels, slurry loops, and distribution pumps, as can be seen in Figure 1-2. As-received slurries were diluted and mixed with chemicals in the daytank and then distributed in the slurry loop using a pumping device. Some studies have shown that positive displacement pumps (e.g., bellows and diaphragm) generate high shear stress and tend to agglomerate particles during slurry handling [Bar99, Lit04, Sin04]. Agglomerated particles can settle on the surface of wafers or increase the mechanical stress that can lead to increased defectivity (e.g., scratches, particle residues, and pits) during the polishing. Therefore, the control and reduction of oversize particles are critical to further reduce surface defectivity during CMP. This especially pertains to the 45 nm semiconductor technology manufacturing node, which is expected to be less tolerant to defects.

This study fundamentally focuses on the effect of stress-induced particle agglomeration and defectivity during CMP of metals and dielectrics. The magnitude of agglomerate

concentrations is determined by the particle types, slurry chemicals, and external mechanical forces applied on the slurry itself during the slurry handling process. The fundamental of slurry stability and stress-induced particle agglomeration has studied. To minimize particle-induced defectivity, we also develop a novel approach to measure the robustness/stability of CMP slurries.

Chapter 4 investigates the effects of shear stress induced by positive displacement pumps and centrifugal pumps on particle agglomeration and polished defectivity. These studies were carried out by measuring the oversize particle distribution and the surface defectivity generated during the CMP of low k dielectrics.

Chapter 5 delineates the chemical effects on pump-induced particle agglomeration. The agglomeration of the slurries was found to depend both on the external shear stress and the interparticle forces acting on the slurries. The correlations were established between the repulsive interaction forces and surface defectivity due to oversize particles.

Chapter 6 studies the slurry formulation in order to stabilize ceria and silica colloidal particles to minimize the process-induced particle agglomeration. The slurry stability was investigated from the polishing performance.

Chapter 7 develops a novel experimental/theoretical approach to determine the degree of agglomeration in highly stable CMP slurries. This approach can be applied to minimize particle-induced defectivity during CMP.

Chapter 8 summarizes the conclusions of this study and suggests future research.

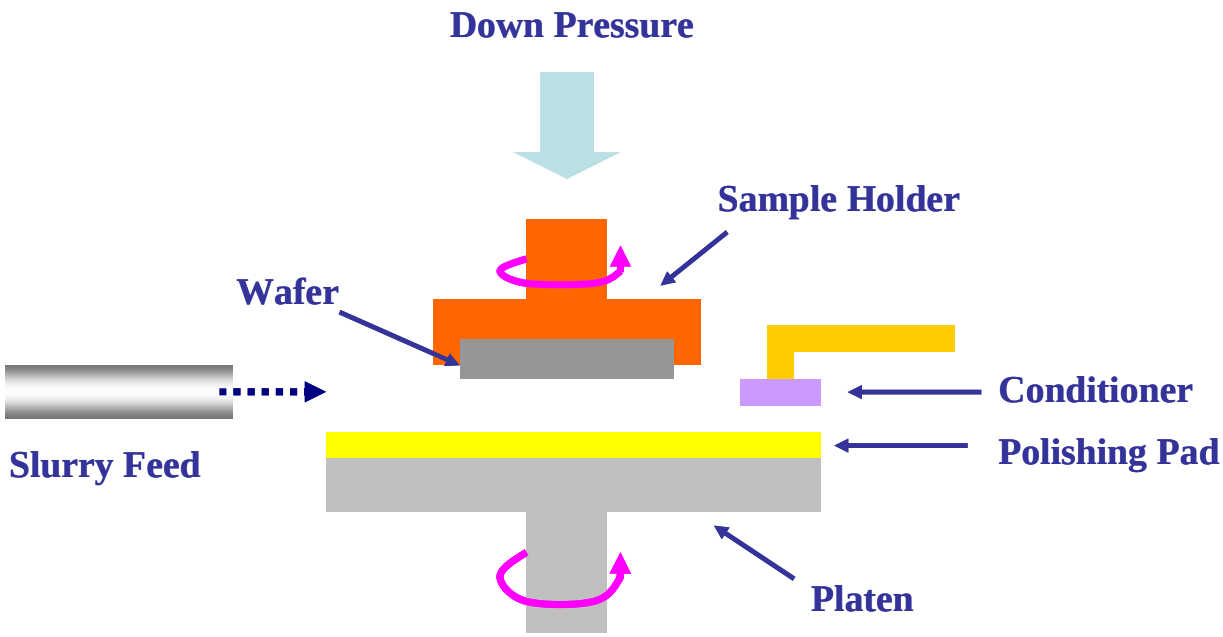

Figure 1-1. Basic process of chemical mechanical polishing.

Table 1-1. Various systems-level variables in CMP [Sin02].

Input variables	Microscale parameters	Nanoscale interaction	Output parameters
Particle Characteristics Size and distribution Shape Mechanical properties Chemistry Concentration Agglomeration Slurry Chemistry Oxidizers Buffering agents Complexing agents Dispersants Down Pressure and Linear Velocity Pad Characteristics Mechanical properties Topography Conditioning Substrate Characteristics Feature size Feature density	Pad Contact angle Pressure on the pad Particles on the Pad Pressure Coverage Chemical Concentration and Distribution Contact Mode Direct Mixed Hydroplaning	Chemomechanical Dynamics of surface layer formation Layer removal mechanism Abrasion frequency Chemical and Mechanical Etching Mechanical removal	Removal Rate Planarization Surface Finish Defectivity

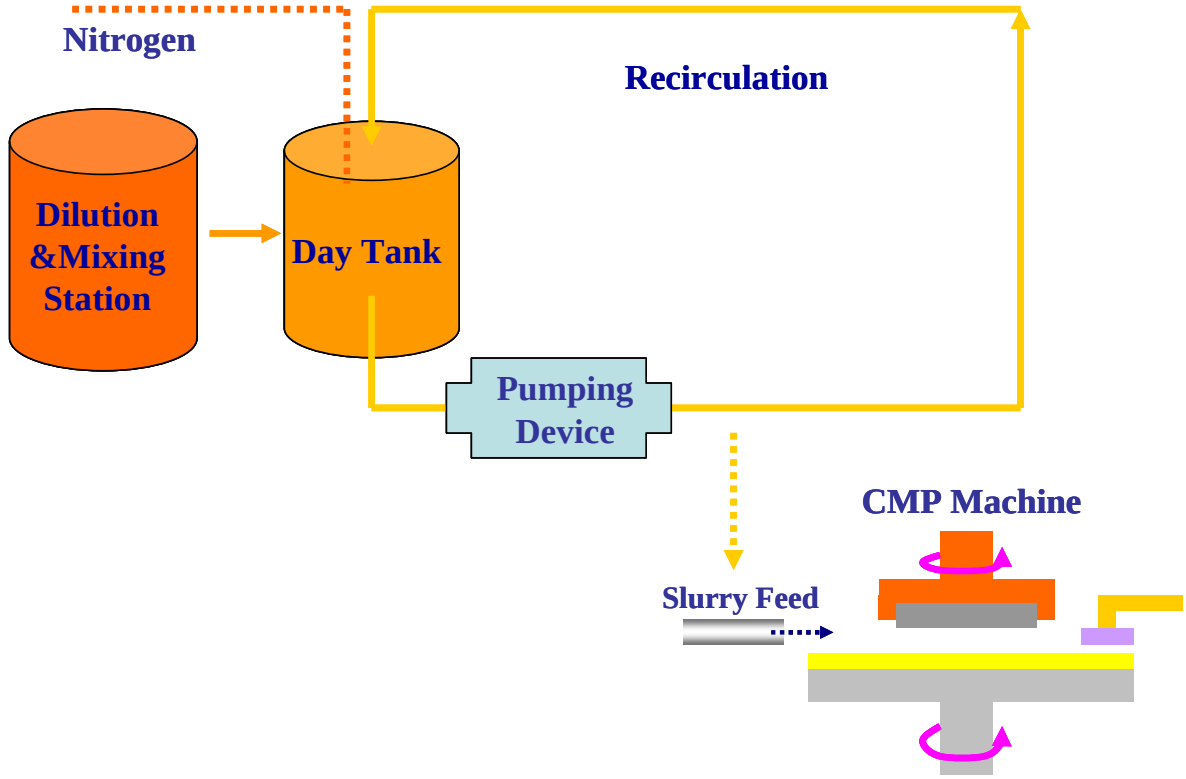

Figure1-2. Typical slurry distribution system.

CHAPTER 2
LITERATURE REVIEW

The CMP Process and Slurry

Chemical mechanical planarization (CMP) is now commonly employed for both the front and back end processing of IC devices due to its unique global planarization capability. This process includes shallow trench isolation (STI), pre-metal dielectrics (PMD), tungsten, inter-layer dielectric (ILD), and copper CMP, as shown in Figure 2-1. Each specific CMP process uses slurries that are specifically designed for that process to ensure the polishing performance (e.g., removal rate and selectivity) and minimize the process-dependent defectivity (e.g., scratches and delamination). In this chapter, we discuss the CMP processes (*e.g.*, Cu/ low k and dielectric polishing), fundamentals of slurry stability, and process-dependent defectivity due to oversize particles.

The Cu/Low K CMP

By miniaturizing the feature size of semiconductor devices, the number of transistors increases: the Semiconductor Industry Association (SIA) has projected that high performance chips will contain more than 3 billion transistors in 2011 [Nai02]. Thus, more reliable and efficient interconnect system in the back-end-of-line (BEOL) technology is essential for manufacturing the new generation of IC devices. Consequently, the multilevel interconnect is a reliable solution to provide direct routing and improve the performance of IC devices, and the CMP process is a dependable technology to manufacture multilevel metallization structures due to its unique global planarization capability.

It is well know that the interconnect delay becomes the dominating issue affecting device speed, called RC delay time, as the feature size of devices continues to scale down [Cha04a and Mur93]. RC time (τ) is the required time to charge nearly 63% of the total voltage and is affected

by the resistance (R) of interconnect and the capacitance (C) of dielectric materials [Sze01]. The RC time is given by

$$R = \rho \frac{l}{w \times t} \quad [2\text{-}1]$$

$$C = \varepsilon_i \frac{l \times w}{d} \quad [2\text{-}2]$$

$$\tau = R \times C \quad [2\text{-}3]$$

where ρ is the resistivity of interconnect, ε_i is the dielectric permittivity, l, w, and t are length, width, thickness of materials, and d is the thickness of dielectric film. The thinner and longer interconnection and larger coupling capacitance can increase the RC delay time due to the decrease in the distance between adjusted metal lines [Sak93]. However, it is difficult to lower the parasitic capacitance by decreasing the thickness of the dielectric film as the device shrinks. Thus, to lower the interconnect delay, an alternative method is to replace aluminum interconnect and silicon dioxide with copper and low k materials, respectively.

The dielectric constant (k) has represented the relative permittivity (ε_r) in the semiconductor industry. When applied to the voltage in the device, the dielectric constant is determined by the polarization of materials. The Debye equation describes the relationship between the relative permittivity and the polarization,

$$\frac{\varepsilon_r - 1}{\varepsilon_r + 2} = \frac{N}{3\varepsilon_0}\left(\alpha_e + \alpha_d + \frac{\mu^2}{3kT}\right) \quad [2\text{-}4]$$

where N is the number of molecules per cubic meter and ε_0 is the permittivity of vacuum. The polarization phenomena are represented by the electronic polarization (α_e), the distortion polarization (α_d), and orientation polarization (μ) [Mae03]. Thus, the dielectric constant can be reduced by introducing the materials, which have smaller molecule densities and less polar bonds, as shown in Figure 2-2 [Sha04].

Furthermore, low k materials can be simply classified as the silica-based, silsesquioxane (SSQ)-based materials, and organic polymers, as shown in Figure 2-3 [Sha04]. The silica-based films, deposited by plasma-enhanced chemical vapor deposition (PECVD) or CVD, have a tetrahedral structure. To lower the k value of silicon dioxide, Si-O bonds are replaced with low polar bonds, such as Si-F and Si-CH_3 bonds. Historically, the fluorinated silicon dioxide glass (FSG) is the first low k dielectric introduced into an ILD layer. The k values range from 3.5 to 3.7. In addition, organosilicate glasses (OSG) are the materials of silicon dioxide doped with carbon or CH_3 to reduce the film density and a number of polar bonds. Their dielectric constants are closed to 2.7 to 3.0. In regard to SSQ-based materials, these films are deposited by spin-coating, and are cured for forming stable polarization. The formula of the SSQ is $(R\text{-}SiO_{3/2})_n$, where R can be H or CH_3. Silicon and hydrogen form a cubic structure and hydrogen and methyl group are connected to the corner of the cubic structure to form hydrogen- silsesquioxane (HSSQ) and methyl-silsesquioxane (MSSQ) structures. Typically, the k-value range of these materials is 2.9 to 3.6. In addition, the organic polymers have low dielectric constants (2.0-3.0) due to the non-polar bonds (e.g. C-C) and asymmetric charge distribution (e.g., C-F and C-F_3). These materials can be deposited by CVD or spin-on polarization [Mae03 and Bor02].

Process flow of Cu/low k CMP

As copper has excellent electronic conductivity and resistance to electromigration, it has successfully replaced aluminum in the process of interconnection metallization. However, a lack of suitable dry-etching solution for removing unwanted Cu materials makes it more difficult to manufacture MLM structure. To address this problem, the dual-damascene process is introduced into Cu/Low k process flow and successfully manufactures the multilevel metallization. The dual-damascene process includes two photolithography and reactive ion etching (RIE) steps to make the vias and trenches, as shown in Figure 2-4 [Sze01]. Afterwards, Ta/TaN and Cu layers

are deposited onto via and trench structures, and the excess copper bulk is removed by CMP. As this structure contains copper bulk, barrier (Ta or TaN), and low k materials, three polishing stages during Cu CMP are required to achieve planarization. The first platen is used mainly for removal of unwanted copper bulk above the patterned features. The Cu slurry used in the first platen must have a high removal rate and high selectivity between the barrier and copper materials. After removing unwanted Cu materials, the nonselective slurry is used in the second platen to remove residual Cu and barrier materials simultaneously. This barrier slurry, composed of silica abrasive particles, can remove copper and barrier metals at approximately the same removal rate to achieve the flat surface. Finally, the third platen is subjected to a buffing step for smoothing the dielectric surface and removing residual barrier metal, as shown in Figure 2-5 [Bal04].

Mechanisms of Cu/low k slurries

Typically, two kinds of slurries, Cu and barrier/low k slurries, are utilized in Cu/low k polishing. First, Cu slurry is designed for a high removal rate and selectivity between barrier and copper bulk materials. The chemicals in Cu slurry are comprised of corrosion inhibitors, complexing agents, and oxidizers. The oxidizer, such as hydrogen peroxide [Ein07 and Den06] and ferric nitride [Ber08], reacts with Cu film to form a soft oxide layer, which is easily removed by abrasive particles. The addition of the complexing agent, such as glycine [Lin08 and Tam02] and oxalic acid [Pan07], can increase the solubility of Cu films or Cu oxides into Cu ions. The addition of corrosion inhibitor into Cu slurry, such as benzotriazole (BTA) [Kim08a and Tam02], forms a protective film to defend against isotropic etching of aggressive chemicals. The phenomena of Cu dissolution and passivation in the Cu-water system can be illustrated from the electrochemical behavior. The copper can dissolve into Cu ions in the acidic solutions, or form Cu oxides in neutral or alkaline solutions. The oxidizer, such as hydrogen peroxide, can further

make a growth of Cu oxide films to obstacle the ion transportation from the Cu surface. Eom et al. [Eom07] indicates that the concentration of Cu dissolution is proportional to the thickness of Cu oxide, which means that Cu oxides can prevent Cu dissolution in the solution. Furthermore, the addition of BTA in Cu slurries can form a monolayer of the Cu-BTA surface to prevent chemical attack on the Cu surface; however, Cu-BTA surface may cause a decrease of the removal rate during Cu CMP [Kim08a and Li08]. Consequently, electrochemical behavior plays an important role in achieving material removal and preventing surface defectivity in metal CMP.

Low k slurries, or Cu barrier slurries, are utilized in polishing barrier and dielectric materials to achieve excellent uniformity and surface finish. The mechanism of dielectric polishing is an extension of glass polishing. Glass polishing for optical applications, such as lens and window sheets, was developed for smooth and planarized surfaces a decade ago. The mechanism of glass polishing is based on the water-oxide interaction [Coo90, Cum95]. During the polishing, the water-silica reaction between siloxane bonds (Si-O-Si) and water forms soft Si-OH layers. The reversible depolymerization reaction can be described as [Ile79]

$$\left(SiO_2\right)_x + 2H_2O \leftrightarrow \left(SiO_2\right)_{x-1} + Si\left(OH\right)_4 \qquad [2\text{-}5]$$

The modified layers are removed by abrasive particles, and the material removal is determined by the hydration rate of siloxane network. The hydration of silanol group (–SiOH) on silica surface, at pH below and above the isoelectric point of silica (IEP ≅ 2.2), creates positive ($–SiOH_2^+$) and negative ($–SiO^–$) charges.

$$-SiOH + H^+ \leftrightarrow SiOH_2^+ \qquad [2\text{-}6]$$

$$-SiOH + OH^- \leftrightarrow -SiO^- + H_2O \qquad [2\text{-}7]$$

Thus, the material removal rate increases rapidly in alkaline slurries due to a significant increase in the dissolution of the silanol group. Choi [Cho04a] studied the pH effect on the removal rate of silicon dioxide during CMP. He found that the surface charges of silica particles increased rapidly with increasing the slurry pH, resulting in raised repulsive forces between silica particle and silica wafer. These repulsive forces not only increased the spatial distance of silica surfaces, but also provided the lubrication effect during the polishing, which caused a decrease in the material removal rate. When the threshold pH reached 9, it caused a dramatic increase in silica polishing due to forming soft layers on the silica surface. The abrasive particles can easily remove these modified layers during the polishing.

The reduction of the dielectric constant is achieved by doping the materials that have low molecule density or polar bonds. These doping materials may affect the removal rate during CMP. For example, the FSG has a higher removal rate than that of an un-doped TEOS oxide because fluorinated doped silica exhibits a lower elastic modulus and hardness [Tse97]. Conversely, the carbon-doped silica films (e.g., OSG, HSSQ, and MSSQ) have a low removal rate during CMP due to the hydrophobicity of the inorganic-organic films [Bor02].

Shallow Trench Isolation CMP

Shallow trench isolation is the device isolation process that achieves a high device-packing density in the front-end-of-line (FEOL) manufacturing [Asa95, Cha96, and Ois00]. As the feature size of the device scales down, the semiconductor industry has replaced the local oxidation of silicon (LOCOS) process with the STI process because the LOCOS process is susceptible to causing a bird's beak structure in the region of the active-isolation transition. This structure reduces the active area and results in a low device-packing density. Consequently, the

STI process has been commonly employed for the technology nodes at 0.25μm and beyond. The comparison between STI and LOCOS processes is listed in Table 2-1[Li08 and Ste96].

Process flow of STI CMP

Figure 2-6 shows a typical process flow of STI CMP. STI process starts with the growth of the oxide thin pad and then the deposition of the nitride film on a raw silicon wafer. The thickness of the oxide thin pad and nitride film are around 15-25 and 100-150 nm, respectively [Kah08]. The following lithography process patterns the isolation area where the nitride and oxide are etched by the reactive ion etching (RIE). Subsequently, the CVD oxide refills the trenches and the over-filled oxides are removed by CMP. Finally, nitride layers are removed by phosphoric acid [Sez01].

Mechanisms of STI slurries

The strategy for designing STI slurry is to consider the slurry selectivity, which is the ratio of material removal rate of silicon dioxide to nitride, during the polishing. If slurry contains high selectivity properties, not only can the unwanted silica be removed quickly, but also the surface uniformity can be achieved by using the endpoint detection [Kim08b and Bib98]. Bu et al. [Bu05 and Bu07] studied the effects of pH and surfactant concentration in silica slurries on polishing selectivity. They studied the effect of sodium dodecyl sulfate (SDS) concentration on the adsorption of silicon dioxide and silicon nitride wafers. Because the isoelectric point of silicon nitride and silicon dioxide wafers are pH 4.5 and 2, silicon nitride exhibited a higher SDS surfactant adsorption at low pH as compared to silicon dioxide wafers due to the electrostatic attraction. Consequently, the maximum SDS adsorption on silicon nitride wafer was found at pH 2; however, an insignificant increase in surfactant adsorption was found on the silicon dioxide wafer. Furthermore, the maximum polishing selectivity of silica slurries was reached when the SDS concentration was beyond the critical micelle concentration (~8mM).

In addition, ceria particles have been commonly employed for glass polishing due to their high removal rate on silicon dioxide. The mechanisms of ceria polishing focus on chemical interactions between abrasive particles and surface groups on the substrate [Oss02 and Sup04]. Cook [Coo90] proposed the following chemical tooth for the glass polishing, listed below:

1. Water penetrates into the glass surface
2. Water reacts with the surface, which leads to the dissolution under particle load
3. Abrasive particles adsorb some dissolution products and leave from the substrate
4. Some dissolution products redeposit onto the substrate
5. Surface dissolution happens between particle impacts

CeO_2 has a high polishing rate because the free energy of the formation of cerium oxide (ΔH_f = -260 kcal/mole) is much less than the free energy of the formation of silicon dioxide (ΔH_f = -216 kcal/mole) [Ste96 and Kub67]. Maximum material removal happens when a neutrally charged CeO_2 particle approaches a silica substrate with negative surface charges to form surface chemical bonds. The condensation reaction can be expressed as

$$-Si-O^{-}+Ce-OH \leftrightarrow -Si-O-Ce-+OH^{-} \qquad [2\text{-}8]$$

The material removal occurs when a silica tetrahedron structure is broken from the silica surface because the strength of Ce–O bonding is greater than Si–O bonding [Oss02].

$$-Si-O-Si-O-Ce- \rightarrow -Si-O+Si-O-Ce- \qquad [2\text{-}9]$$

Furthermore, the bonding effect on ceria polishing can be proven by measuring particle size and zeta potential in ceria slurries. Abiade et al. [Abi05] studied the material removal rate as a function of ceria slurry pH in silica polishing. They concluded that the maximum material removal rate occurred near neutral slurry pH. The polished slurry at nearly neutral pH had a larger particle size, and the zeta potential showed much more negative potential as compared to un-polished slurry. That means Si-O^{-} is adsorbed onto ceria particles during the polishing.

Slurry Stability

Highly stable colloidal suspension plays an important role in chemical mechanical polishing (CMP) slurries as it determines the quality of polishing performance. To minimize process-dependent defectivity (e.g., scratches and particle residue), abrasive particles should not agglomerate or settle down during the slurry blending and handling process. The dispersion stability can be achieved by two methods: the electrostatic interaction between particles and polymer stabilization.

Electrostatic Stability

When two colloidal particles with the same charges approach each other, osmotic pressure tends to push particles away due to its high counterion concentrations, as shown in Figure 2-7 [Hun01, Ros04]. The overlapping of the electrical double layer potential causes a raise of repulsive potential. The repulsive double layer potential can be determined by Debye length $1/\kappa$:

$$1/k = \sqrt{\frac{\varepsilon_r \varepsilon_0 RT}{4\pi F^2 \sum_{i=1}^{n} C_i Z_i^2}} \qquad [2\text{-}10]$$

where ε_r is the relative permittivity, ε_0 is the permittivity of a vacuum, R is a gas constant, T is temperature, F is the Faraday constant, C_i is the molar concentration of any ion in the solution phase, and Z_i is the valence of ions in the solution phase. For two spherical particles of radius a, when ka << 1 (i.e., small particles and a relatively thick electrical double layer), the repulsive potential can be expressed as

$$V_R = \frac{\varepsilon_r a^2 \psi_0^2}{R} e^{-kH} \qquad [2\text{-}11]$$

where ψ_0 is the surface potential. Thus, the magnitude of the repulsive double layer potential is dependent on surface potential and chemical in the solution.

Further, total surface potential in colloidal systems is illustrated by the Derjaguin-Landau-Verwey-Overbeek (DLVO) theory, which demonstrates that the stability of colloidal particles is dependent on a balance between attractive Van der Waals potential and repulsive double layer potential. The total potential energy between colloidal particles is expressed as the sum of repulsive (V_R) and attractive (V_A) potential:

$$V_{total} = V_A + V_R \qquad [2\text{-}12]$$

Thus, the potential attraction energy for similar spherical particles with radius *a* whose centers are separated by distance *R* can be expressed as

$$V_A = \frac{-Aa}{12H} \qquad [2\text{-}13]$$

where *H* is the nearest distance between particle surfaces and *A* is the Hamaker constant.

Polymer Stabilization

Highly stable dispersions in an aqueous system can also be achieved by the addition of surfactants (e.g., ionic and nonionic polymers) in the presence or absence of electrostatic interaction. Basim et al. [Bas03] indicate that the addition of cationic surfactants into silica slurries can provide barrier forces to stabilize colloidal suspensions. When the concentrations of C_nTAB (trimethylammonium bromide) exceeded a critical micelle concentration, micelles were formed and adsorbed onto silica surfaces to provide repulsive electrostatic interactions between particles to defend against the coagulation. The magnitude of repulsive forces was also dependent upon the polymer chains. They indicate that the potential barriers between silica particles were observed while the carbon chains of the C_nTAB were larger than 8 ($n > 8$). Although higher repulsive barrier forces can stabilize colloidal particles, lower material removal rates were found during CMP because of the lubricant effect.

The other polymer stabilization, steric stabilization, utilizes non-ionic surfactant to stabilize colloidal particles [Mor02 and Hun01]. The repulsion occurs when two adsorbed polymer layers on the particles approach each other. Napper [Nap83] demonstrated that polymer stabilization occurs due to disfavored thermodynamics. The change of the free energy of two approaching polymer particles, ΔG_F, can be expressed

$$\Delta G_F = \Delta H_F - T\Delta S_F \qquad [2\text{-}14]$$

where subscript F represents the flocculation, ΔH_F and ΔS_F are the change of the enthalpy and entropy, and T is the temperature. Three conditions may achieve steric stabilization. The first approach is the *enthalpic stabilization*: positive changes of the enthalpy and entropy. If ΔH_F is larger than ΔS_F, the flocculation is disfavored. The flocculation can be caused by raising the temperature. The second approach is *entropic stabilization*: negative changes of the enthalpy and entropy. ΔS_F is dominated by the change of energy. By lowering the temperature, the flocculation can occur. The third method is *enthalpic-entropic stabilization*: a positive change of enthalpy and a negative change of entropy. The flocculation can not be caused by changing temperature.

Furthermore, Palla et al. [Pal00] investigated the stability of alumina particles in the presence of a mixture of surfactants. They indicate that a mixture of anionic and nonionic surfactants can efficiently stabilize alumina particles because the anionic surfactants were attracted by charge surface of alumina particles and nonionic surfactants penetrated into anionic surfactant layers due to hydrocarbon chain interactions. The mechanisms of surfactant adsorption involved three phenomena. First, the driving force of the adsorption of ionic surfactants depended on the length and concentration of hydrocarbon chains. Second, the hydrocarbon chains interact with anionic and nonionic surfactants. Finally, the magnitude of polymer-solvent

interaction should be larger than that of the polymer-polymer interaction to prevent coiled polymers, and the steric stabilization occurred when nonionic surfactants were adsorbed onto particle surfaces.

Particle Agglomeration

CMP slurry is a synergistic combination of particles and chemicals, and is perhaps the most critical consumable in the semiconductor industry as it controls the uniqueness and technical performance of the CMP process. Slurry stability plays an important role in ensuring the polishing performance. If the agglomeration happens in the slurry storage or delivery, agglomerated particles not only can reduce the lifetime of filter in the slurry distribution system, but can also result in the increase of surface defectivity during the polishing process. Thus, the understanding of fundamental of particle agglomeration helps address these issues.

Slurry Agglomeration

Slurry agglomeration is influenced by particle types, slurry chemicals, and the external mechanical forces applied on the slurry itself during the slurry handling process. Typically silica, ceria, and alumina are the most common abrasive particles in the CMP slurries. These solid oxides not only provide the mechanical behavior to remove unwanted materials during the polishing, but also exhibit the interparticle forces to stabilize the suspensions. However, these abrasive particles along with numerous chemicals could deteriorate the slurry stability and influence the polishing performance.

Effect of chemicals on particle agglomeration

Chemicals in CMP slurries include oxidizers, buffering agents, dispersants, complexing agents, and pH [Sin02 and Ste96]. Each chemical has its unique function applied in the polishing process. For example, adjusting pH in CMP slurries is used to dissolve surface wafers for an increase in material removal rate. However, agglomerated particles increase significantly when

slurry pH is close to the isoelectric point of the solid oxide due to weak interaction forces between particles [Par65, Ram00, and Fran00]. Furthermore, slurries have varying ionic strengths that can change the electrostatic interaction between particle-particle and particle-wafer. The strength of the interaction depends on the concentration of salt addition in the slurry. The salt addition in CMP slurries can reduce the repulsive forces between particles and wafer, leading to an increased material removal rate during CMP [Hay95]. However, the introduction of salt in CMP slurries can also reduce the strength of electrostatic interaction between particles, resulting in increased particle agglomeration and surface defectivity during CMP [Bas02]. Choi [Cho04b] studied the effect of ionic salts on slurry stability and the polishing rates. He found that the polishing rate increased with ionic strength in stable slurry due to the uniform contact area between agglomerated particles and wafer. However, larger agglomerated particles caused non-uniform contact in unstable slurries, resulting in a decrease in material removal rate. In addition, Palla et al. [Pal99] studied the effect of oxidizer addition on the stability of alumina slurry in tungsten CMP. Typically, oxidizer can form a passive layer on tungsten surface to prevent the underlying tungsten substrate from corrosion. He found that, after adding 0.1 M potassium ferricyanide to alumina slurry, particles were agglomerated and settled due to numerous counter-ions shielding the surface charges on the particles.

Effect of pump-induced particle agglomeration

To minimize the process-dependent defectivity, particle size distribution, especially the tail region representing oversized particles, should be as small as possible and should not increase with time during slurry delivery. Some studies have shown that positive displacement pumps (e.g., bellows and diaphragm) may generate high shear stress and cause particles to agglomerate during the slurry handling [Bar99 and Lit04]. Singh et al. [Sin01] investigated the pump effect on slurry agglomeration. Silica, ceria, and alumina slurries were utilized to circulate in the slurry

delivery systems, which were comprised of a bellows pump and a vacuum-pressure-dispense-technology pump. They indicate that circulated silica-based slurries contained more agglomerated particles as compared to ceria and alumina-based slurries. Furthermore, more agglomerated particles were found in the bellows pump system than those of a vacuum-pressure-dispense-technology pump system.

Model of the Particle Agglomeration

Colloidal particles present a behavior of Brownian random motion in an aqueous system. The coagulation of colloidal particles occurs due to particle collisions. If we do not consider repulsive forces between colloidal particles, the collision frequency increases with raising shear flow, which is called rapid coagulation. On the other hand, if electrostatic interactions present between colloidal particles, the potential barrier can defend against shear flow and then reduce the frequency of particle collision. This phenomenon is called slow coagulation. The kinetic theory of particle coagulation was first worked by von Smoluchowski [Smo17, Rus89, and Hun01]. His kinetic model follows the Brownian random motion and the rapid coagulation. The model assumes that the particle collisions are binary and proportional to the particle concentration. The aggregation rate of the k-fold aggregates, *dNk/dt*, is given by the time evolution of the cluster size aggregates, *i* and *j*-folds,

$$\frac{dN_k}{dt} = \frac{1}{2}\sum_{i+j=k}^{l=k-1} k_{ij} N_i N_j - N_k \sum_{k=1}^{\infty} k_{ki} N_i \qquad [2\text{-}15]$$

where k_{ij} is the second-order aggregation constant. If colloidal particles are subjected to the uniform laminar flow, this aggregation constant, k_{ij}, can be expressed as a function of shear rate, *G*, and particle size, *a*,

$$k_{ij} = \frac{4}{3} G(a_i + a_j) \qquad [2\text{-}16]$$

Furthermore, the efficiency of particle collision is influenced by the electrostatic interaction between particles in the aqueous system. Total electrostatic interaction provides a potential barrier to hinder particle agglomeration, resulting in a decrease of the aggregation rate. Thus, the rate of k-fold aggregates can be revised by introducing the stability ratio (W), which is the ratio of rapid aggregation rate to the slow aggregation ratio. The aggregation rate can be expressed as

$$\frac{dN_k}{dt} = \frac{1}{2}\sum_{i+j=k}^{l=k-1}(k_{ij}/W_{ij})N_iN_j - N_k\sum_{k=1}^{\infty}(k_{ki}/W_{ki})N_i \qquad [2\text{-}17]$$

Thus, the Smoluchowski theory of shear aggregation [Hig82] is an applicable method to model the effect of pump-induced particle agglomeration in CMP slurries.

Particle-Induced Defectivity

Abrasive particles in the CMP slurry typically provide the mechanical component of the polishing process. Some polishing models based on the interaction between particles and wafer surfaces have been developed. Cook [Coo90] first proposed the indentation model for glass polishing. In this model, the indentation depth or material removal is taken to be in proportion to the particle size and down pressure, but is inversely proportional to material properties (e.g., elastic modulus and hardness). Thus, an indentation depth (R_s) as a function of particle size (ϕ) is given by

$$R_s = \frac{3}{4}\phi\left(\frac{P}{2KE}\right)^{2/3} \qquad [2\text{-}18]$$

where P is the down pressure, K is the surface particle fill factor, and E is Young's modulus. Thus, large particles or agglomerate are more likely to cause an increase in the defectivity of fragile materials. Mahajan et al. [Mah00 and Bas00] reported that the presence of larger particles (>0.5 μm) in the slurry not only changed the removal rate, but also caused surface defectivity (e.g., pits and micro-scratches) during CMP. As the particle size increases, the polishing

mechanism changes from a contact area-based mechanism to an indentation-based mechanism. Thus, the presence of agglomerated particles (>0.5 μm) in the slurry is the dominant factor contributing to the deterioration in the quality of the polished surface and the material removal rate during CMP.

Typically, four different types of particle-induced defectivity (i.e., killer scratch, triangle scratch, shallow scratch, and embedded particle) were found during Cu CMP [Teo04]. The killer scratches can cause significant damage or cut through the copper interconnects. The triangle scratches could be as deep as 2000 Å, resulting in the formation of metal residual on a sequent metal layer, leading to an electrical short circuit. Furthermore, shallow scratches and embedded particles may influence the dielectric reliability. In addition, the introduction of low k materials into the interlayer dielectrics is expected to have more challenges in the device integration during CMP of Cu/low-k dielectrics because the modulus and hardness of low-k materials decrease with decreasing the dielectric constant [Xu02]. Those materials with poor mechanical properties have a tendency to form more surface defects (e.g. scratches, embedded particles, and film delamination) during CMP [Klo02 and Hij04]. Chandrasekaran et al. [Cha04b] investigated polishing conditions on surface defects in three different types of low k materials. The dielectric constants and mechanical properties (elastic modulus and hardness) of those materials are shown in Table 2-2. They indicate that black diamond (BD) wafer, with a dielectric constant (*k*) of 3, had smooth surface finishing after the polishing. However, porous methyl silsesquioxane (MSQ) wafer, with a *k* of 2.5 and 2.2, exhibited rough surface finishing and some surface defects (e.g., pits and microscratches) after polishing due to an exposed underlying pore structure.

As manufacturing nodes continue to scale down, less tolerance for defect and particle densities on the wafer is expected to ensure device reliability. The International Technology

Roadmap for Semiconductors (ITRS) has predicted the required reduction of surface defects, such as killer defect density and critical particle diameter, in the near-term technology nodes, as shown in Table 2-3 [ITRS07]. Thus, robust CMP slurries may play an important role in minimizing process-induced agglomeration and particle-induced defectivity during CMP of metals and dielectrics.

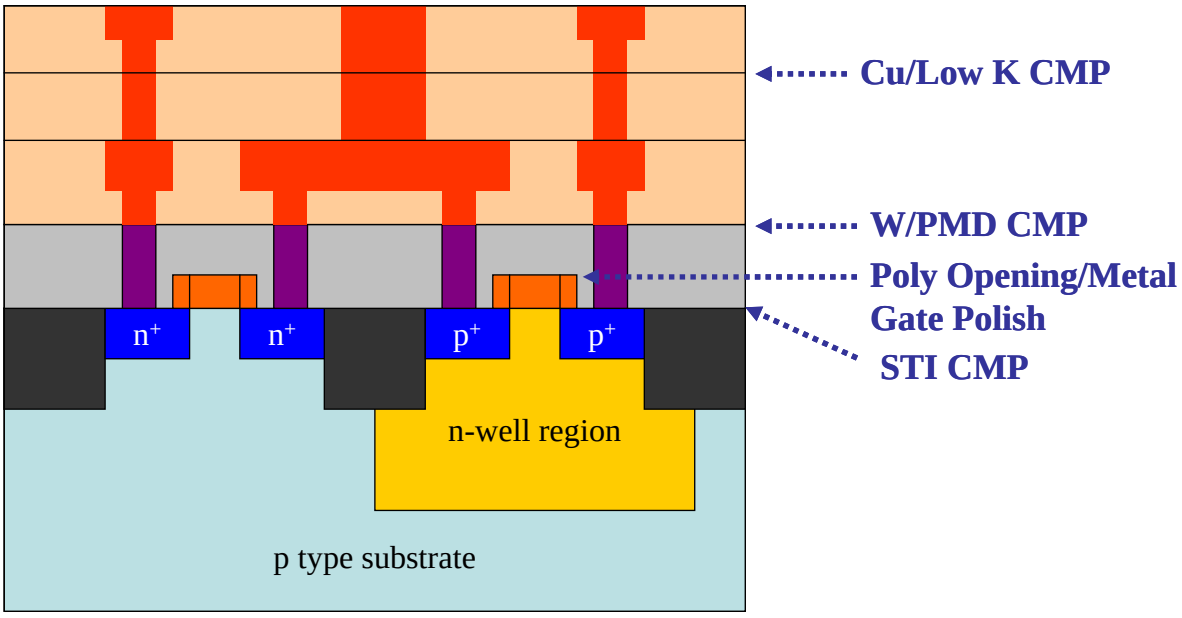

Figure 2-1. Role of CMP process in the manufacture of a microprocessor device.

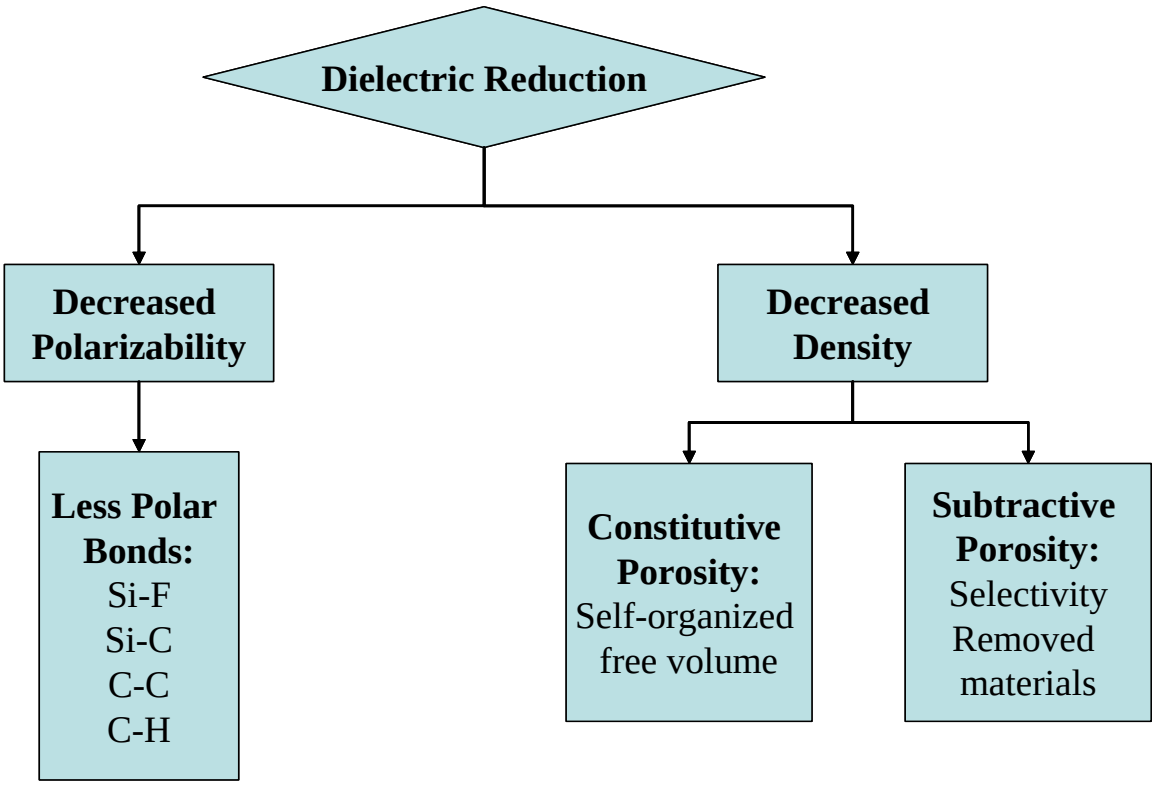

Figure 2-2. Possibilities for reducing the dielectric constant [Sha04].

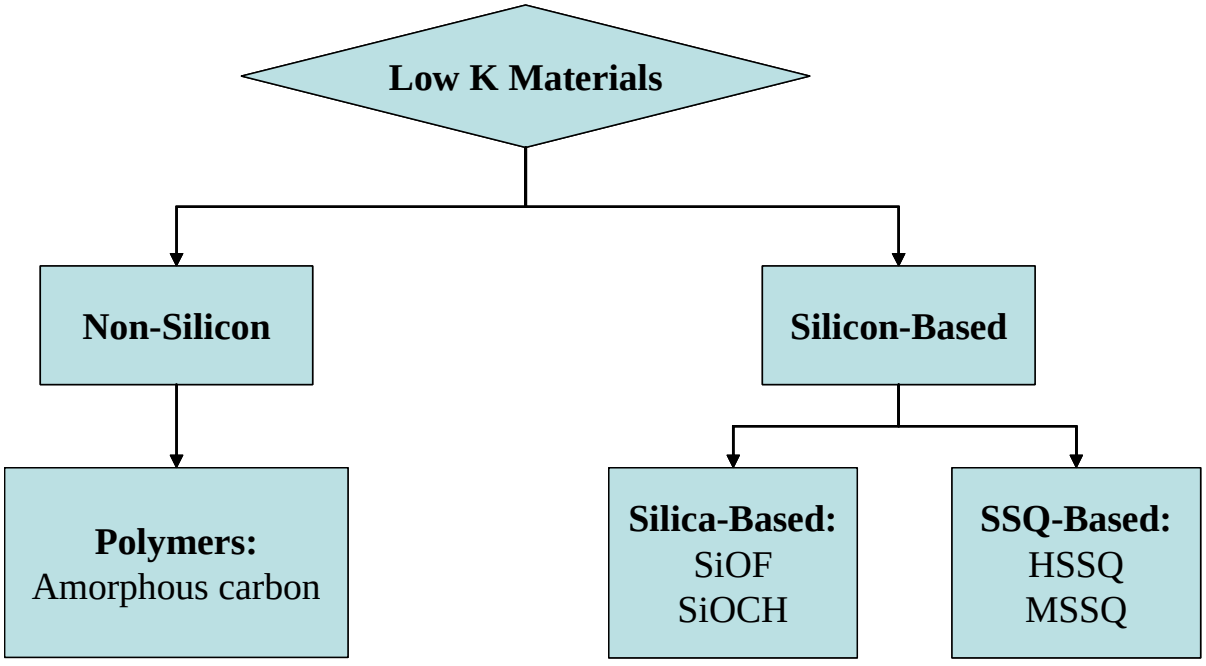

Figure 2-3. The classification of low k materials [Sha04].

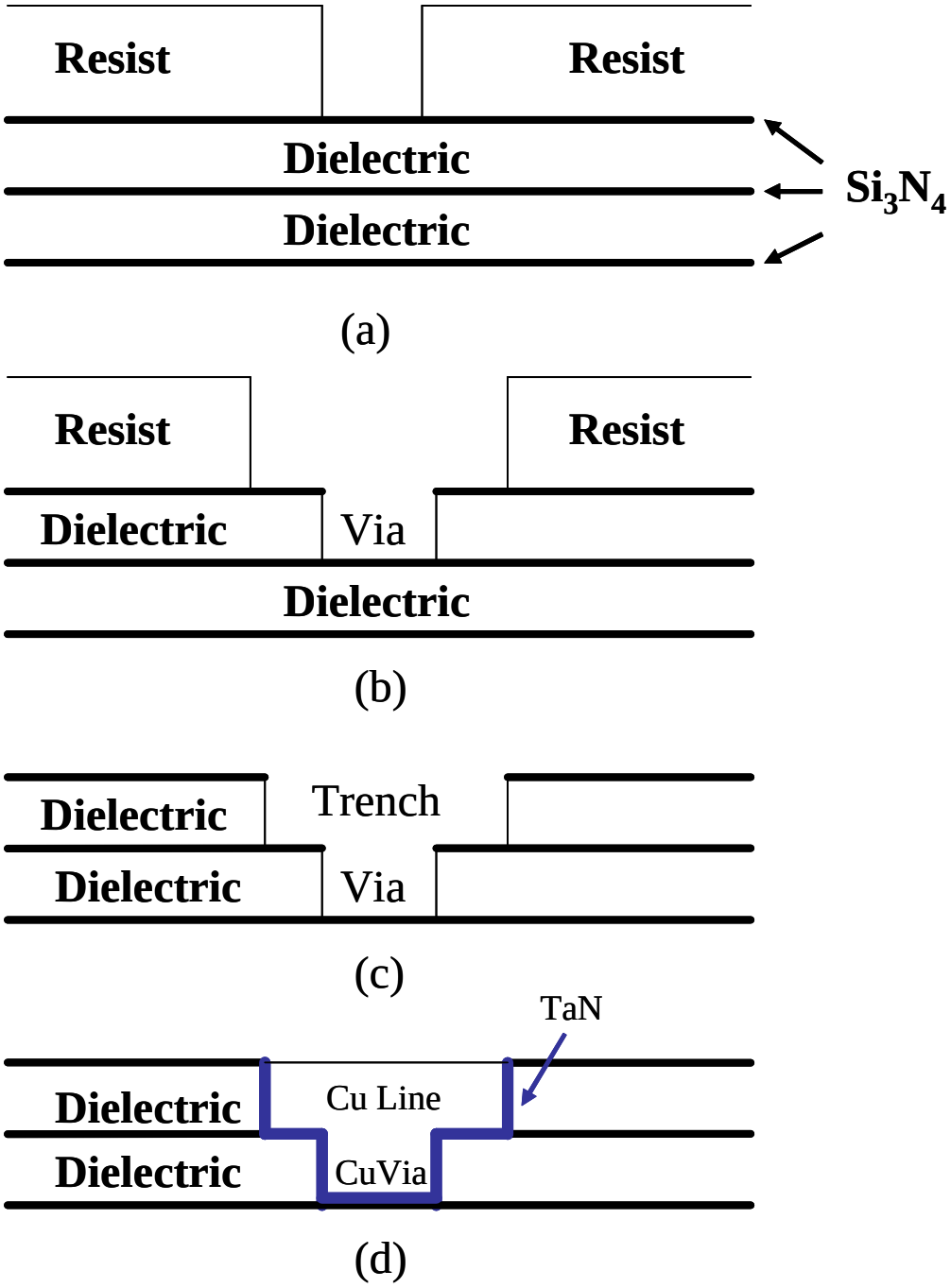

Figure 2-4. Daul-Damesence Process Flow for making MLM structure: (a) resist patterning, (b)RIE and resist patterning, (c) RIE achieved trench, and (d) Cu deposition and CMP [Sze01].

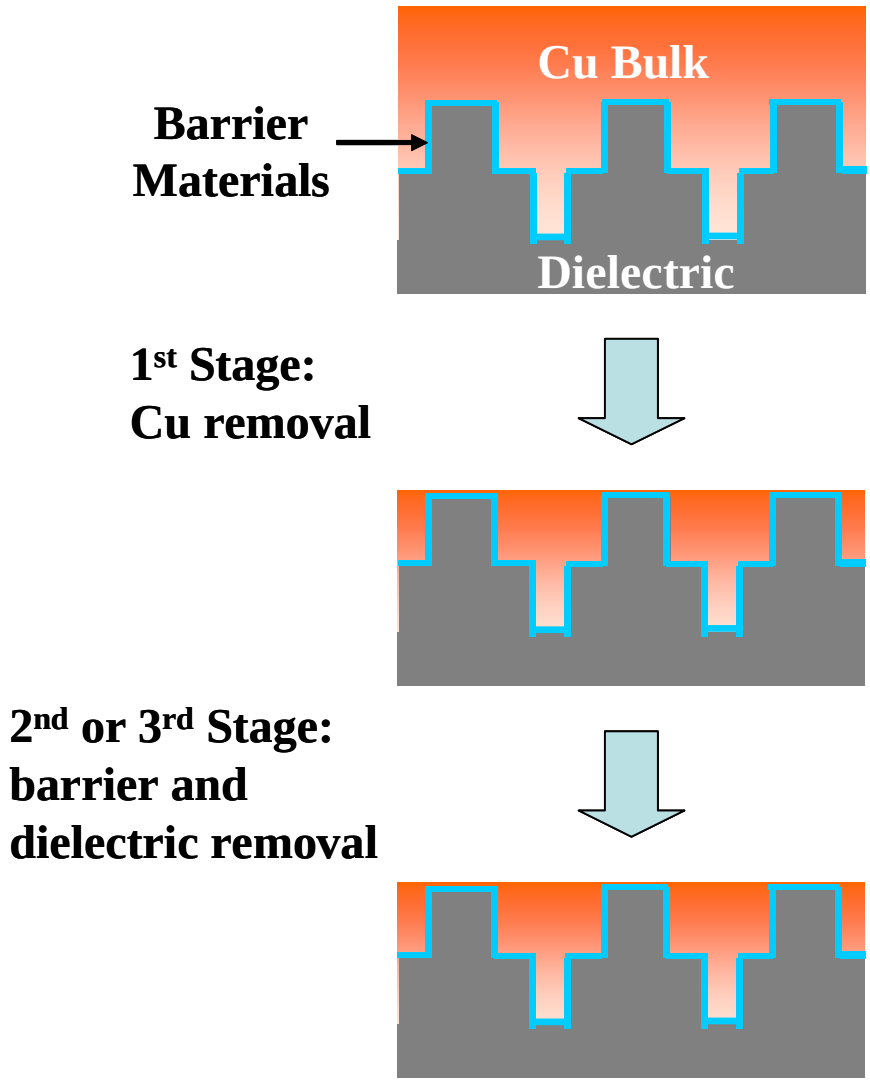

Figure 2-5. Three polishing stages during Cu/Low k CMP.

Table 2-1. Comparison between LOCOS and STI processes.

Process	LOCOS	STI
Advantages	1. Simple Process 2. Low Cost	1. Eliminated Bird's Beak 2. High Device Packing Density (node ≤ 0.25μm)
Disadvantages	1. Uncontrollable geometry 2. Bird's Beak 3. Low Device Packing Density (node ≥ 0.25μm)	1. Defects (e.g. micro-scratches and dishing) 2. Increased Leakage Current

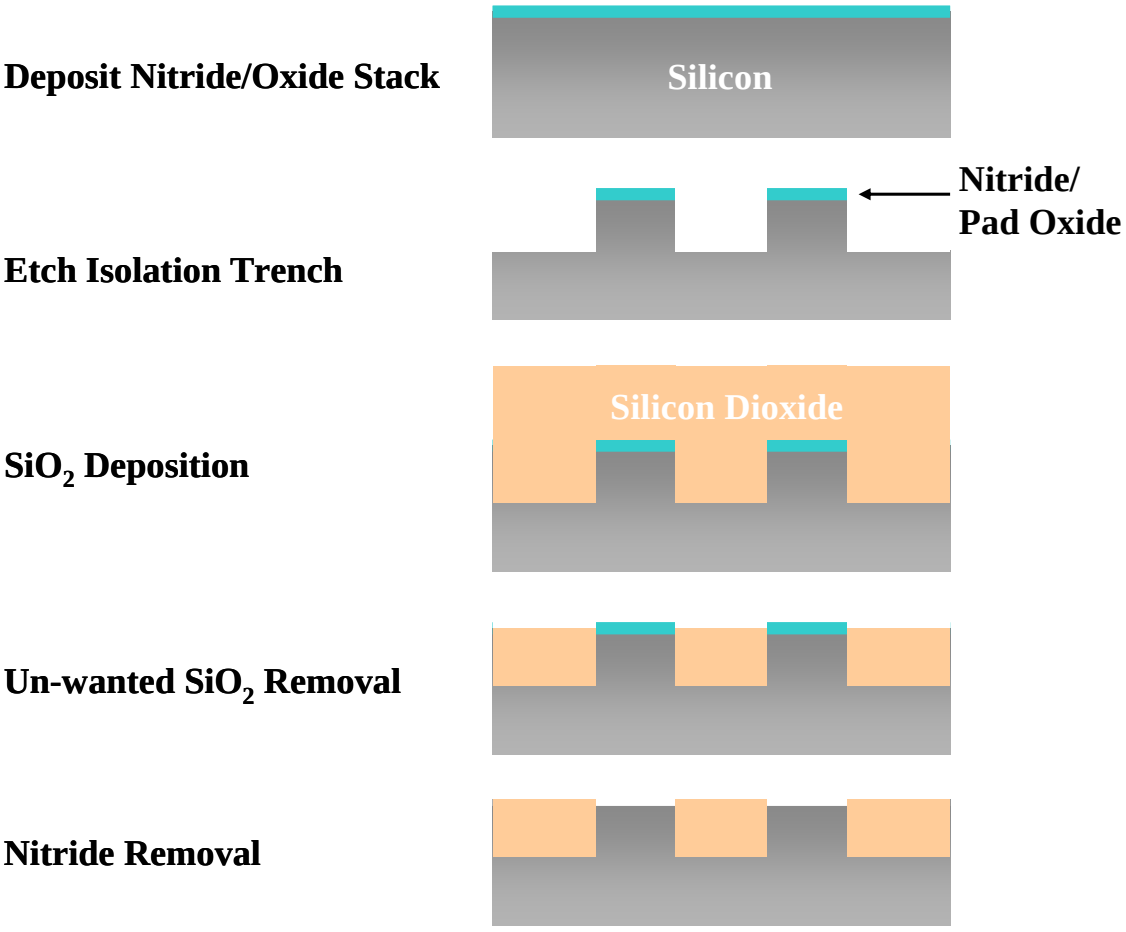

Figure 2-6. STI process flow.

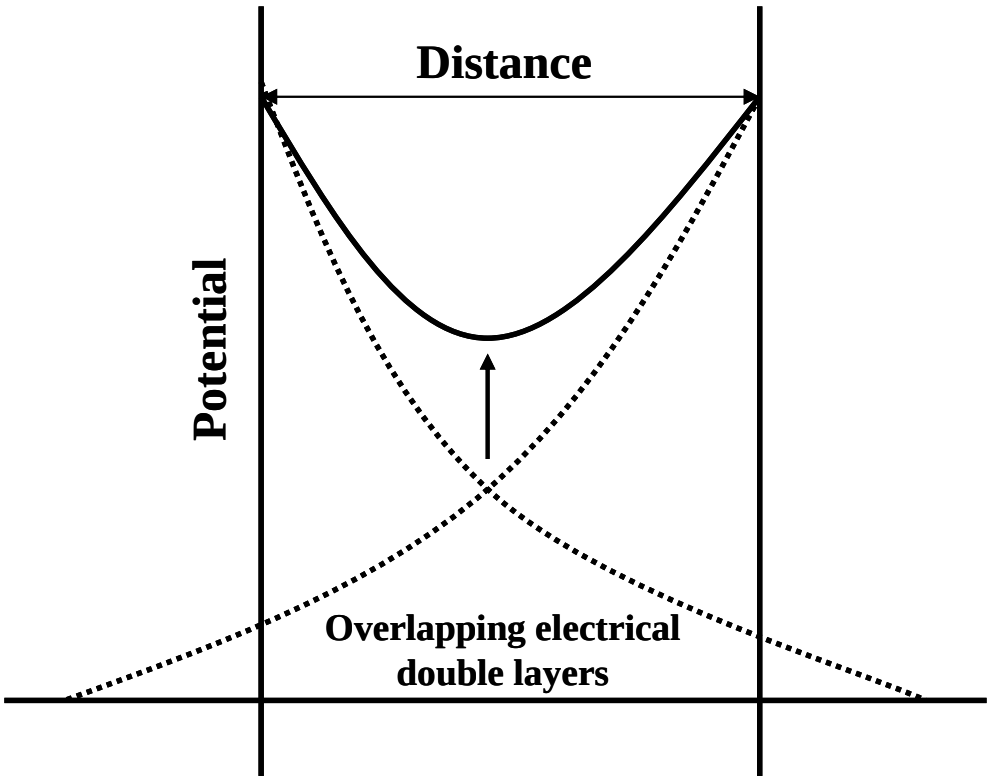

Figure 2-7. Overlapping of two electrical double layers [Hun01].

Table 2-2. Properties of dielectric films [Cha04].

Types of Dielectrics	Dielectric Constant	Hardness (GPa)	Elastic Modulus (GPa)
Organosilicate glass (OSG)	3	4.6	24.9
Silsesquioxane (SSQ)	2.5	1.24	8.63
Silsesquioxane (SSQ)	2.2	0.68	4.98

Table 2-3. Interconnect surface requirements at near-term technology nodes [ITRS07].

Year of Production	2008	2010	2012	2014
Technology Node (nm)	59	45	36	28
# of Metal levels	12	12	12	13
Average dielectric constant	2.7-3.1	2.4-2.8	2.2-2.6	2.2-2.6
Dishing Planarity (nm)	20	16	14	11
Min. defect particle size (nm)	28.5	22.5	17.5	14

CHAPTER 3
CMP CHARACTERIZATIONS

CMP System and Consumables

A CMP system basically consists of CMP polisher and slurry distribution. In our studies, different types of slurries, including silica slurries for Cu/ low k dielectric polishing and ceria based slurries for STI polishing, were utilized to polish 1-inch square BD1 low-k (k=3.0), JSR ultra low-k (k=2.2), copper, and tetraethyl orthosilicate (TEOS) wafers from a TegraPol-35 Table Top Polisher, Struers Co. The 1-inch square sample holder was made by a stainless cylinder of 2.25 inches in diameter and 1.125 inches in height. The following conditions were applied to each run: a down pressure of 3 psi, polishing time of 1 min, slurry flow rate of 100 ml/min, and rotation speed of 150 rpm. During the polishing process, CMP slurries with varying chemicals were poured down a soft polymeric polishing pad, which provides a transport of slurry to achieve a local and global planarization.

Furthermore, Figure 3-1 shows a slurry distribution system, which consisted of pumping devices and a slurry delivery loop. A distribution loop consisted of a 12-foot long PFA tubing (Teflon poly-fluoroalkoxy), slurry tank (10 gallons), pressure gauge flowmeter, pressurized air supply outlet/inlet, and 220 volt power supply system. Pumping devices can be simply classified as positive displacement pumps (e.g., bellows or diaphragm pumps) and centrifugal pumps (e.g., a magnetically levitated centrifugal pump). Both pumping devices have different operating principles, causing to different magnitudes of shear stress and degrees of particle agglomeration during slurry delivery. For example, a positive displacement pump can be considered a constant volume pump because the slurry is transported from the suction nozzle to the discharge nozzle. The volume of captured slurry depends on the chamber size. However, this pumping device may generate highly localized shear stresses near the wall during the pump stroke, resulting in a

significant increase in agglomerated particles. On the other hand, a magnetically levitated centrifugal pump, which is a constant pressure head device, provides a smooth pulseless flow due to a contact-free impeller in the pump housing, resulting in an insignificant increase in agglomerated particles. Thus, the magnetically levitated centrifugal pump can be considered a low shear pumping device.

Particle Characterization

As CMP slurries are a synergistic combination of particles and chemicals, the properties of abrasive particles can influence the slurry stability and polishing performance (e.g., removal rate and roughness). In the present studies, particle characterization involves the measurements of particle size, interparticle force, and surface charge. These measurements can help in understanding the particle properties for the CMP application.

Particle Size Measurement

Numerous particle size instruments can be utilized to measure particle size distribution in the slurry, as listed in Table 3-1 [Bow02]. These instruments are based on several principles (e.g., microscopy, sedimentation, sieving, single particle counter, light scattering, and gas adsorption) and their limitation to determine particles in the size range of a few nanometers to thousand microns. As the abrasive particles utilized in the polishing are below 1μm, some particle size instruments, such as dynamic light scattering, laser diffraction, photo-centrifuge, and a single-particle optical sensor (SPOS) system, are employed for measuring the particle size and distribution.

To detect the agglomerates or oversize particles in CMP slurries, the particle size measurement system “AccuSizer 780,” consisting of a single-particle optical sensor (SPOS), was used to measure the oversize particle distribution in the size range of 0.51 to 200 μm [Pro98].

This instrument has two stages of the autodilution system to obtain an acceptable particle concentration for the SPOS sensor. The total extent dilution of initial sample suspension is equal to the dilution factor 1 (DF1) of first stage multiplied by the dilution factor 2 (DF2) of the second stage, defined as

$$C_i / C_2 = (C_i / C_1) \times (C_1 / C_2) = DF1 \times DF2 \qquad [3\text{-}1]$$

where C_i, C_1, and C_2 are defined as initial particle concentration and first and second stage of particle concentrations. Thus, the advantage of this instrument is that it is capable of starting a concentrated particle concentration. In our experiment, 1 ml of circulated slurry was dropped into the solution chamber and diluted with deionized water. Particles in the dilute slurry flow through a sensor zone, a laser diode, to cause a detected pulse. The magnitude of pulse depends on the particle diameter and the physical method, light extinction and light scattering. Figure 3-3 shows the cumulative concentration tails of oversize particles in 60nm silica slurry (5 wt%) at 0 and 1,000 turnovers. The cumulative concentration tail can clearly demonstrate the stress effect on particle agglomeration during the handling process.

Furthermore, the primary sizes for sub-micron particles in CMP slurry are measured by dynamic light scattering, photo-centrifuge, and laser diffraction techniques [Bow02 and Sta02]. The principle of photo-centrifuge is a combination of sedimentation theory and light adsorption. The centrifugal sedimentation can be expressed by the Stokes' law: the particle diameter (d) is dependent on the time (t) required to settle down a known distance.

$$d = \sqrt{\frac{18\eta_0 In(x_1 / x_2)}{(\rho - \rho_0)\omega^2 t}} \qquad [3\text{-}2]$$

where ρ is the sample density, ρ_0 is the dispersing liquid density, x_1 is the starting radius, x_2 is ending radius, and ω is the rotational angular velocity. During the measurement, small amounts

of particles at a particular size pass through the light beam and cause an intensity reduction. The particle concentration can be obtained by the Beer-Lamberts Law.

$$\log I_0 - \log I_i = A\sum_{i=1}^{n} K(d_i) N_i d_i^{\,2} \qquad [3\text{-}3]$$

where I_0 is the maximum intensity of the initial light beam, I_i is the reduction intensity while detecting particles, A is optical coefficient of the cell, N_i is the number of particles, and $K(d_i)$ is the efficiency of light extinction. For example, Figure 3-4 shows the particle size distribution of 80 nm silica slurry measured by Disc Centrifuge from CPS instruments. The measurable particle size range of Disc Centrifuge is 20nm to 30 μm.

Furthermore, a light scattering technique has been commonly employed for measuring particle size. This technique can be divided into two groups, dynamic light scattering (or quasi-elastic light scattering or photon correlation spectroscopy) and low angle laser light scattering (or laser diffraction). Dynamic light scattering can quickly and accurately measure the particle size range from 0.8 nm to 6.5 μm (Nanotrac®). When the particle size is smaller than a sub-micron, colloidal particles have a behavior of Brownian motion due to thermal vibration. Thus, for a monodisperse distribution of spherical particles, an intensity of autocorrelation function is employed for analyzing the intensity fluctuations.

$$g(t) = \exp(-Dq^2 t) \qquad [3\text{-}4]$$

where $g(t)$ is the normalized autocorrection function, and D, q, and t are the Brownian diffusion coefficient (Stokes-Einstein relation), scattering vector, and delay time of the autocorrelation function.

$$D = K_B T / 3\pi\eta d \qquad [3\text{-}5]$$

where K_B is Boltzmann constant, T is the absolute temperature, η is the liquid viscosity, and d is the particle diameter. Thus, smaller particles move more rapidly and have more intensity fluctuations than bigger particles. Furthermore, the laser diffraction has been commonly employed for detecting large particles. When a particle size is larger than incident wavelength, the diffraction phenomenon occurs while light beam interacts with particles. The smaller particles have a higher angle of diffraction than bigger particles [Mor02].

Interparticle Force Measurement

When particles approach each other closely, the overlapping of the repulsive electrical double layer forces have the capability to defend against the external mechanical forces applied on slurry itself. In this experiment, the silica-silica and silica-ceria interparticle forces were measured using the wet cell arrangement in the Digital Instruments Nanoscope III atomic force microscope (AFM). Before the force measurement, colloidal probes and substrates must be prepared. A silica micro-spherical particle can be attached to the end of the cantilever using epoxy resins to simulate the interparticle forces. The liquid used in the measurement will be the supernatant of the specific slurry used (e.g., silica slurry, low k slurry etc.). The strength of the interaction will depend on the chemistry and additives in the slurry and the nature of the particles. Such measurements will be conducted on respective slurries. It should be noted that the defectivity in CMP can be simulated with particle interactions with the respective substrate (e.g. copper, tungsten etc.). In this case, the plate for AFM measurement would be the same as the surface to be polished.

The AFM force measurement was conducted by a colloidal probe technique, as shown in Figure 3-2 [But91 and But95]. The force-distance curve was the cantilever deflection (Δz_c) versus the height position of the sample (Δz_p). During the measurement, the cantilever deflection

was measured by a laser diode beam, reflecting from the back of the cantilever to a position-sensitive photodiode, and the sample position was controlled by a piezoelectric translator. The force measurement began with a large tip-surface separation in an aqueous electrolyte, as shown in Figure 3-2 (top). When the tip approaches the wafer surface, the interaction forces between the silica probe and substrate can bend the cantilever, resulting in the cantilever deflections. When a colloidal probe moved closely at a certain distance, where the attractive Van der Waals force was larger than the repulsive electrical double layer force, the tip rapidly jumped onto the sample surface. Once the tip was in contact with the surface, the cantilever deflection increased as Δz_p decreases, pulling the cantilever upward. When the sample was retracted from the substrate, the silica probe may stick on the wafer surface due to the adhesion force. When the bending force was greater than the adhesion force, the sample abruptly jumped from the surface and returned to its starting position. The interaction force between silica probe and substrate was calculated by multiplying the spring constant of the cantilever with the separation distance. Thus, the magnitude of the interparticle force can be converted from the interaction force between silica probe and substrate because the interparticle force is half the value of the particle-plate force.

Measurement of Electrical Potential (Zeta Potential)

The electrical double layer potential plays an important role in stabilizing the colloidal particles. However, there is no experimental approach to measure such potentials. The alternative method is to measure the zeta potential, which is the surface potential at the shear plane in an aqueous system, by means of the electrokinetic experiments.

In this study, the zeta potential of abrasive particles in CMP slurries was measured by the Brookhaven ZetaPlus, which is utilized an electrophoresis method to measure the electrophoretic velocity (v_E) of colloidal particles [Ste05 and Hun01]. When the electrical double layer (*1/k*) is

much smaller than particle size, the Smoluchowski equation can be applied to measure the zeta potential (ζ).

$$\zeta = \frac{\eta}{\varepsilon}\frac{\upsilon_E}{E_0} \qquad [3\text{-}6]$$

where ηand ε are the values of viscosity and dielectric constant in the solution and E_0 is the electric field. If the electrical double layer (*1/k*) is much larger than the particle size, the Huckel equation can be applied, and expressed as

$$\zeta = \frac{3}{2}\frac{\eta}{\varepsilon}\frac{\upsilon_E}{E_0} \qquad [3\text{-}7]$$

Polishing Characterization

Polishing Parameter for Cu/Low K CMP

The process of Cu/low CMP is a dependable technology to manufacture multilevel metallization structures. The introduction of low polar bonds or low density materials into silicon dioxide for reducing dielectric constant causes mechanical properties to deteriorate and presents many challenges (e.g., Cu/low-k delamination and scratching) in the device integration during CMP. In our experiment, 5 wt% 80nm silica slurries at pH 9 were used to polish low k wafers (BD1) in the TegraPol-35 Table Top Polisher at down pressure of 1.7, 3.4, and 5.0 psi to determine the best polish parameters in low k CMP. Figure 3-3(a) shows the material removal rate as a function of down pressure. Although removal rate was proportional to down pressure, broken wafers were found at down pressure of 5 psi due to the poor mechanical strength of low k wafer. Thus, the down pressure for polishing was subjected to 3.4 psi.

For metal CMP, chemical dissociation and passivation on a metal surface can dramatically affect the polishing performance. According to the Pourbaix diagram, Cu starts to form a passivation layer above pH 6. In our experiment, 75nm silica slurries at pH 6, 6.5, and 7.0 were

used to polish Cu wafers at a down pressure of 3.4 psi to investigate the effect of passivation layer on material removals. Figure 3-3(b) shows the material removal rate as a function of slurry pH. The Cu removal rates decreased with slurry pH due to the growth of the passivation layers on Cu surface. Thus, acidic slurries with a corrosion inhibitor were utilized to polish Cu wafers to get a higher removal rate. Although a corrosion inhibitor can protect the Cu layer from adramatic chemical dissociation below pH 6, it can decrease the Cu removal rate, as shown in Figure 3-3(c).

Characterization of Polished Wafer

Polished Cu, low k, and TEOS wafers were characterized by using an atomic force microscope (AFM), ellipsometry, and a scanning electron microscope (SEM), optical microscope, and four-point probe to measure the material removal rate, surface roughness, and polished defectivity.

AFM has been commonly employed for measuring the root mean square, RMS = $(\Sigma h_i/N)^{1/2}$ (h and N are height values and numbers of measurements), and maximum height (R_{max}) of polished substrates to determine the surface roughness and defectivity. Typically, the principle of AFM is to measure the near-filed forces between cantilever tip and substrate, and its operational modes can simply divide into the contact and tapping modes [Len08]. In the case of contact mode, the AFM tip constantly contacts with substrate during the measurement, and the cantilever deflection is measured by positive-sensitive photodiodes, which is utilized to detect laser beam reflections from the back of a cantilever, as illustrated in Figure 3-4. On the other hand, the tapping mode AFM measures the surface topography by means of the amplitude of the cantilever oscillation. The decrease and increase in the oscillation amplitude corresponds to a protruding and a concaving surface, respectively, as shown in Figure 3-5. Furthermore, to obtain an

accurately scanned position, the three dimensional scanning is controlled by X-Y-Z piezoelectric tubes.

The surface images of polished defectivity can also be detected by a SEM, which has a resolution up to1-10nm, and magnification range from 10x to 10^6x [Len08]. The image resolution is determined by the beam brightness, which is dependent on the electron gun (i.e., field emission gun, LaB_6 thermionic gun, and tungsten thermionic gun). Typically, the secondary electrons and the backscattered electrons can be applied to the surface topographic images and compositional images, respectively. When a high energy electron beam interacts with the sample, the secondary electrons escape from the near-surface region in the depth range of 5 to 50 nm due to its weak electron energy (< 50 eV). Because the backscattered electrons have a greater electron energy (>50 eV), they can escape from a deeper depth range of 50 to 300nm [Eva92]. Thus, the secondary electron image is the best choice to observe the surface defectivity of polished wafers.

The thickness of oxide films can be measured by ellipsometry, which is a nondestructive technique. The advantages of this instrument are that it requires no vacuum and has a large detected range (1-1000nm) [Eva92]. Typically, the principle of ellipsometry is to measure the change in the polarization of thin films after reflection or transmission. By measuring the change of the amplitude factor (ψ) and phase shift (Δ), the complex ratio (ρ), defined as a ratio of reflection coefficient r_p (electric field parallel to the plane of incidence) to r_s (electric field perpendicular to the plane of incidence), can be obtained.

$$\rho = \frac{r_p}{r_s} = \left(\tan\psi\right)e^{i\Delta} \qquad [3\text{-}8]$$

In this study, the thickness of silica and low k wafers were measured by a Woollam EC110 Ellipsometer to obtain the material removal rate.

In addition, four-point probe technique has been commonly used to measure the sheet resistance for determining the thickness of the Cu film due to its accurate and reliable measurement [Sze01]. During measurements, two outer probes were passed through applied current and inner probes were measured a voltage drop by voltmeter. By separating the probes of supplied current and measured voltage using two pairs of probes, this instrument can eliminate the measurement errors from probe and contact resistances because large impedance of voltmeter caused to negligible parasitic resistances (probe and contact resistances) in inner probes [Doe08]. Thus, it accurately measured voltage difference of tested sheet. When the probe spaces were equal, the sheet resistance (R_s) can be expressed:

$$R_s = \frac{\rho}{t} = \frac{\pi}{\ln 2}\frac{V}{I} \qquad [3\text{-}9]$$

where ρ is the resistivity, t is the thickness of thin film, V and I are measured voltage and applied current. By determining the sheet resistance, the thickness of the Cu film can be obtained. In addition, the geometrical error, arising from slight variation of probe spacing and closing to wafer edges, can be eliminated by its dual-configuration technique.

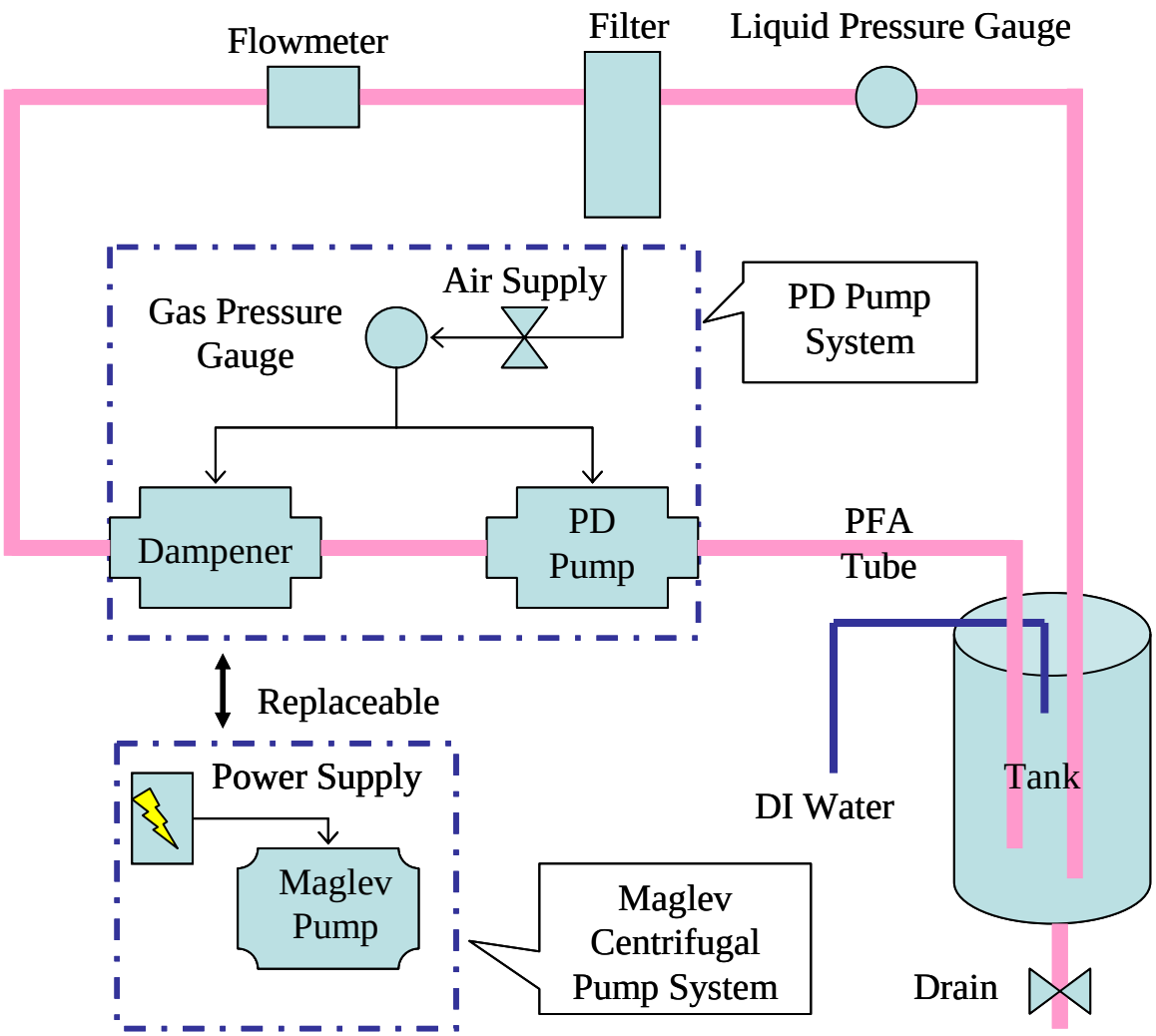

Figure 3-1. Schematic illustration of a slurry distribution system.

Table 3-1. Various measurement methods for particle size [Bow02].

Method	Medium	Size Range (μm)	Diameter Measured
Microscopy			
Optical	Liquid/Gas	400–0.5	Projected area
Electron	Vacuum	400–0.001	Feret
Sieving	Air	8000–37	Sieve
	Liquid	5000–5	
Sedimentation			Stokes
Gravity	Liquid	100–0.5	
Centrifuge	Liquid	300–0.01	
Ultracentrifuge	Liquid	300–0.001	
Single particle counters			
Electrical sensing			
Zone	Liquid	1200–0.3	Volume
Time of flight	Gas	700–0.2	Aerodynamic
Light scattering			
Diffraction (LALLS)	Liguid/Gas	1800–0.5(0.1)	Volume
Dynamic (PCS)	Liquid	0.5(1)–0.002	Hydrodynamic
Gas adsorption	Gas/Vacuum	5–0.005	Surface-Volume

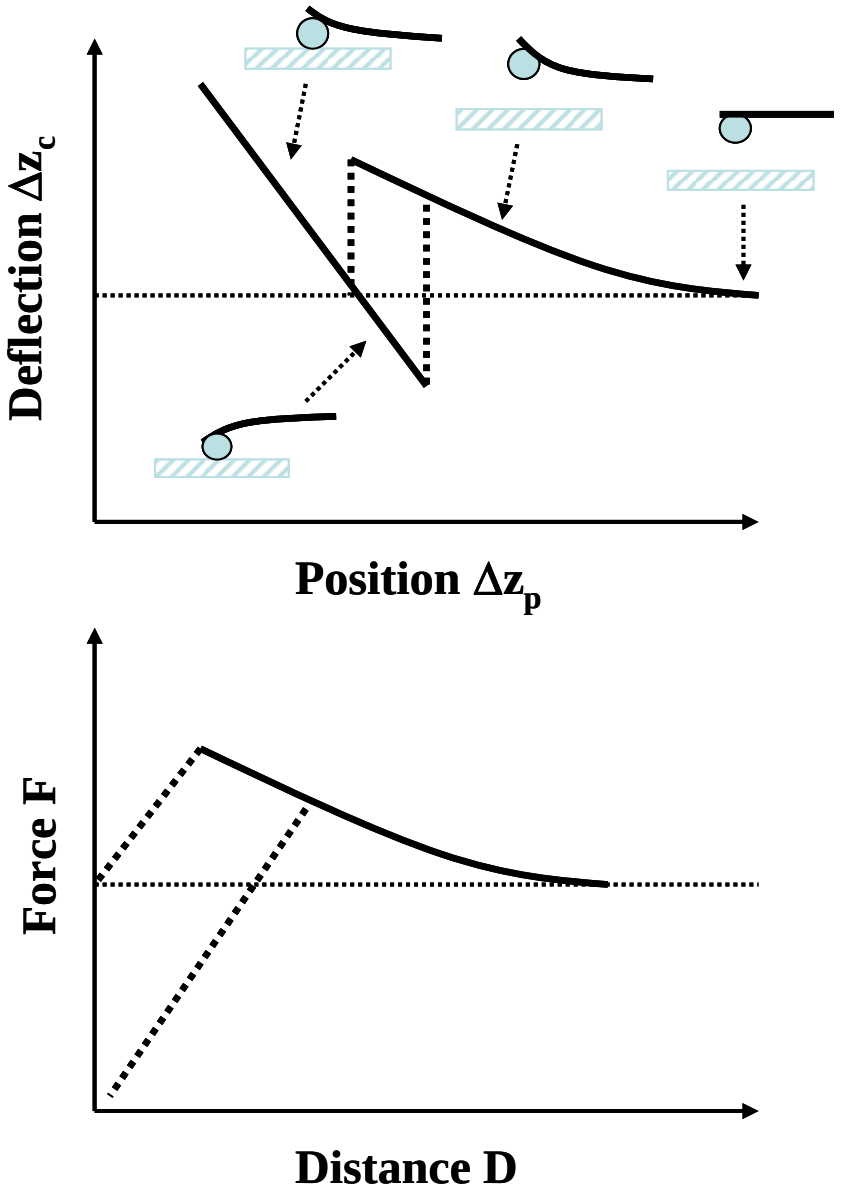

Figure 3-2. Schematic illustration of the colloidal probe technique: cantilever shapes and cantilever deflection Δz_c versus height position of sample Δz_p (top); force–distance curve (bottom) [But91].

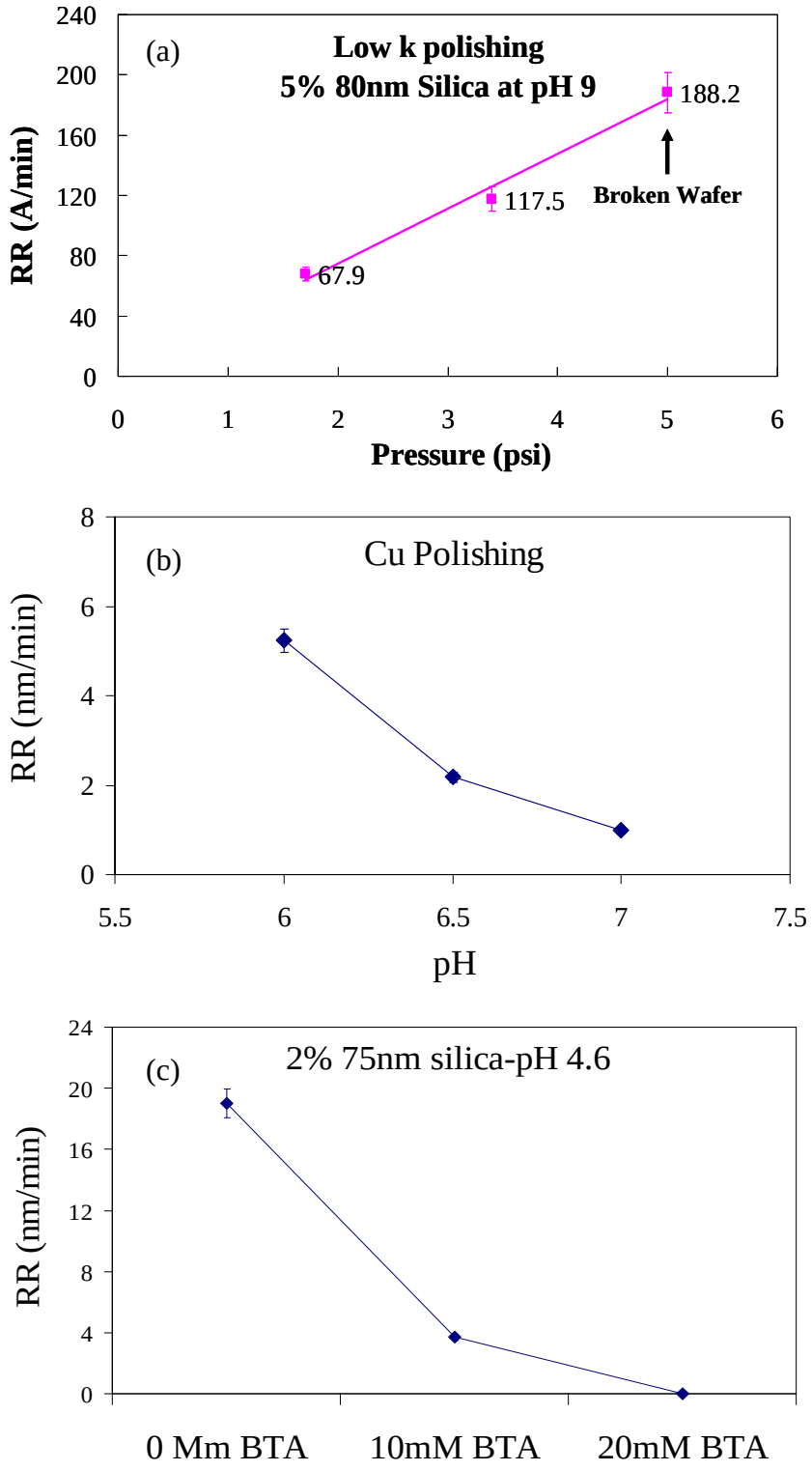

Figure 3-3. Polishing parameters: (a) the material removal rate as a function of down pressure in low k CMP, (b) the material removal rate as a function of pH in Cu CMP, (c) the material removal rate as a function of BTA concentrations in Cu CMP.

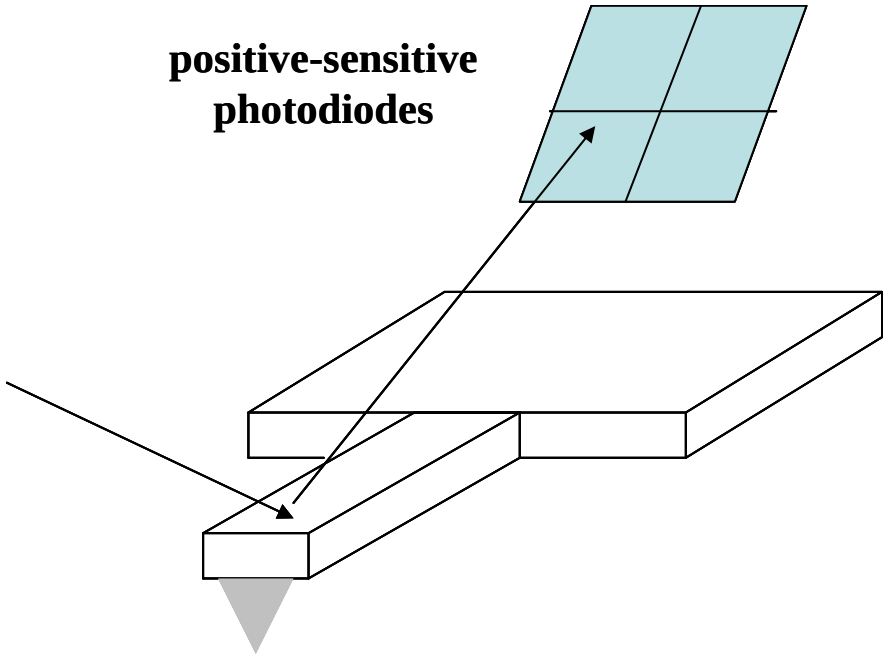

Figure 3-4. Contact mode AFM: the cantilever deflection is measured by positive-sensitive photodiodes, which is utilized to detect laser beam reflections from the back of the cantilever [Len08].

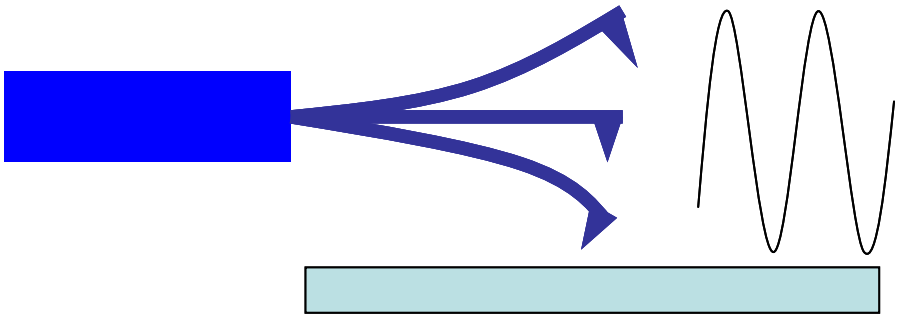

Figure 3-5. Topping mode AFM: the surface topography is measured by detecting the amplitude of the cantilever oscillation [Len08].

CHAPTER 4
EFFECTS OF STRESS-INDUCED PARTICLE AGGLOMERATION ON DEFECTIVITY DURING CMP OF LOW-K DIELECTRICS

Introduction

Chemical mechanical planarization (CMP) is now commonly employed for both the front and back end processing of IC devices due to its unique global planarization capability [Ste96 and Sin02b]. With the miniaturization of semiconductor devices, multilevel interconnect plays an important role in providing a reliable and an efficient interconnect system for new generation of IC devices. The CMP process of Cu/low-k dielectrics is a dependable technology to manufacture multilevel metallization structures. This process is used for removing the excess copper, barrier layer, and underlying low-k dielectrics. As low-k films exhibit poor mechanical properties, many remaining challenges (*e.g.*, Cu/low-k delamination and scratching) in the device integration during CMP of Cu/low-k dielectrics need to be solved [Cha04b, Bal04, and Xu02].

The presence of larger particles in CMP slurries is among the foremost factors that introduces defects (*e.g.*, scratches and embedded particles) during the polishing process [Rem06]. Mahajan *et al.* [Mah00 and Bas00] studied the effect of particle size on the surface roughness and removal rate during CMP of oxide thin films. They reported that large particles (>0.5 μm) in the slurry not only changed the removal rate, but also deteriorated the quality of the oxide surface (*e.g.*, pits and micro-scratches) during CMP. These large particles in CMP slurries can increase mechanical stress that can lead to increase in surface defectivity during the polishing; especially for low-k dielectrics with low elastic modulus and hardness [Hij04]. These surface damages have a significant negative impact on the manufacturing process and the reliability of dielectrics.

Large particles can exist in CMP slurry, or be generated from the slurry blending and slurry distribution system, which utilizes a pumping device to circulate CMP slurry in the global

distribution loop [Joh03]. Some studies have shown that positive displacement pumps (*e.g.*, bellows and diaphragm) generate high shear stress and tend to agglomerate particles during slurry handling [Sin01, Sin04, and Lit04]. Litchy *et al.* [lit05] reported clogging of the filters in a slurry distribution system by agglomerated particles, resulting in a pressure drop across the filter. Diaphragm and bellows pumps caused a larger pressure drop as compared to a magnetically levitated centrifugal pump as larger amounts of agglomerated particles were produced during slurry handling.

As some CMP slurries are shear-sensitive, which means that particles tend to agglomerate under the shear flow, low shear pump is in urgent need in slurry distribution system to prevent defect generation due to agglomerated particles during polishing. In the present study, we investigated the stress effects of three different types of pump on particle agglomeration and particle-induced defectivity during CMP of low-k dielectrics, and established a correlation between the roughness/defect density and the degree of agglomeration.

Experimental

A slurry distribution system was designed and built to observe the effects of stress on particle agglomeration. This system consisted of a 12-foot long tubing distribution loop (Teflon poly-fluoroalkoxy), a slurry tank, a pressure gauge, a flow meter, and a pressurized air supply outlet/inlet. Positive displacement pumps (*e.g.*, bellows or diaphragm pumps) and magnetically levitated centrifugal pumps, provided by Levitronix LLC, were placed in the system to circulate the CMP slurry. The slurry used was Cu barrier slurry comprised of 10 wt% silica, designed to remove the residual Cu, the barrier metal, and a portion of the low-k dielectric. The flow rate of the silica slurry was held constant at 12 L/min by fixing the gas pressure at 30 psi for the positive displacement pumps and 5900 rpm for the magnetically levitated centrifugal pump. The effects of pump-induced particle agglomeration were examined at 250, 500, and 1000 turnovers.

The particle size measurement system "AccuSizer 780," consisting of a single-particle optical sensor (SPOS), was used to characterize the oversize particle distribution in circulated slurries and can detect particle in the size range of 0.51 to 200 μm. To measure the particle size, 1 ml of circulated low-k slurry was dropped into the solution chamber and diluted with deionized water to prevent slurry re-agglomeration. Single oversize particle was detected by the photozone, a narrow laser diode, and the cumulative oversize particle tail was obtained after measurements had been taken. Furthermore, the primary particle size can be measured by dynamic light scattering technique. In this experiment, the as-received and circulated slurries were measured by Nanotrac®, which can detect the particle size range from 0.8 nm to 6.5 μm.

Subsequently, silica slurries circulated by positive displacement and magnetically levitated centrifugal pumps were used to polish 1-inch square BD1 low-k (k = 3.0, Hardness/Elastic modulus = 4.6/24.9 GPa) and JSR ultra low k (k = 2.2, Hardness/Elastic modulus = 0.68/4.98 GPa) wafers [Cha04] in a Struers RotoPol-31 Table Top Polisher with a down pressure of 3 psi, polishing time of 1 min, slurry flow rate of 100 ml/min, and rotation speed of 150 rpm. The surface roughness of polished low-k wafers was characterized using a Digital Instruments Nanoscope III atomic force microscope (AFM). The defect density was determined by counting the number of defects per square millimeter by optical microscopy at 200× magnification.

Results and Discussion

Characterization of Oversize Particle Distribution

Silica slurries (10 wt%) were circulated using positive displacement and magnetically levitated centrifugal pumps (Maglev pump) in the slurry distribution system to observe the effects of stress on particle agglomeration. Figure 4-1 shows the primary particle size of low-k slurries as a function of slurry turnovers. The results indicate that the primary particle sizes

remained constant in all pumping devices and were independent of numbers of slurry turnovers. Thus, the pumping devices would not change the primary particle size in highly stable slurries during the handling process.

Figure 4-2 shows the cumulative distribution curves of oversize particles in low-k slurries at 0, 250, and 500 turnovers from different pumps obtained by cumulatively summing the number of particles above a certain size from 10 to 0.51 μm. The cumulative concentration at 0.51 μm was 15,377 (particles/ml) in as-received slurry (0 turnovers). The increase in the concentration of oversize particles depends on the shear stress, which arises from the different types of pumps used, and the number of turnovers. The cumulative concentrations of oversize particles for 250 and 500 turnovers at 0.51 μm were 44,613 and 66,916 (particles/ml) in the bellows pump system, 41,435 and 61,481 (particles/ml) in the diaphragm pump system, and 16,485 and 18,809 (particles/ml) in the magnetically levitated centrifugal pump system. Based on experimental results, the cumulative concentrations of oversize particles were shown to significantly increase with slurry turnovers in the positive displacement pump system. In contrast, increasing the number of turnovers did not increase the concentration of oversize particles significantly in the case of magnetically levitated centrifugal pump system.

The normalized oversize particle distribution, which is defined as the ratio of cumulative concentrations at 500 slurry turnovers to cumulative concentrations at 0 slurry turnovers, can clearly determine the effect of stress on particle agglomeration, as shown in Figure 4-3. In the positive displacement pump system, the normalized distributions exhibited greater and wider distributions as compared to the magnetically levitated centrifugal pump system. Furthermore, the mean value of normalized oversize concentrations in the positive displacement pump system was 6 times higher than that of a magnetically levitated centrifugal pump system. The mean

value of normalized number of oversize concentrations was calculated in the particle size range of 0.51 to 1 μm because most oversize particles were generated in this region during slurry delivery. The magnetically levitated centrifugal pump did not increase the normalized oversize particle distribution significantly at 500 turnovers.

The phenomena of stress-induced particle agglomeration can be explained by the Smoluchowski theory [Smo17, Hig82, and Ste05] in which a model is proposed that considers the shear flow and the electrostatic interaction between particles. This model assumes that the particle collisions are binary and proportional to the particle concentration. The aggregation rate of k-fold aggregates, dN_k/dt, is given by the time evolution of the cluster size aggregates, *i* and *j*-fold,

$$\frac{dN_k}{dt} = \frac{1}{2}\sum_{i+j=k}^{l=k-1}(k_{ij}/W_{ij})N_i N_j - N_k\sum_{k=1}^{\infty}(k_{ki}/W_{ki})N_i \qquad [4\text{-}1]$$

$$k_{ij} = \frac{4}{3}G(a_i + a_j) \qquad [4\text{-}2]$$

where the aggregation constant, k_{ij}, is a function of the shear rate (G) and particle size (a). The stability ratio (W) is the ratio of the rapid aggregation rate in the absence of electrostatic interaction to the slow aggregation rate when there are electrostatic interactions between particles. According to this model, during slurry delivery, the shear flow causes particles to approach each other. When the particles are sufficiently close to each other that the attractive Van der Waals force is greater than the repulsive interparticle force, particle agglomeration occurs. The degree of particle agglomeration that occurs is determined by the slurry properties (*e.g.*, interparticle forces), external shear stress (*i.e.*, type of pump), and the number of turnovers of the slurry. In our experiment, the normalized oversize particle distribution was measured from the same slurry at fixed slurry turnovers (500 turnovers). Thus, the magnitude of shear stress induced by pumps can be distinguished by the degree of particle agglomeration. Lower

agglomeration of particles during slurry handling by a magnetically levitated centrifugal pump was because of its contact-free impeller in the pump housing which provided a smooth pulseless flow, whereas the positive displacement pump generated highly localized shear stresses near the wall during the pump stroke, resulting in a significant increase in oversize particles. Thus, the magnetically levitated centrifugal pump is a low shear pumping device.

Characterization of Low-k CMP

The effects of oversize particles present in the slurry on the defectivity during CMP of low-k dielectrics were investigated by analyzing various operating conditions (*e.g.*, turnovers and pump types) and corresponding output parameters (*e.g.*, RMS roughness and defect density) to investigate the correlation between the roughness/defect density and the degree of particle agglomeration. First, low-k and ultra low-k wafers polished by circulated slurries at 1000 turnovers were characterized by optical microscopy at 200× magnification, as shown in Figure 4-4. As ultra low-k wafers exhibited poor mechanical properties (i.e., elastic modulus and hardness) as compared to BD1 wafers, more surface defects were found on polished ultra low-k wafers. In addition, the defect density, determined as the number of defects per square millimeter, was calculated from those images. Figure 4-5 shows the defect densities of BD1 and ultra low k wafers as a function of slurry turnovers. Insignificant increase in defect density with slurry turnover was observed in the case of maglev pump processed slurries due to less agglomerated particles. Consequently, the defect density or surface defects increased with increasing agglomerated particles caused by pumping devices and decreasing with mechanical properties of thin films.

Furthermore, the example of the surface roughness (RMS and R_{max} characterized by contact mode AFM) of polished BD1 wafers as a function of turnovers is shown in Figure 4-6. In the positive displacement pump system (*i.e.*, bellows and diaphragm pumps), the surface

roughness increased with slurry turnover, but the increase was not significant in the magnetically levitated centrifugal pump system. As a result, a positive correlation was observed between the roughness/defect densities and mean value of normalized oversize concentrations, as shown in Figure 4-7. The normalized oversize concentration in this figure was defined as the mean value of normalized oversize concentrations in the particle size range of 0.51 to 1 μm because a large number of oversize particles in this range can cause most surface defectivity during CMP of low-k dielectrics. In both graphs, points closer to and further from the y-axis correspond to slurries circulated by the magnetically levitated centrifugal pump and positive displacement pump, respectively. The maximum defect density was 4.4 (numbers/mm^2) on low-k wafers polished by circulated slurries from the positive displacement pump system, and 1.1 (numbers/mm^2) in the case of the magnetically levitated centrifugal pump system. Consequently, positive displacement pump system caused more particle agglomeration with slurry turnovers, resulting in significant increases in the surface roughness and defect density as compared to the magnetically levitated centrifugal pump system.

Summary

We examined the effects of stress on particle agglomeration occurring in silica slurries circulated by both positive displacement and magnetically levitated centrifugal pumps. Our results indicate that the magnetically levitated centrifugal pump had less effect of stress on particle agglomeration and did not increase the concentration of oversize particles significantly with slurry turnovers. The mean value of normalized oversize concentrations in the positive displacement pump system was 6 times higher than that of a magnetically levitated centrifugal pump system. The roughness/defect density and the degree of agglomeration were found to be positively correlated. In addition, more surface defects were found on polished ultra low-k

wafers because ultra low-k wafers exhibited poor mechanical properties (i.e., elastic modulus and hardness) as compared to BD1 wafers. Consequently, the magnetically levitated centrifugal pump was a low shear device and caused less process-dependent defectivity (e.g., scratches and embedded particles) during CMP of low k dielectrics.

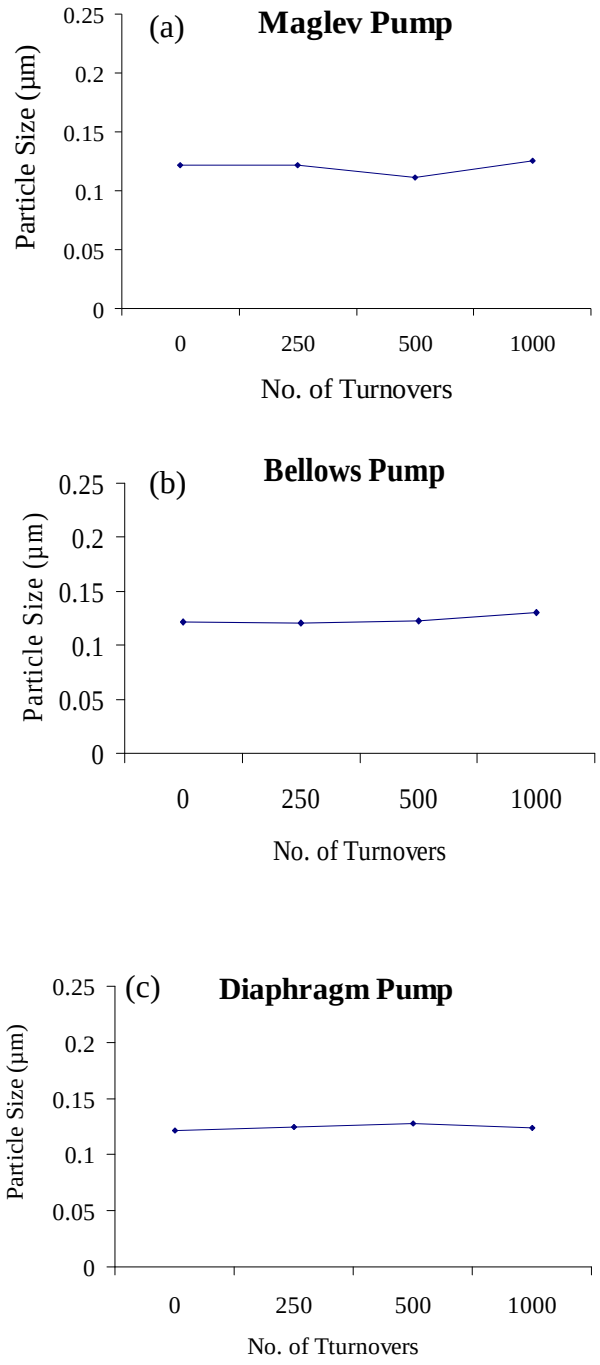

Figure 4-1. Primary particle size as a function of slurry turnovers: low-k slurries circulatedby (a) maglev, (b) bellows, and (c) diaphragm pumps.

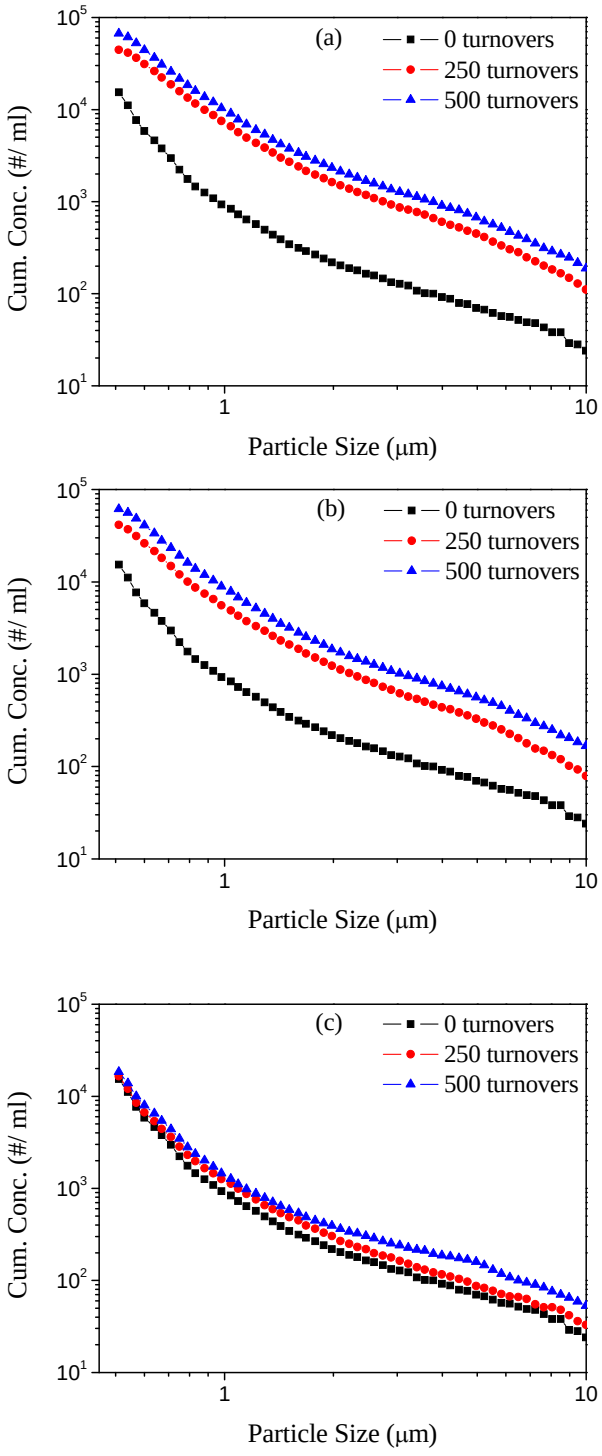

Figure 4-2. Cumulative concentration *vs*. particle size at 0, 250, and 500 turnovers for (a) Bellows, (b) diaphragm, and (c) magnetically levitated centrifugal pump systems. The magnetically levitated centrifugal pump caused less particle agglomeration as the tail portion did not change significantly with increase in the number of slurry turnovers.

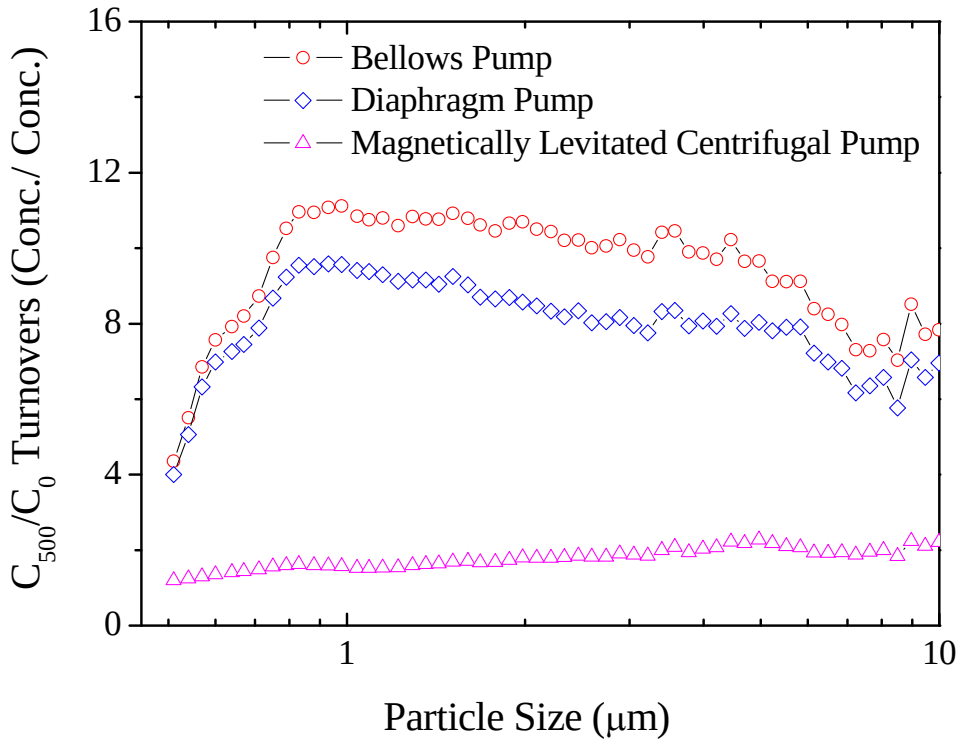

Figure 4-3. Normalized oversize particle distribution for positive displacement and magnetically levitated centrifugal pumps.

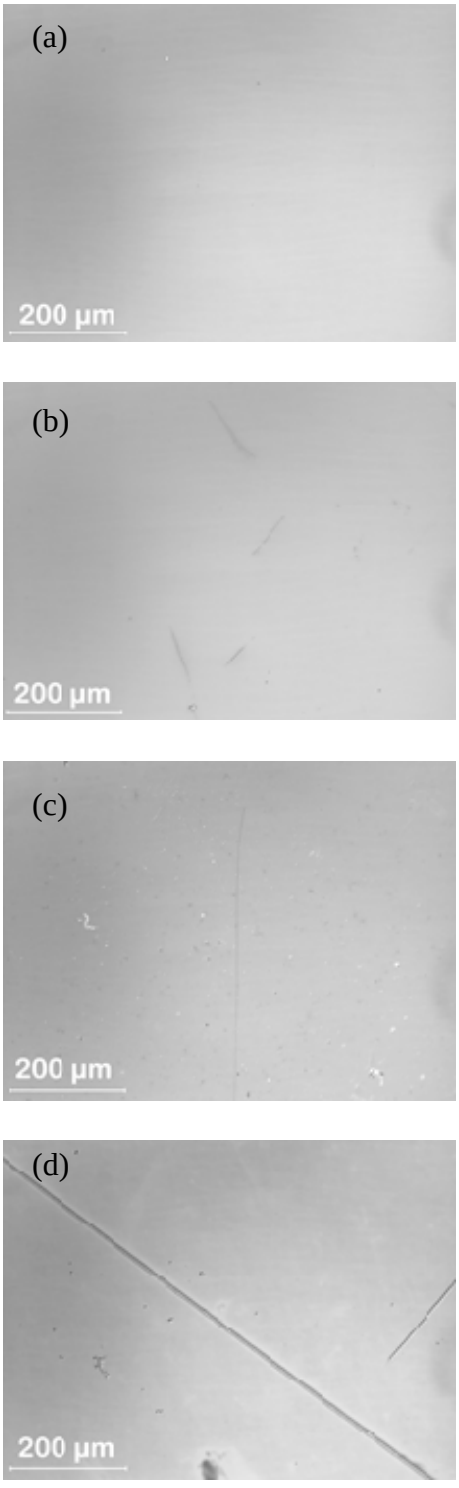

Figure 4-4. Optical images: (a) BD1 and (c) ultra low k wafers polished by maglev pump processed slurries, and (b) BD1 and (d) ultra low k wafers polished by positive displacement pump processed slurries.

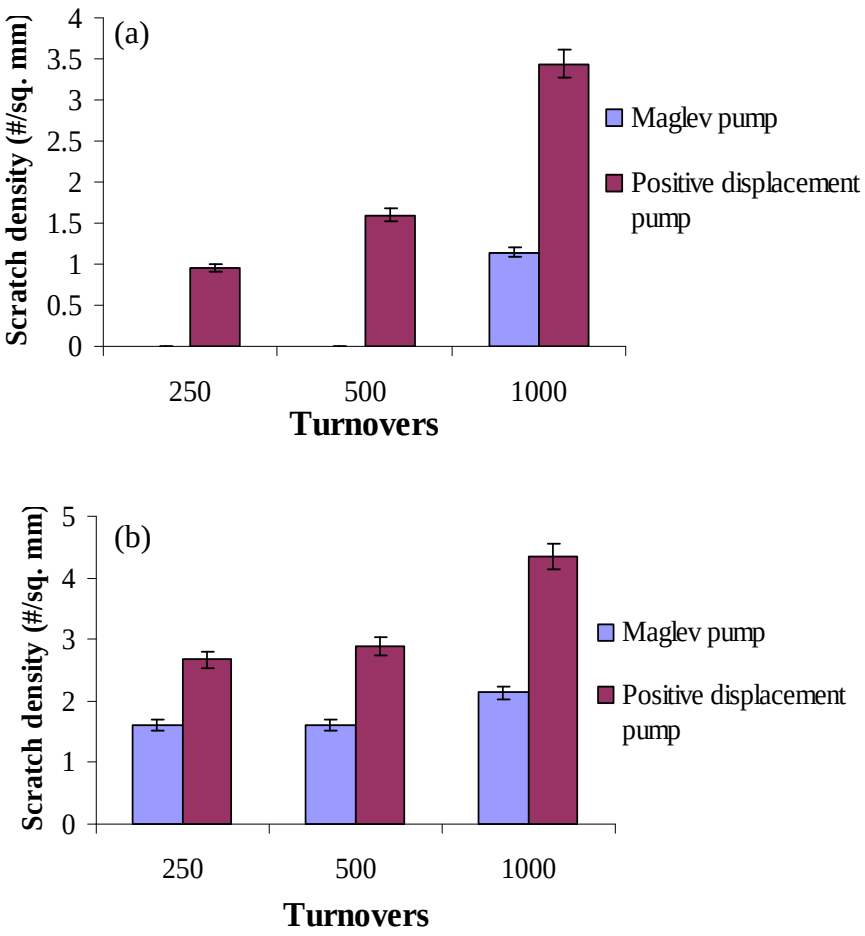

Figure 4-5. Scratch density as a function of turnovers: (a) BD1 wafers and (b) ultra low k wafers.

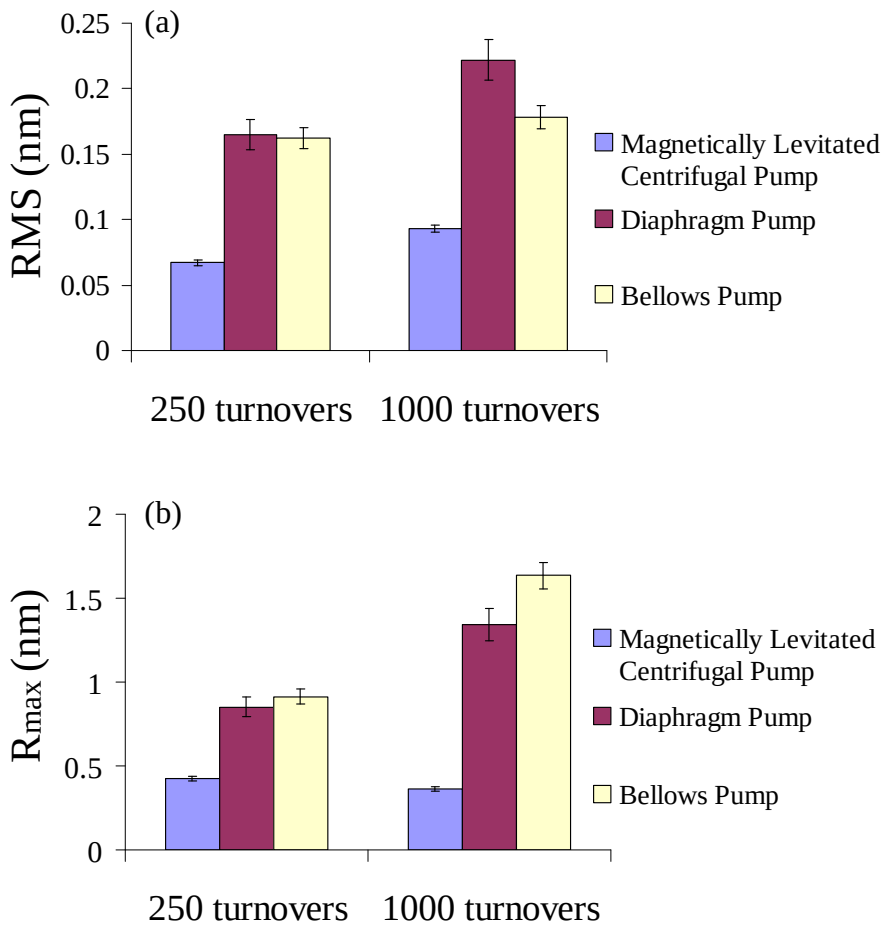

Figure 4-6. Comparison of surface roughness (a) RMS and (b) R_{max} of low-k wafers polished by circulated slurries from diaphragm, bellows, and magnetically levitated centrifugal pumps.

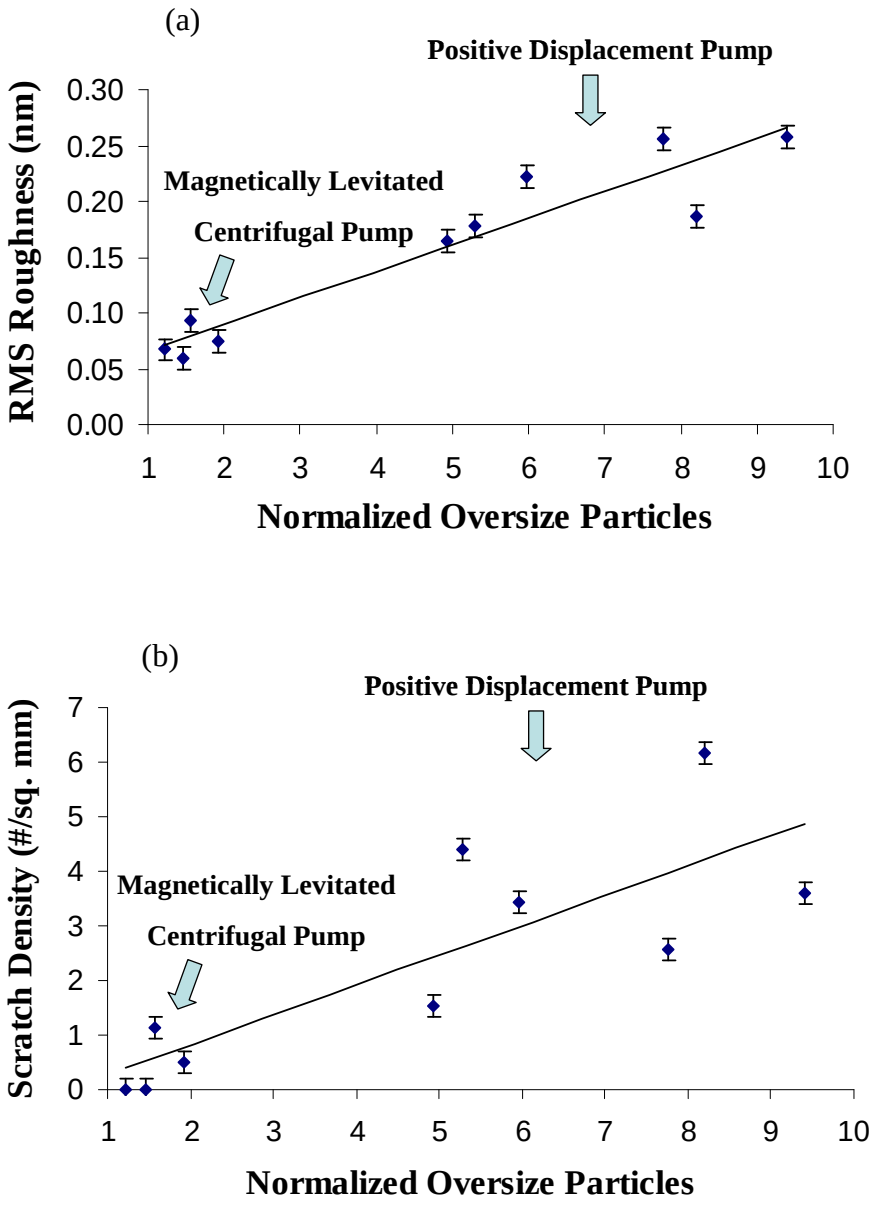

Figure 4-7. Defectivity *vs*. normalized oversize particles. (a) Scratch density *vs*. normalized oversize particles. (b) RMS roughness *vs*. normalized oversize particles.

CHAPTER 5
ROLE OF INTERPARTICLE FORCES DURING PUMP-INDUCED AGGLOMERATION OF CMP SLURRIES

Introduction

With the miniaturization of semiconductor devices, chemical mechanical polishing (CMP) is commonly employed for both the front and back end processing of such devices for local and global planarization. The CMP slurry is a synergistic combination of abrasive particles and chemicals, and is perhaps the most critical consumable in the semiconductor industry as it controls the uniqueness and technical performance of the CMP process [Sin02a and Ste96]. Thus, highly stable particles in chemical mechanical polishing (CMP) slurry play an important role to ensure a superior polishing performance and minimize the process-dependent defectivity.

Stable suspensions in CMP slurry are achieved by overlapping the similar surface charges from the dissociation of the metal oxide groups (M^+OH^-). The degree of slurry stability depends on intrinsic properties of particles and slurry pH. However, abrasive particles (*e.g.*, ceria, silica, and alumina) along with numerous chemicals (e.g., oxidizers, salts, and complexing agents) can deteriorate the stability of abrasive particles and cause surface defectivity during CMP [Sin02b and Bie99]. Typically, the introduction of salt in CMP slurries can increase the polishing rate due to screening the surface charges between abrasive particles and substrate, leading to an increase in friction force during the polishing [Cho04b]. However, slurries containing high ionic strengths can also diminish the repulsive forces between abrasive particles, resulting in a significant increase in agglomerated particles. Basim *et al.* [Bas02] investigated the effect of salt concentration on particle agglomeration and surface quality in silica polishing. They indicate that the abrasive particles tended to agglomerate each other at high salt concentration (NaCl > 0.2 M). These soft agglomerates deteriorated the quality of polished surface during CMP.

To minimize the polishing defectivity, the particle size distribution, especially the tail region representing oversized particles, should be as small as possible and should not increase with time during slurry delivery. Our recent study indicates that some pumping devices in the slurry distribution system may generate high shear stress and cause to a significant increase in agglomerated particles during slurry handling [Cha08]. The phenomenon of pump-induced particle agglomeration can be explained by the Smoluchowski theory of shear aggregation, as listed in Equation 2-17. The degree of particle agglomeration that occurs is determined by the slurry properties (*e.g.*, interparticle forces) and the external shear stress applied on the slurry itself during the slurry handling process.

In our study, formulated slurries were recirculated in the slurry distribution system to examine the slurry stability. The agglomeration of the slurries was found to depend both on the external shear stress and the interparticle forces acting on the slurries. The interparticle forces were determined by means of the interaction forces between silica probe and silica wafer, measured by the colloidal probe technique in the supernatant slurries with varying chemicals.

Experimental

We circulated 30 nm silica slurries (5 wt %) at various pH values (2, 7, and 11), with and without 0.1 M KCl in the slurry distribution system for 1000 turnovers to observe the stress effect on particle agglomeration. The slurry distribution system consisted of a positive displacement pump (*e.g.*, bellows or diaphragm pumps), a 12-foot long tubing distribution loop (Teflon poly-fluoroalkoxy), a slurry tank, a pressure gauge, a flow meter, and a pressurized air supply outlet/inlet. The flow rate of the slurry was held constant at 12 L/min by fixing the gas pressure at 30 psi.

Agglomerated particles in circulated slurries were characterized using the particle size measurement system “AccuSizer 780,” consisting of a single-particle optical sensor (SPOS).

This system can detect particle sizes from 0.51 to 200 μm. To measure the particle sizes, 1 ml of circulated silica slurry was dropped into the solution chamber and diluted with deionized water to prevent slurry re-agglomeration. The single oversize particle was detected by the photozone, a narrow laser diode, and the cumulative oversize particle tail was obtained after measurements had been taken. Furthermore, the surface potential of silica particles was characterized by zeta potential (Brookhaven ZetaPlus), measuring the velocity of charged particles at shear plane in the solution.

The interparticle force measurement can be achieved by means of the colloidal probe technique using the atomic force microscope (AFM). Ducker *et al.*[Duc91 and Duc92] and Butt *et al.*[But91 and Kap02] first used colloidal probe technique to measure directly interaction forces between colloidal probe and sample surface. In this experiment, a 5 μm spherical silica particle from Bangs Laboratories Inc. was attached to the end of cantilever using epoxy resins and the micromanipulator under the control of an optical microscope. Figure 5-1 shows the scanning electron microscope (SEM) image of 5 μm spherical silica particle glued on the top of the AFM tip. This experiment was performed with the wet cell arrangement by AFM force measurement in the supernatant slurries at various pH values (2, 7, and 11), with and without 0.1 M KCl. The surface forces were measured by the cantilever deflection as a function of the distance between silica probe and plate surface. The plate used was silica wafer deposited by a plasma-enhanced chemical vapor deposition (PECVD) technique. The definition of zeros of both force and tip-substrate separation is necessary to analyze deflection data. The zero of force was chosen where the deflection was constant, and the zero of tip-substrate separation was defined as the region of constant compliance. The surface force was calculated by multiplying the tip deflection with the spring constant (0.58 N/m) of the cantilever.

Subsequently, circulated silica slurries (30nm) were used to polish 1-inch square BD1 low-kwafers in a Struers RotoPol-31 Table Top Polisher with a down pressure of 3 psi, polishing time of 1 min, slurry flow rate of 100 ml/min, and rotation speed of 150 rpm. The surface roughness of polished low-k wafers was characterized using a Digital Instruments Nanoscope III atomic force microscope (AFM).

Results and Discussion

To investigate the stability of formulated slurries, 30nm silica slurries (5 wt%) at pH 2, 7, and 11, with and without 0.1 M KCl, were circulated in the slurry distribution system for 1000 turnovers. Figure 5-2 shows the cumulative distribution curves of oversize particles in silica slurries obtained by cumulatively summing the number of particles above a certain size from 10 to 0.51 μm. The cumulative concentrations of oversize particles increased rapidly as pH values decreased, as shown in Figure 5-2(a). The particle concentrations at 0.51 μm were 95,717, 59,577, and 45,373 (particles/ml) at pH 2, 7, and 11, respectively. The introduction of salt in silica slurries further accelerated slurry agglomeration at all pH values, as shown in Figure 5-2(b). The particle concentrations at 0.51 μm were 118,457, 69,811, and 54,150 (particles/ml) at pH 2, 7, and 11 with 0.1 M KCl, respectively. In addition, the mean value of normalized oversize particle distributions, defined as the ratio of cumulative concentrations at 1000 slurry turnovers to 0 slurry turnovers in the particle size range of 0.51 to 1 μm, can clearly determine the effect of pump-induced particle agglomeration, as shown in Figure 5-2(c). We found the mean values of normalized oversize concentrations at pH 2, 7, and 11 to be 4.5, 2.6, and 2.1 times higher than those of as-received slurries. In the case of salt addition, the mean values of normalized oversize concentrations at pH 2, 7, and 11 with 0.1 M KCl were 6.6, 3.9, and 3.3 times higher. These

results indicate that silica slurries at acidic pH, and with salt addition, were unstable, resulting in a significant increase in agglomerated particles during the handling process.

The agglomeration of the slurries was found to depend both on the external shear stress acting on the slurries and the stability of colloidal particles, expressed from Equation 2-17. The stability ratio (W) is a criterion for slurry stability and dependent on the total electrostatic interaction (V_{total}) at a particle separation distance (d), can be expressed as

$$W = 2\int_0^{\infty} \frac{\exp\left(V_{total} / KT\right)}{\left(u+2\right)^2} du \qquad [5\text{-}1]$$

where u is equal to d/a for same particle size (a), K is the Boltzmann's constant, and T is temperature [Eli98]. Based on Derjaguin-Landau-Verwey- Overbeek (DLVO) theory, the total electrostatic interaction, a sum of repulsive electrical double layer potential (V_r) and attractive Van der Waals potential (V_a), provides a potential barrier to prevent particle agglomeration [Hun01]. However, some pumping devices may generate high shear stress that causes particles to approach each other. When the particles are sufficiently close to each other that the attractive Van der Waals force ($\partial V_a/\partial d$) is greater than the repulsive interparticle force ($\partial V_r/\partial d$), particle agglomeration occurs. Thus, the repulsive interparticle forces play an important role to stabilize the colloidal particles. The strength of repulsive interparticle forces can be controlled by varying chemicals (*e.g.,* pH and salt) and colloidal particles (*e.g.,* ceria and silica).

Based on Derjaguin approximation, the force of sphere-sphere ($F_{s\text{-}s}$) is half the value for sphere-plate interaction forces ($F_{s\text{-}p}$) [Isr91]. Thus, the interparticle force is determined by means of the interaction forces between a silica probe and a silica wafer measured by the colloidal probe technique in the supernatant slurries. The normalized interaction force (F/R) as a function of separation distance between the silica probe and the silica wafer in supernatant slurries at various pH values, with and without salt addition (0.1 M KCl), was shown in Figure 5-3. When

the silica probe was far away from the silica wafer (separation distance > 25 nm), no interaction force was observed from all supernatant slurries. As the separation distance consecutively decreased, the cantilever bent upward due to repulsive surface forces, generated by overlapping the electrical double layers between the silica probe and the silica substrate. Afterwards, when the silica probe approached to the silica wafer at a certain interactive distance, the silica probe suddenly jumped onto the substrate (jump-in) because the gradient of attractive Van der Waals force exceeded the gradient of repulsive surface force plus the spring constant of the cantilever, and the normalized repulsive forces became vertical at this contact region, defined as zero of separation distance. As the isoelectric point (IEP) of silica is around pH 2, the increase of the slurry pH raised a repulsive surface force due to increasing negative charges ($-SiO^-$) on silica surface [Par65]. The maximum normalized repulsive interaction forces in supernatant slurries at pH 2, 7, and 11 were 0.66, 1.0, and 1.82 (mN/m), respectively. However, smaller repulsive interaction forces were observed from all supernatant slurries with adding 0.1 M KCl because of the screening effect. The maximum normalized repulsive interaction forces at pH 2, 7, and 11 with 0.1 M KCl were 0.33, 0.79, and 1.49 (mN/m), respectively. Consequently, alkaline silica slurries without salt addition exhibited larger repulsive interaction forces between silica surfaces.

In addition, the screening effect caused by the salt addition in silica slurries can also be proved by zeta potential measurement, as shown in Figure 5-4. The zeta potentials of silica slurries at pH 2, 7, and 11 were -3.5, -33, and -39.6 (mV), respectively. In the case of salt addition, smaller surface potentials were observed. The zeta potentials of silica slurries at pH 2, 7, and 11 with 0.1 M KCl were -0.45, -27.8, and -34.5 (mV), respectively.

Based on experimental results, excellent correlations were established between the repulsive interaction forces and the mean values of normalized oversize particles as a function of

pH, with and without 0.1 M KCl, as shown in Figure 5-5. The increase in slurry pH raised a repulsive interaction force and corresponded to a considerable decrease in agglomerated particles during the handling process. Silica slurries at pH 11 without salt addition exhibited the largest repulsive interaction forces and the smallest mean values of oversize particles. The addition of salt in silica slurries further reduced the repulsive interaction forces and caused more agglomerated particles during slurry handling. These results can prove that interparticle forces in colloidal suspension play an important role to prevent process-induced particle agglomeration.

In addition, agglomerated particles in slurries may increase the mechanical stress that leads to increase surface defectivity during the low k polishing. Circulated silica slurries (5wt% 30nm) at varying pH and salt addition were used to polish low k wafers. Figure 5-6 show the surface roughness (i.e., RMS and R_{max}) as a function of slurry pH and the AFM images of polished low k wafers at pH 2, 7, and 11. Our results indicate that larger surface roughness and more surface defectivity (e.g., micro-scratches) were found in low k wafers polished by circulated silica slurries at acidic and neutral pH, with and without salt addition because lower interparticle forces between silica particles caused more agglomerated particles during the handling process. The maximum surface roughness (RMS = 1.47nm, Rmax = 35.96nm) was found at silica slurry at pH 2 with 0.1 M KCl; whereas less surface defectivity and minimum surface roughness (RMS = 0.79nm, Rmax = 13.01nm) was observed at silica slurry at pH 11.

Summary

Our results indicate that silica slurries at acidic pH, and with salt addition, tended to agglomerate more oversize particles during the handling process. The agglomeration of the slurries was dependent both on the external shear stress acting on the slurries and interparticle forces in a colloidal suspension. The interparticle forces were determined by means of the interaction forces between a silica probe and a silica wafer measured by the colloidal probe

technique in the supernatant slurries with varying chemicals. Larger repulsive interaction forces were found in alkaline silica slurries. However, the addition of salt in silica slurries reduced the strength of repulsive interaction forces because of the screening effect. As a result, excellent correlations were established between the repulsive interaction forces and the mean values of normalized oversize particles. The increase in slurry pH raised a repulsive interparticle force to defend against shear flow, resulting in less agglomerated particles during slurry handling. Least particle-induced defectivity was observed on polished low k wafers, utilized highly alkali slurries. Thus, alkaline silica slurries would be the best condition for robust slurries to minimize the process-induced particle agglomeration and surface defectivity during CMP of metals and dielectrics.

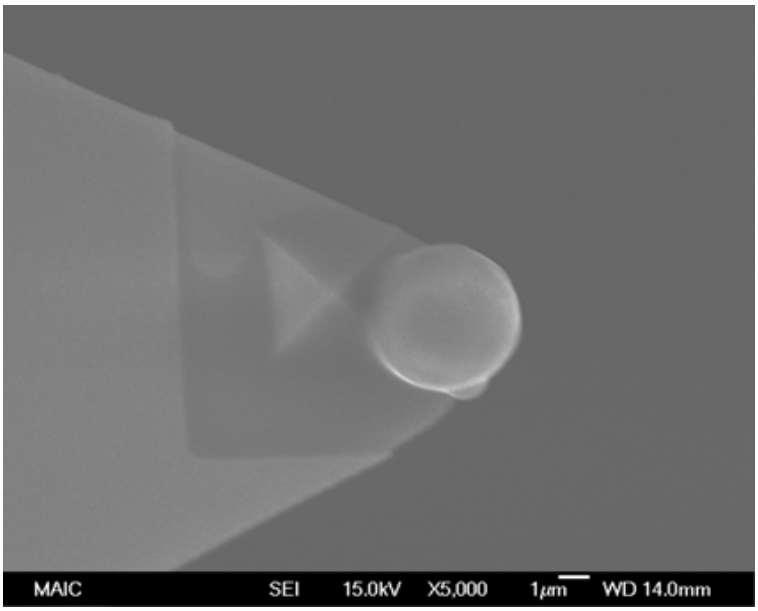

Figure 5-1. SEM image of 5μm silica probe.

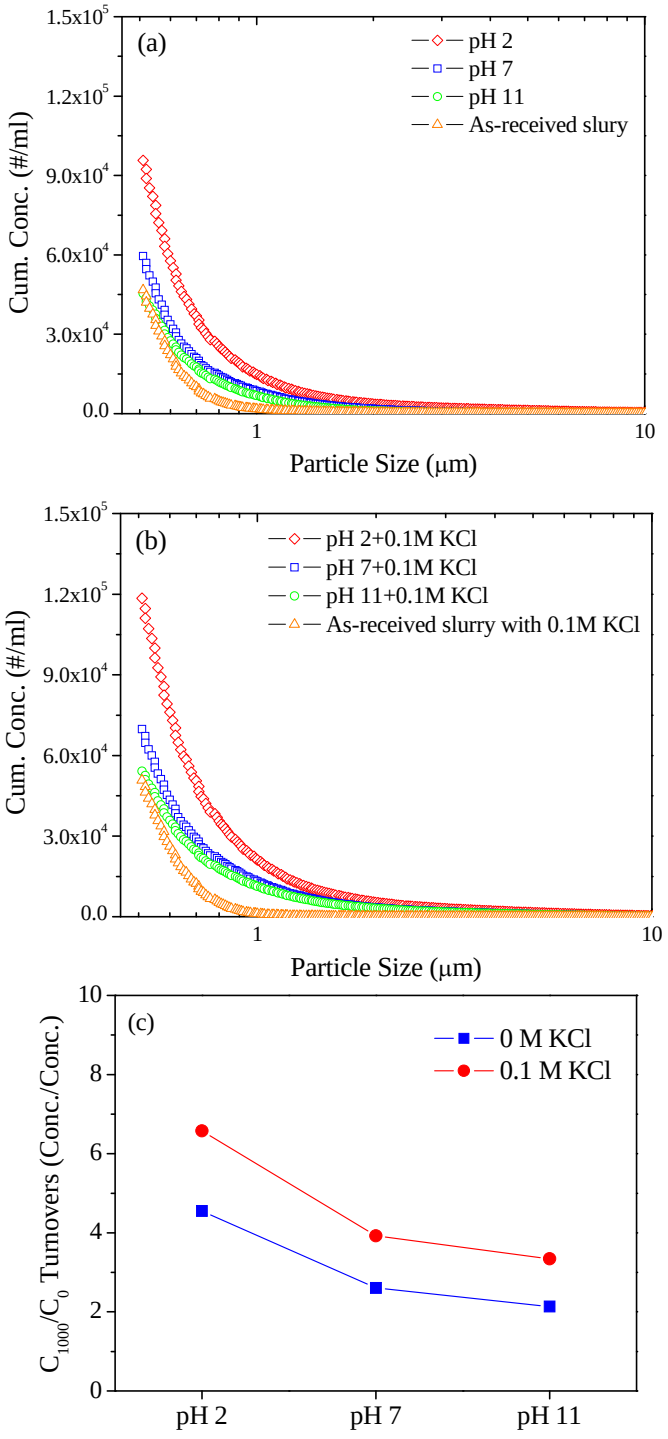

Figure 5-2. Circulated silica slurries for 1000 turnovers at pH 2, 7, and 11: (a) cumulative concentration without salt, (b) cumulative concentration with 0.1 M KCl, and (c) the mean value of normalized oversize particles in the particle size range of 0.51 to 1 μm.

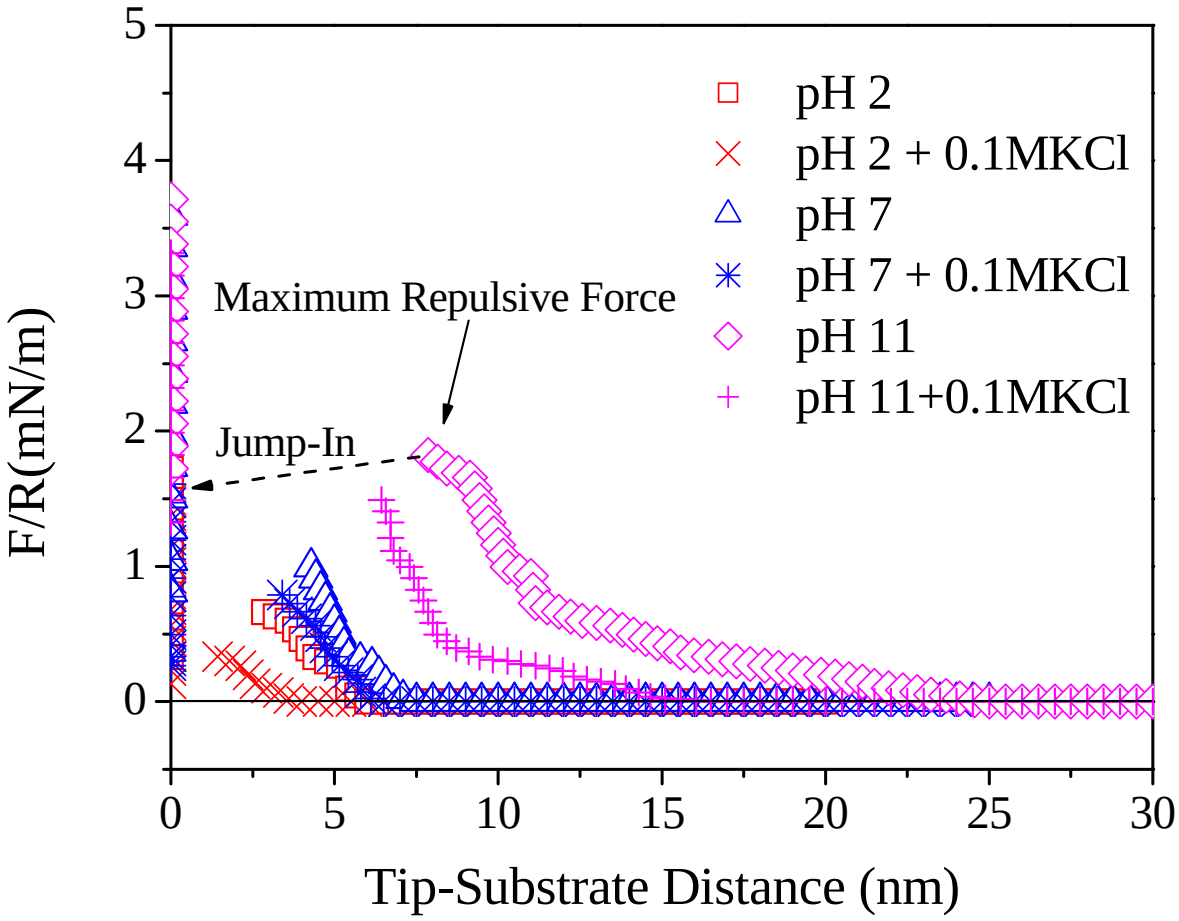

Figure 5-3. Force versus distance between a silica substrate and silica probe in supernatant slurries at pH 2, 7, and 11, with and without 0.1 M KCl.

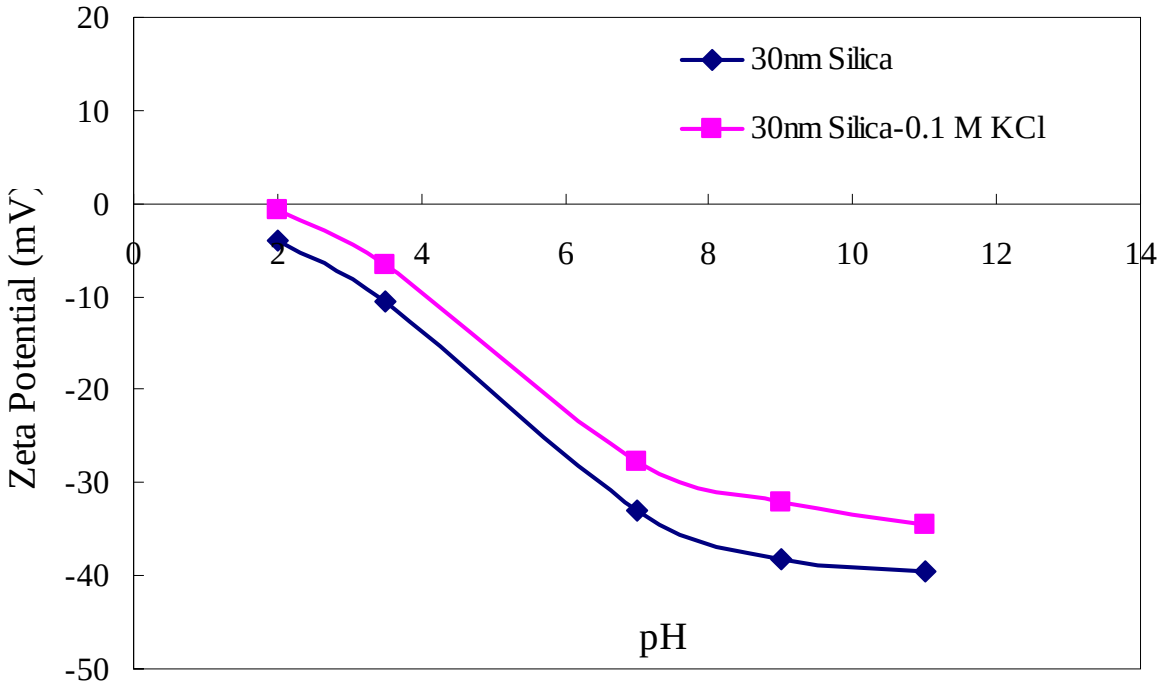

Figure 5-4. Zeta potential of 30 nm silica slurries as a function of pH, with and without 0.1 M KCl.

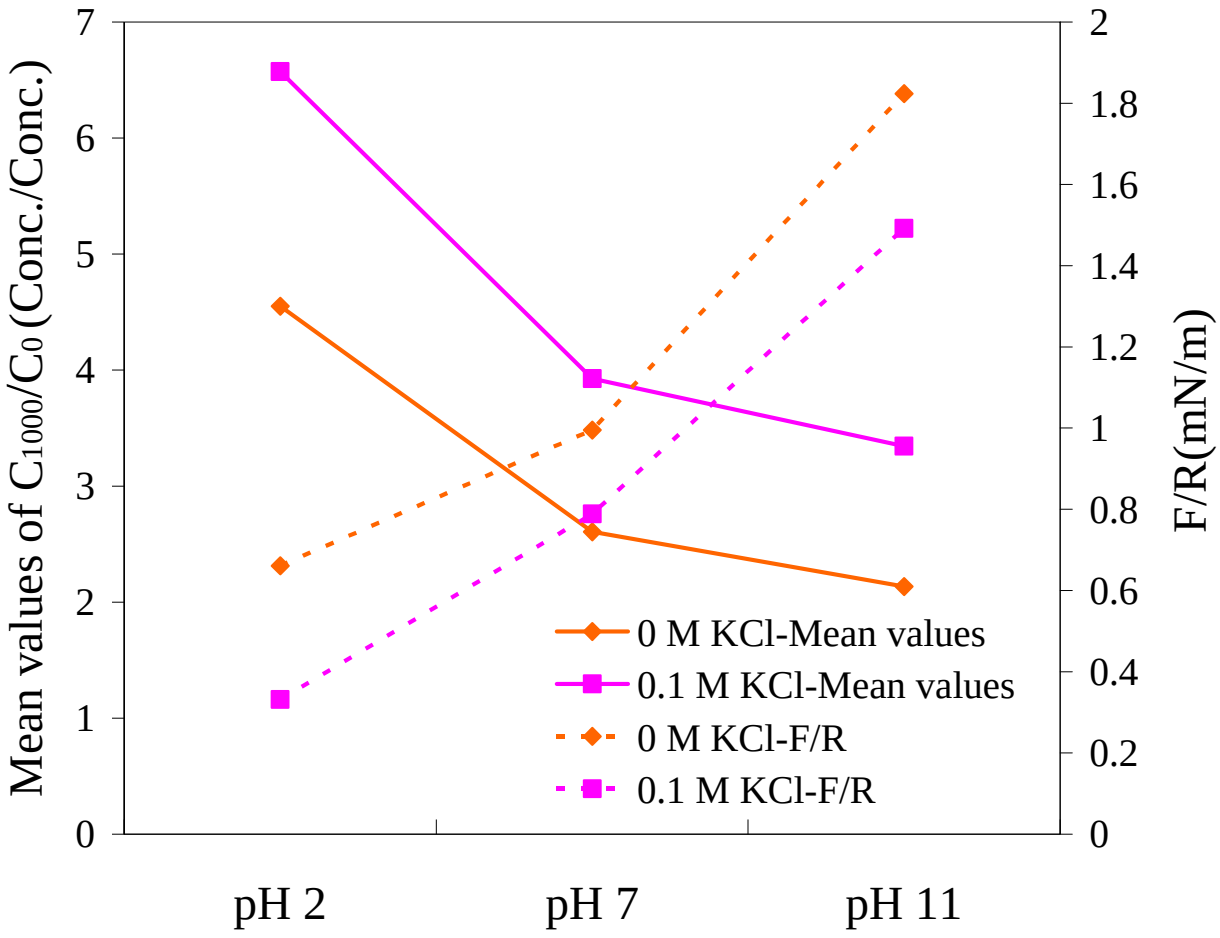

Figure 5-5. Correlations between repulsive interaction forces and mean values of normalized oversize particles as a function of pH, with and without 0.1 M KCl.

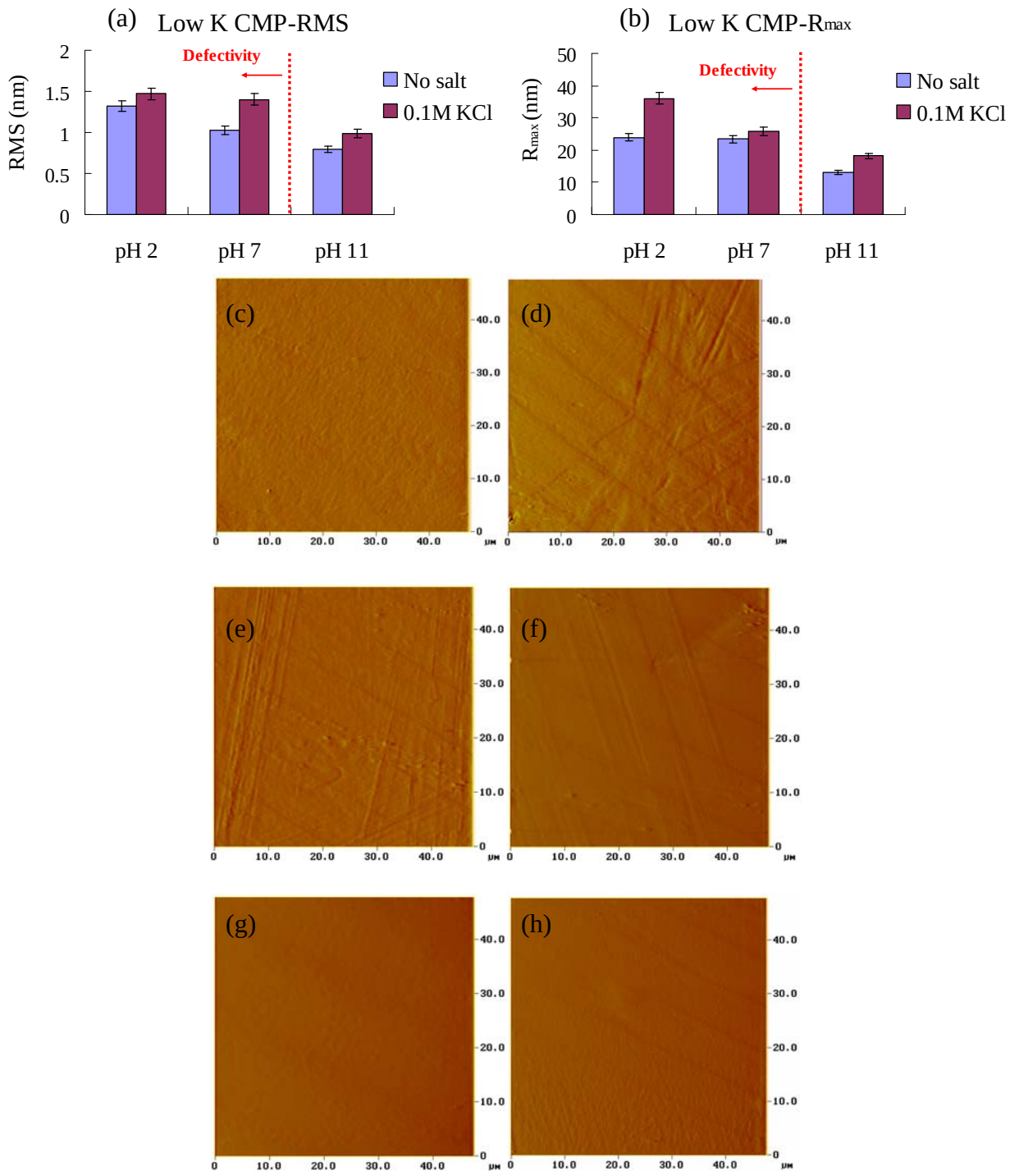

Figure 5-6. Surface roughness as a function of pH: (a) RMS and (b) Rmax, and AFM images of low k wafers polished by circulated silica slurries at (c) pH 2, (d) pH 2 with 0.1M KCl, (e) pH 7, (f) pH 7 with 0.1M KCl, (g) pH 11, and (h) pH 11 with 0.1M KCl.

CHAPTER 6
ROLE OF SLURRY CHEMISTRY ON STRESS-INDUCED AGGLOMERATION

Introduction

The presence of colloidal dispersions is thermodynamically disfavored due to large surface area of colloidal particles and particle collisions (Brownian motion). If a lack of potential barriers between colloidal dispersions, particles have a tendency to agglomerate during the storage and the slurry blending. Thus, electrostatic and polymeric stabilization are commonly employed for stabilizing abrasive particles in CMP slurries.

Palla *et al.* [Pal 99 and Pal02] studied the effect of the surfactant addition on the stability of alumina slurry with oxidizer agent. Typically, oxidizer can form a passive layer on tungsten surface to prevent underlying tungsten substrate from corrosion. However, with adding 0.1 M potassium ferricyanide to alumina slurry, particles were agglomerated and settled because of numerous counter-ions shielding surface charges on the particles. On the other hand, the addition of a mixture surfactant (nonionic and anionic surfactants) into the slurry can efficiently stabilize alumina particles because anionic surfactants were attracted by charge surface of alumina particles and nonionic surfactants penetrated into anionic surfactant layers due to hydrocarbon chain interactions. The polishing results in tungsten CMP indicate that the addition of a mixture surfactant in alumina slurry can reduce surface roughness and particle residues during W CMP [Bie99]. In addition, Hackley [Hac97] demonstrated the role of polymer dispersant in the dispersion of silicon nitride particles. The polyacrylic acid (PAA) formed a protective film onto the surfaces of silicon nitride particles, resulting in a wide pH range of the colloidal stabilization due to shifting the isoelectric points of silicon nitride particles induced by the ionization of PAA. Thus, the addition of polymer surfactants in the absence or presence charge effects can form protective barriers to stabilize colloidal suspensions.

In our study, formulated and un-formulated ceria and silica slurries were subjected to high shear forces and then measured the particle agglomeration characteristic of their tail distribution to investigate the effect of surfactants on the slurry stability. The slurry stability was investigated from the polishing performance.

Experimental

During the slurry handling, some pumping devices in a slurry distribution system may generate high shear flow and cause to agglomerate particles in the tail distribution of oversize particles. In this study, as-received and formulated slurries were used to circulate in the slurry distribution system, utilized by high shear pumping device (e.g., positive displacement pump), to examine the slurry stability. The slurries used for shear testing included different types of particles (e.g., ceria and silica) and surfactants (e.g., anionic, nonionic, and cationic surfactants).

The primary particle size and size distribution were measured by the dynamic light scattering technique, Nanotrac® from Microtrac Inc., can quickly and accurately measure the particle size in the range of 0.8 nm to 6.5 μm. In addition, the tail distribution of oversize particles in circulated slurries can be characterized using the particle size measurement system "AccuSizer 780," consisting of a single-particle optical sensor (SPOS). This system can detect particle sizes from 0.51 to 200 μm. To measure the particle sizes, 1 ml of circulated silica slurry was dropped into the solution chamber and diluted with deionized water to prevent slurry re-agglomeration. The single oversize particle was detected by the photozone, a narrow laser diode, and the cumulative oversize particle tail was obtained after measurements had been taken.

The surface potentials of abrasive particles were characterized by zeta potential, ZetaPlus from Brookhaven Instruments Corporation, utilizing an electrophoresis method to measure the

electrophoretic velocity of colloidal particles. In this experiment, the Smoluchowski model was applied to measure the zeta potentials of CMP slurries.

Results and Discussion

Typically, to obtain high removal rates of dielectric substrates, the ceria slurry was taken near its isoelectric point (IEP) (*i.e.*, pH 6~7), and silica slurry was at alkaline solutions (i.e., pH 9~11). Thus, un-formulated ceria slurry at pH 6 and silica slurry at pH 9 were circulated in the slurry distribution system for 1000 turnovers to determine the stability of ceria and silica slurries. Figure 6-1 shows the normalized distribution curves of oversize particles, defined as the ratio of cumulative particle concentrations at 1000 turnovers to 0 turnovers. A significant increase in oversize particle distribution was found in ceria slurry as compared to silica slurry. This phenomenon can be demonstrated by measuring the surface potential. Figure 6-2 shows the zeta potentials of un-formulated ceria and silica slurries as a function of slurry pH. The zeta potentials of ceria slurry at pH 6 and silica slurry at pH 9 were 0.41 (mV) and -46.4 (mV), respectively. A weakly repulsive electrostatic interaction between ceria particles caused to a significant increase in particle agglomeration under the external shear stress applied on slurry itself.

To improve the stability of CMP slurries, varying surfactants (e.g., anionic and cationic surfactants) were introduced into ceria and silica slurries for providing the polymer stabilization. Figure 6-3 shows the zeta potentials of formulated ceria slurries as a function of pH. The addition of anionic ionic surfactant (sodium dodecyl sulfate) and polymer dispersant (PAA) to ceria slurry can shift the IEP of ceria to more acidic pH due to lots of negative charges adsorbed onto ceria surface. On the other hand, the addition of cationic surfactants, decyltrimethyl-ammonium bromide (C_{10}TAB) and tetramethylammonium hydroxide (TMAH), can shift the IEP to more alkaline pH due to the positive charges of hydrophilic heads. A comparison of normalized tail distributions between the circulation of formulated (cationic surfactant) and un-

formulated ceria slurries at pH 6 is shown in Figure 6-4. The formulated ceria slurry can significantly minimize the magnitude of stress-induced particle agglomeration during the handling process because the adsorption of cationic surfactant onto ceria surfaces provided the stronger repulsive electrostatic interaction between ceria particles as compared to un-formulated ceria slurry (Figure 6-5).

Furthermore, the effect of surfactant addition on the stability of silica slurries was measured by dynamic light scattering and SPOS. Figure 6-6 shows the primary particle size distribution of 80nm silica slurries with cationic (CTAB) and anionic surfactants (SDS) at pH 9. The addition of cationic surfactant can neutralize the charges on silica surface that can reduce the magnitude of repulsive forces between silica. The agglomeration behavior was found during the slurry formulation and the handling process. However, an insignificant change in particle size distribution was observed in silica slurries with anionic surfactant. Furthermore, the magnitude of stress-induced particle agglomeration can be clearly determined by the normalized tail distribution of oversize particles, as shown in Figure 6-7. The addition of anionic surfactant into silica slurry can provide the stronger electrostatic interactions between silica particles to defend against shear stress during slurry handling. The magnitude of surface charges was observed by zeta potential (Figure 6-8). Consequently, alkaline silica slurry with SDS (anionic) surfactant exhibited better slurry stability due to increasing the strength of the electrical double layer.

In addition, the stability of un-formulated and formulated slurries can be investigated by the polishing performance. For example, Figure 6-9 shows the surface roughness and AFM images of silica wafers polished by un-formulated and formulated ceria slurries at pH 6. Silica wafers polished by un-formulated ceria slurries showed a smooth surface and low surface roughness (RMS = 2.06 nm and R_{max}= 10.6 nm), as shown in Figure 6-9(c). However, higher

surface roughness (RMS = 10.3 nm and R_{max}= 272 nm) and deep micro-scratch were observed on silica wafers polished by un-formulated ceria slurries circulated for 1000 turnovers because high shear stress generated by pumping device can significantly increase agglomerated particles during the handling process, as shown in Figure 6-9(e). Conversely, the addition of cationic surfactant into ceria slurry can provide a stronger potential barrier to defend against shear stress and significantly reduce the magnitude of stress-induced particle agglomeration, as shown in Figure 6-4. Thus, a small increase in surface roughness (RMS = 2.18 nm and R_{max}= 40.8 nm) was found in formulated ceria slurry circulated for 1000 turnovers, as shown in Figure 6-9(d).

Summary

Highly stable slurry plays an important role to minimize the process-induced particle agglomeration and ensure a superior polishing performance. The stability of slurry can be obtained by adding surfactants (e.g., anionic and cationic surfactants) to provide the polymer stabilization between particles. In this study, the stability of un-formulated and formulated ceria and silica slurries was determined by their primary particle size distribution and oversize distribution. As the ceria slurry near its isoelectric point (IEP = 6~7) exhibited the amphoteric properties, the addition of anionic and cationic surfactants into ceria slurries at pH 6 can provide a stronger potential barrier to defend against the stress-induced particle agglomeration, resulting in the minimization of surface defectivity during CMP of dielectric materials. However, the addition of cationic surfactant into silica slurries deteriorated the stability and caused more agglomerates during the handling due to neutralizing the surface charges.

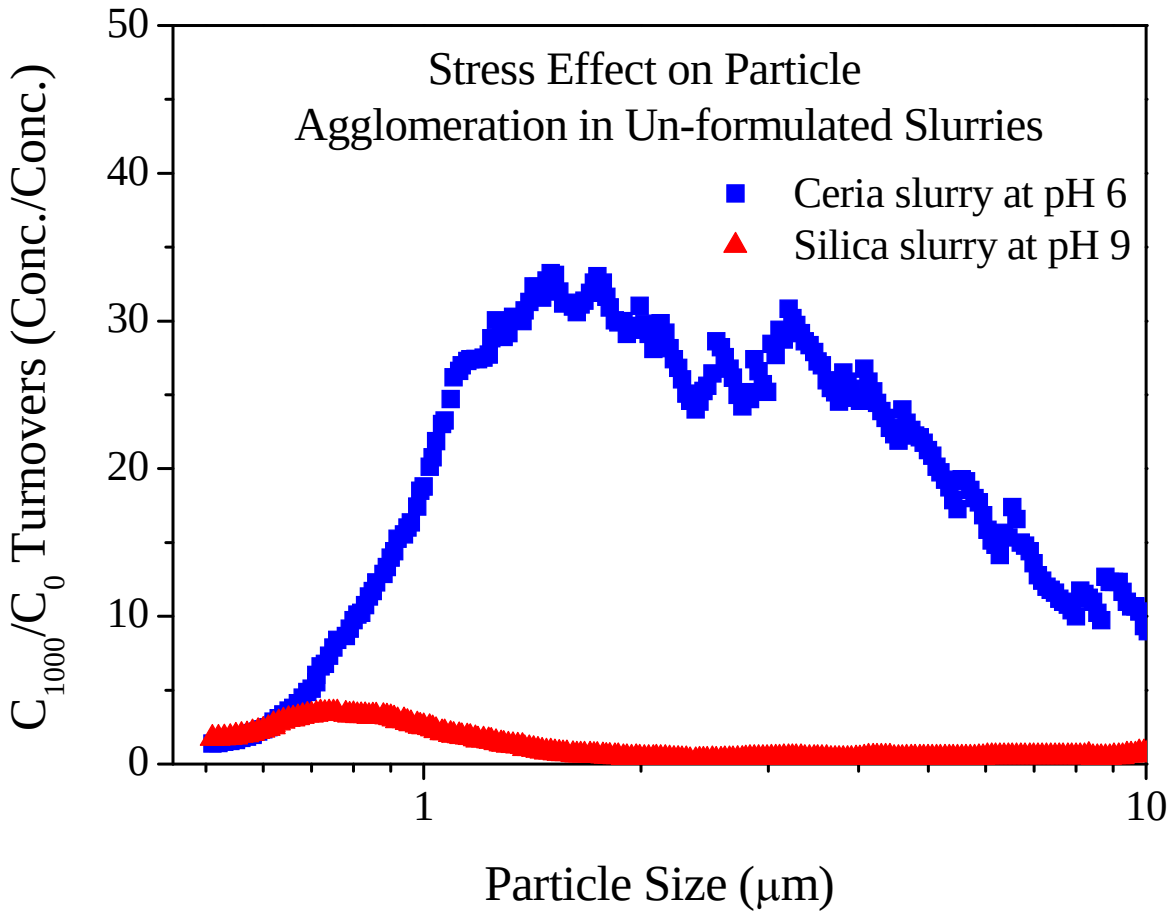

Figure 6-1. Effects of stress-induced particle agglomeration in un-formulated ceria and silica slurries.

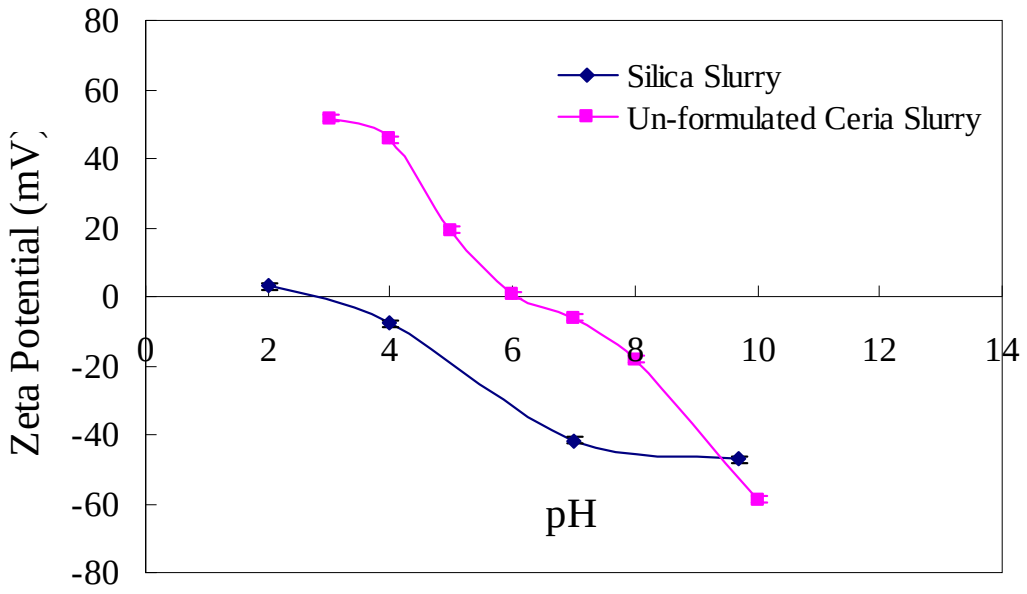

Figure 6-2. Plot of zeta potential vs. pH: the potential curves of un-formulated silica and ceria slurries.

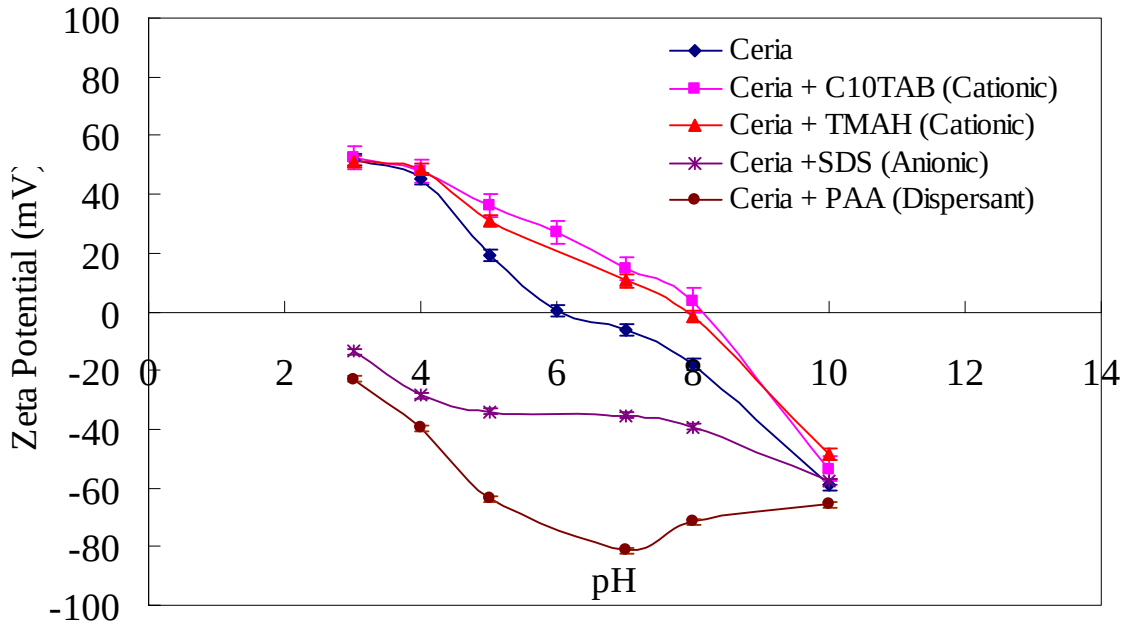

Figure 6-3. Plot of zeta potential vs. pH: the potential curves of formulated ceria slurries with varying surfactants.

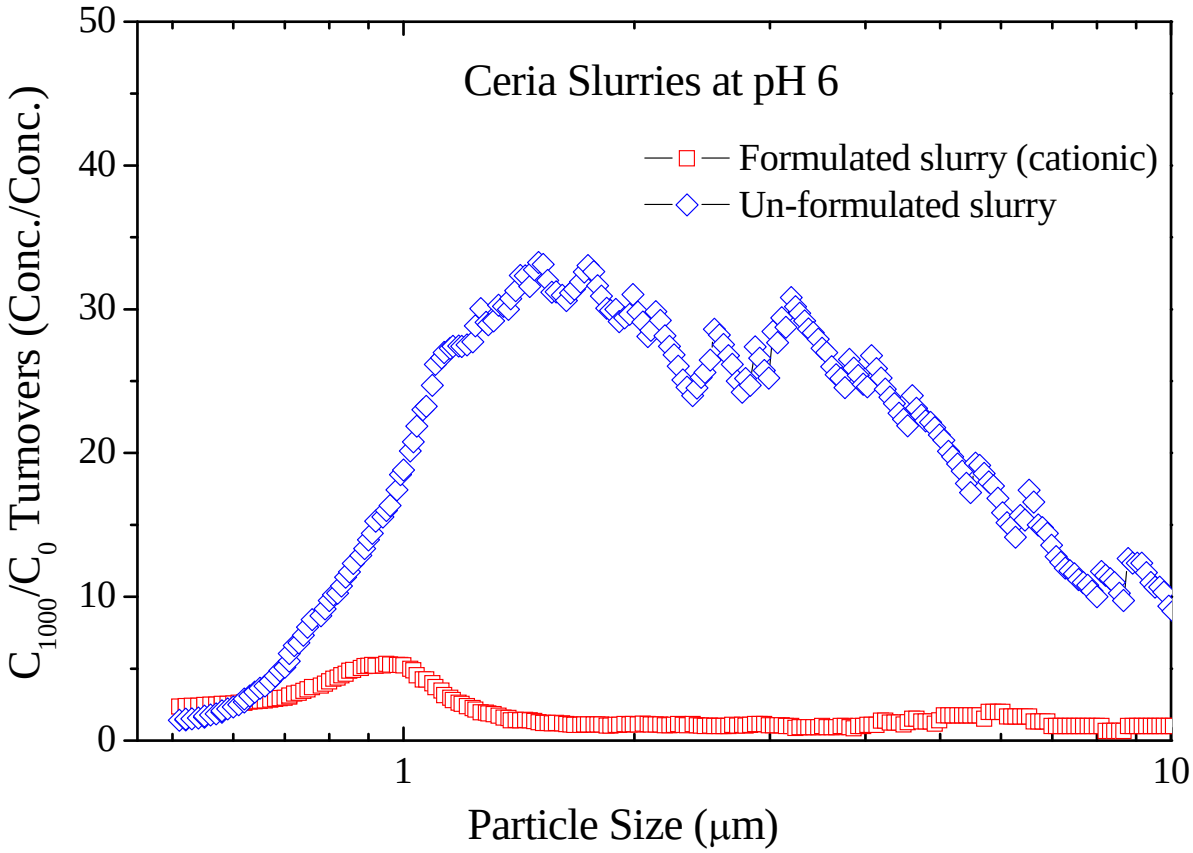

Figure 6-4. Comparison of particle agglomeration in formulated and un-formulated ceria slurries due to stress effect.

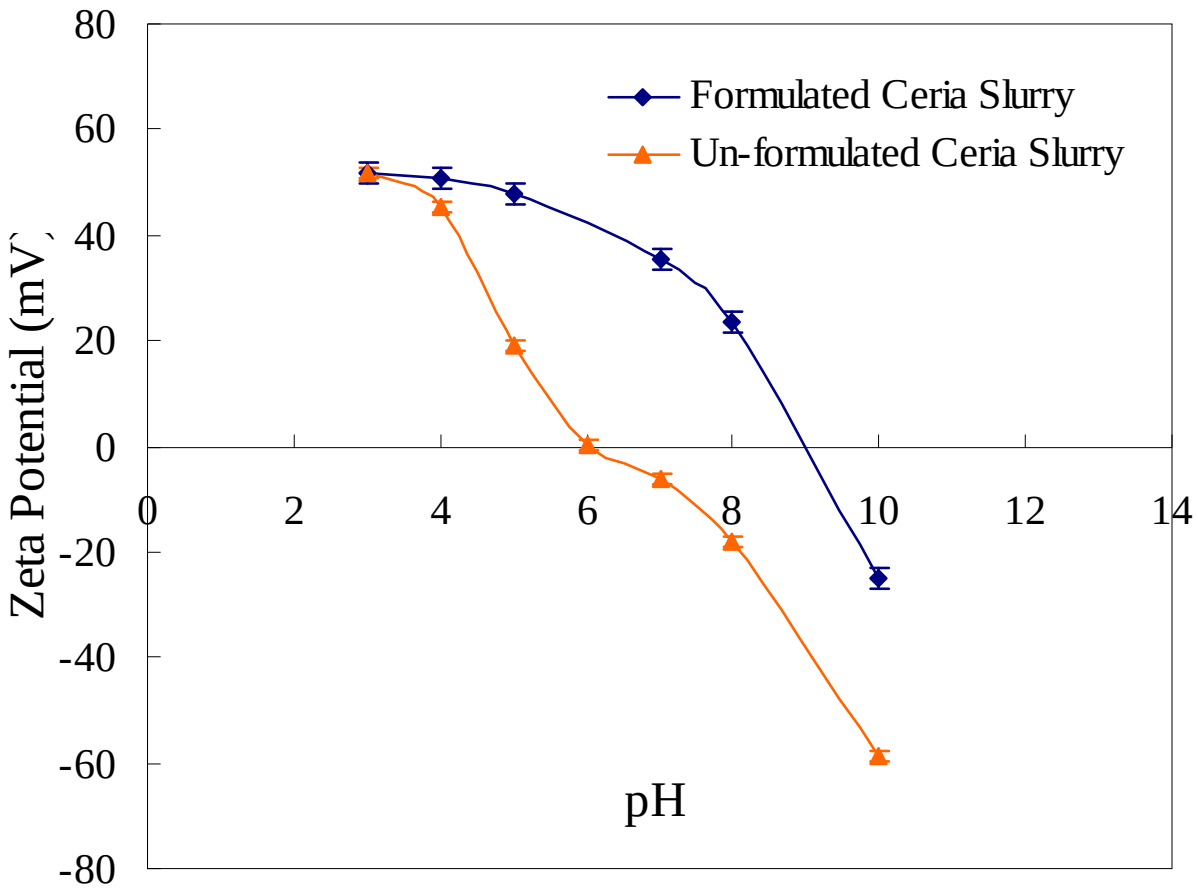

Figure 6-5. Plot of zeta potential vs. pH in ceria slurry with cationic surfactant.

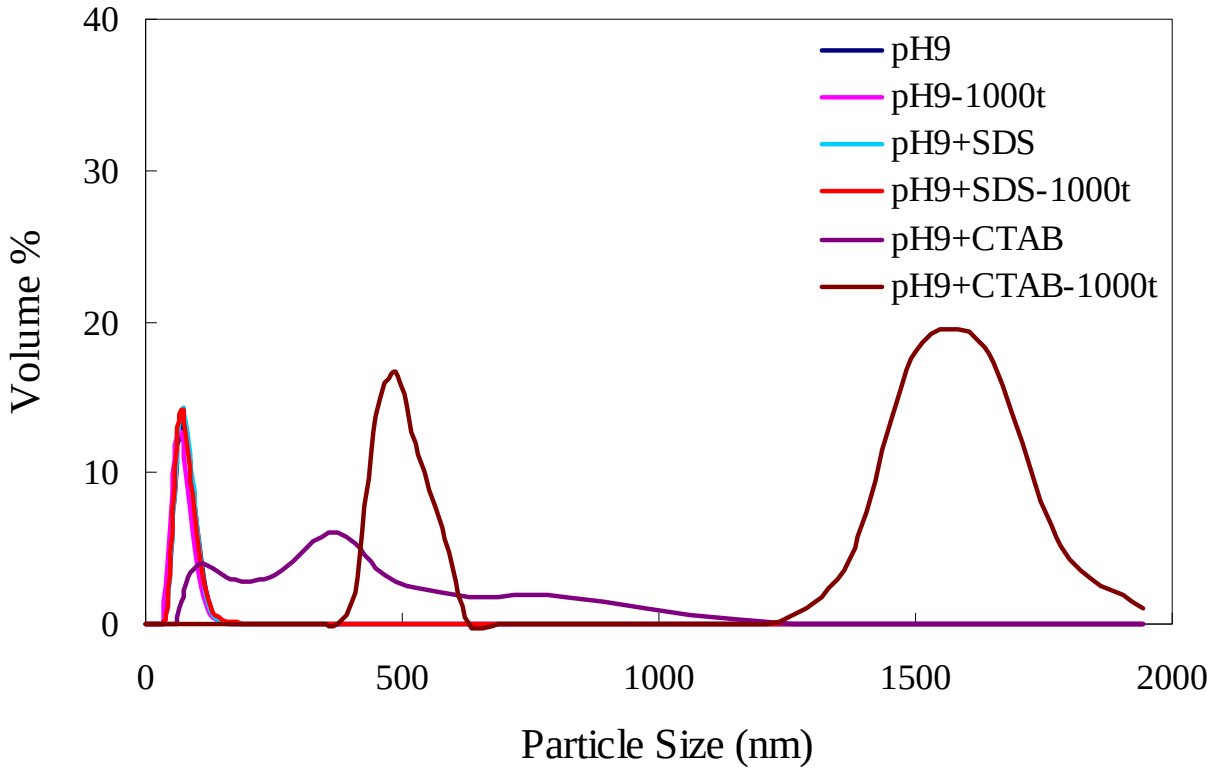

Figure 6-6. Dynamic light scattering (DLS) experiment: the particle size distributions of 80nm silica slurries with surfactants.

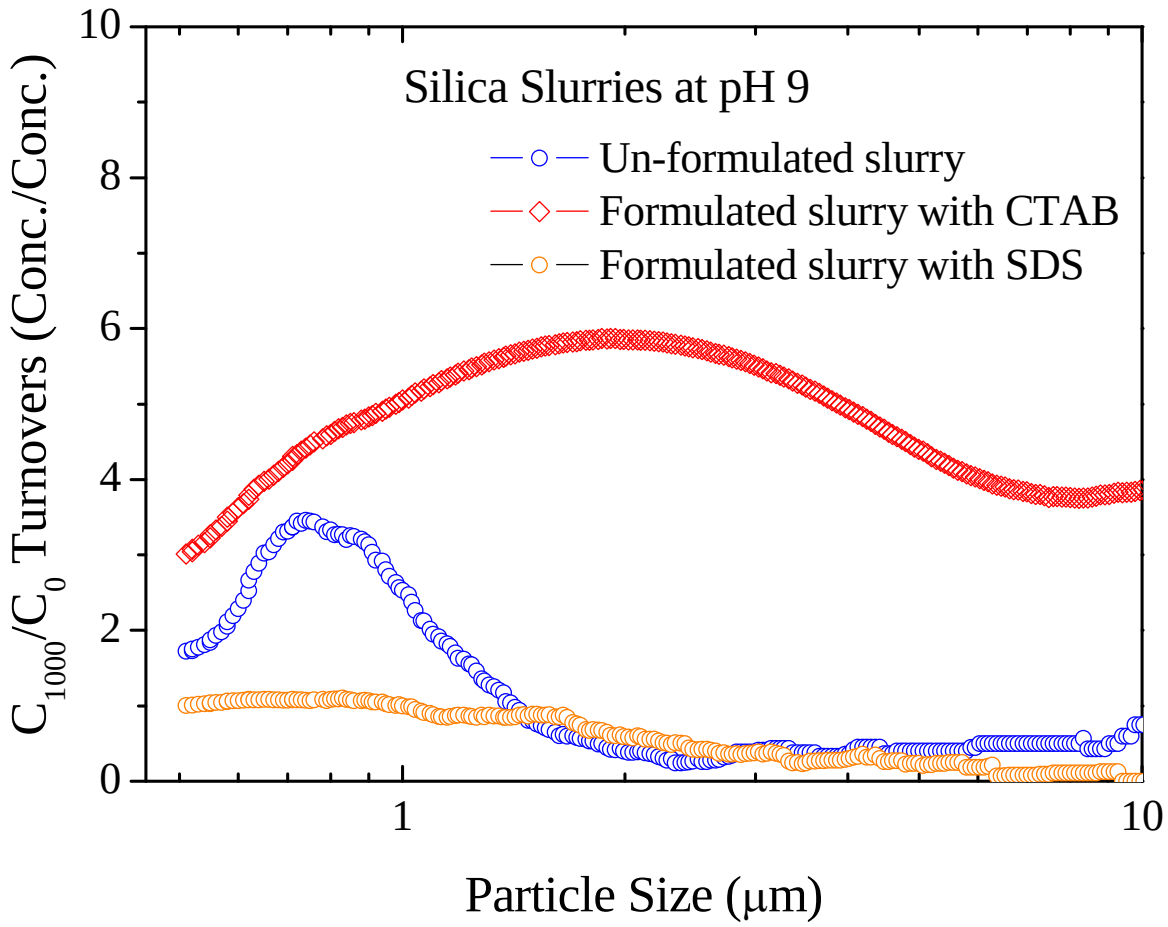

Figure 6-7. Comparison of particle agglomeration in formulated and un-formulated silica slurries.

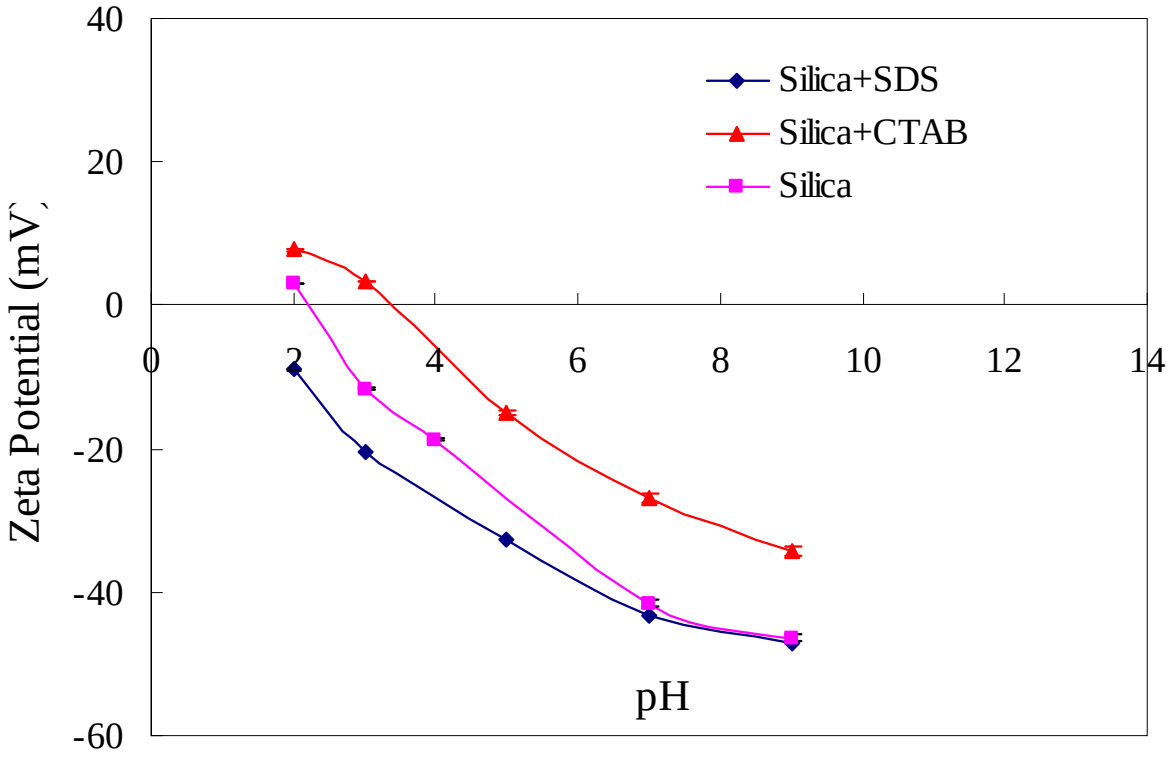

Figure 6-8. Plot of zeta potential vs. pH in silica slurry with surfactants.

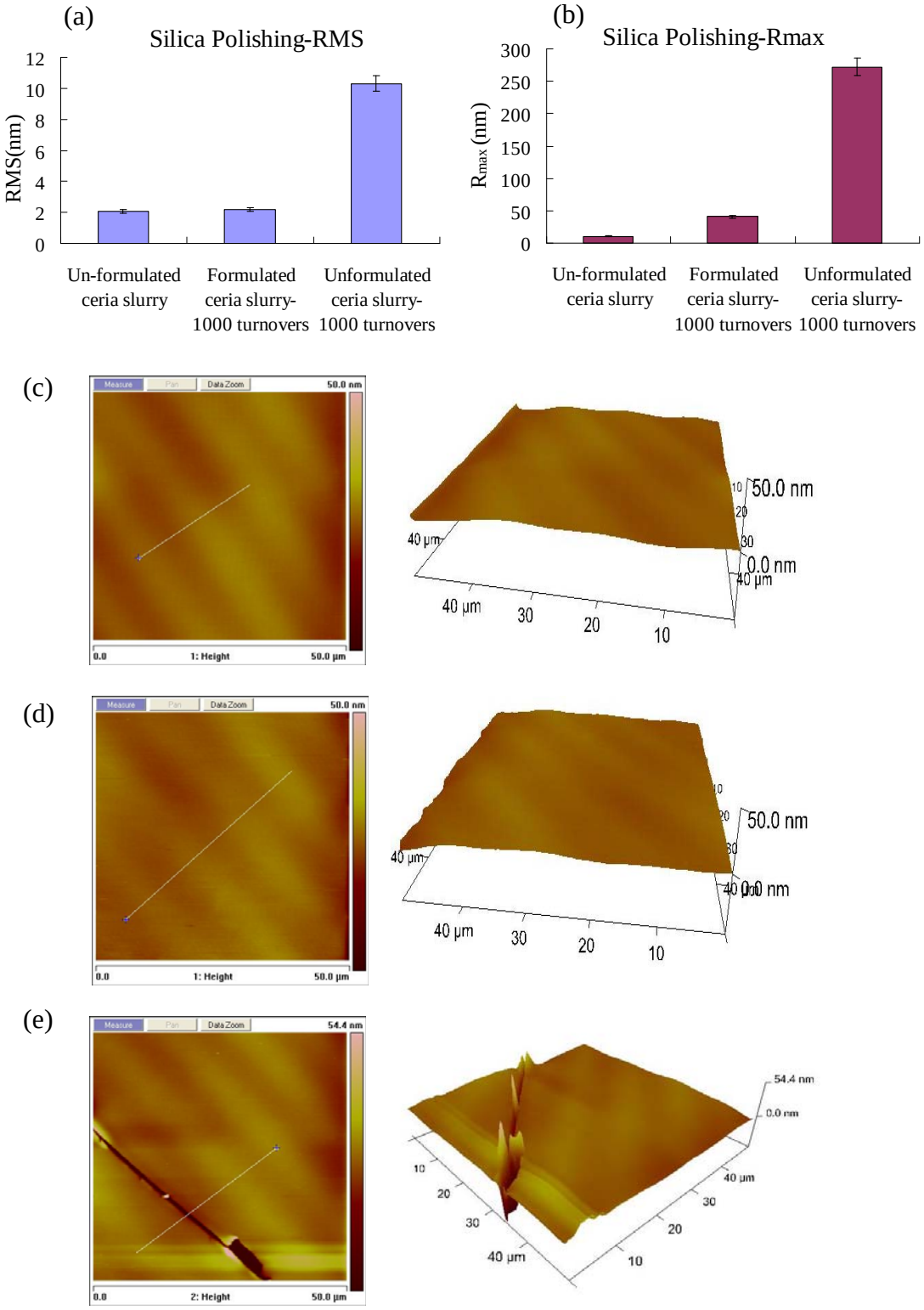

Figure 6-9. Silica CMP: (a) surface roughness (RMS), (b) R_{max}, (c) AFM images of silica wafers polished by un-formulated ceria slurry at pH 6, (d) formulated ceria slurry (cationic surfactant) at pH 6 (1000 turnovers), and (d) un-formulated ceria slurry at pH 6 (1000 turnovers).

CHAPTER 7
NOVEL METHOD TO QUANTIFY THE DEGREE OF AGGLOMERATION IN HIGHLY STABLE CMP SLURRIES

Introduction

Highly stable slurry plays an important role in chemical mechanical polishing (CMP), as it minimizes particle-induced defectivity. The presence of agglomerated particles in a CMP slurry is one of the main causes of defects during polishing [Bas02]. The degree of agglomeration depends on external shear stress (e.g., slurry delivery) and internal slurry chemistry (e.g., interparticle force) [Cha08]. As manufacturing nodes continue to scale down, it is becoming increasingly important to control and reduce agglomerated particles to minimize defectivity during CMP. Thus, a reliable and accurate method for measuring agglomeration phenomena in CMP slurries is important to prevent particle-induced defectivity.

Typically, measurements of interparticle force and/or zeta potential are used to assess the stability of CMP slurries qualitatively. Basim *et al.* [Bas03] studied surfactant effects on repulsive interaction forces between silica particles at high ionic strengths. They found that repulsive interaction forces, correlated to the length of surfactant chains, determined the stability of colloidal particles. Slurries with shorter surfactant chain lengths (less repulsive forces) were unstable (large particle size). Other researchers have measured zeta potential and light scattering (e.g., dynamic light scattering and laser diffraction) to investigate how slurry chemicals (e.g., organic acids, ionic concentrations, and surfactants) affect colloidal dispersion behavior [Gop06, Vid05, and Eom02]. They observed agglomeration behavior when colloidal particles exhibited low zeta potential values.

These measurements, however, do not fully describe agglomeration phenomena in CMP slurries because of complicating factors such as high ionic strength and multiple additives. In addition, light scattering techniques are inadequate for determining the degree of agglomeration

in CMP slurries, due to their inability to detect changes in slurry characteristics [Nic01]. Therefore, we developed a novel method for quantifying the degree of agglomeration in a CMP system. We circulated typical CMP slurries using a high shear pumping device, and measured particle agglomeration characteristics using a single-particle optical sensor (SPOS). We used Smoluchowski's theory to model changes in tail distribution, and developed an agglomeration index to quantify the degree of agglomeration.

Experimental

Determining the Agglomeration Index

The agglomeration index (*AI*) of CMP slurries can be determined in three steps: (1) subject CMP slurries to high shear forces, (2) measure the slurry characteristics of oversize tail distributions, and (3) model changes in oversize tail distribution.

High shear stress, generated by pumping devices, causes particle agglomeration during the handling process [Cha09]. We used magnetically levitated (Maglev) centrifugal and positive displacement pumps to circulate various types of slurries (e.g., various surfactants, particle sizes and types, ionic concentrations, and pH) in a slurry distribution system, to investigate how external shear stress and internal slurry chemistry affect the tail distribution of oversize particles. In this experiment, slurries were subjected to a constant slurry flow rate of 12 L/min, and were circulated in a slurry loop to a maximum of 1000 turnovers, where a turnover was defined as the cycling of the total volume of each slurry (2 L) through the entire slurry loop once.

We measured the particle agglomeration characteristics of tail distribution using the "AccuSizer 780" particle size measurement system, which consists of a single-particle optical sensor (SPOS). Its auto-dilution component can obtain a particle concentration that allows its photozone sensor to detect single particles ranging in size from 0.51 to 200 μm.

To calculate the agglomeration index, we used Smoluchowski's slow coagulation theory to model changes in particle tail distribution under external shear stress [Eli98 and Rus89]. Slow coagulation is defined as the presence of electrostatic interaction between particles, which defends against coagulation. We assumed that particle collisions were binary and proportional to particle concentration. The total change in the rate of agglomerate concentrations, such as singlet (dN_1/dt), doublets (dN_2/dt), and triplets (dN_3/dt), can be expressed as:

$$\frac{dN_1}{dt} = -(k_{11}/W_{11})N_1^2 - (k_{12}/W_{12})N_1N_2 - (k_{13}/W_{13})N_1N_3 \cdots\cdots\cdots \quad [7\text{-}1]$$

$$\frac{dN_2}{dt} = (k_{11}/W_{11})N_1^2/2 - (k_{12}/W_{12})N_1N_2 - (k_{23}/W_{23})N_2N_3 \cdots\cdots\cdots \quad [7\text{-}2]$$

$$\frac{dN_3}{dt} = (k_{12}/W_{12})N_1N_2 - (k_{13}/W_{13})N_1N_3 - (k_{23}/W_{23})N_2N_3 \cdots\cdots\cdots \quad [7\text{-}3]$$

where the aggregation constant, $k_{ij} = 4G(a_i + a_j)/3$, is a function of the particle size (a) aggregates, i and j-folds, and the shear rate (G), described by the orthokinetic theory. Individual agglomerate concentrations can be derived from the above equations as follows:

$$N_k = \frac{N_0(t/\tau)^{k-1}}{(1+t/\tau)^{k+1}} \quad [7\text{-}4]$$

$$\tau = \frac{W_{ij}}{k_{ij}N_0} \quad [7\text{-}5]$$

where N_0 is the total particle concentration, t is the aggregation time, and W is the stability ratio, defined as the ratio of the rapid aggregation rate in the absence of electrostatic interaction to the slow aggregation rate when electrostatic interactions occur between particles [Ste05]. Thus, we can define the agglomeration index (AI) as a logarithm ratio of external shear stress to the stability ratio (Log (G/W)). Therefore, a slurry with a lower agglomeration index will have a more stable colloidal suspension.

We determined the agglomeration index of CMP slurries by modeling changes in the tail distribution. Figure 7-1 schematically illustrates how we determined the agglomeration index.

First, we used the initial tail distribution of oversize particles to simulate the growth of individual agglomerates. By fitting both experimental and modeling changes to tail distributions, we were able to determine the value of the agglomeration index.

Effect of Agglomeration Index on Polishing Performance

To investigate how the agglomeration index affected polishing performance, we used circulated slurries to polish 1-inch square Cu, TEOS, and low k wafers in a TegraPol-35 Table Top Polisher, from Struers Co., with a down pressure of 3 psi, polishing time of 1 min, slurry flow rate of 100 ml/min, and rotation speed of 150 rpm. The surface roughness (RMS) of polished Cu wafers was characterized using a Digital Instruments Nanoscope III atomic force microscope (AFM).

Results and Discussion

To investigate how external shear stress affected the agglomeration index, we used pumping devices to circulate silica slurries at pH 10 (primary particle size: 150 nm). As-received slurries were circulated by maglev centrifugal and positive displacement pumps for 500 turnovers (5000 seconds). Figure 7-2 illustrates the changes in the fraction of oversize tail distributions, defined as a ratio of particle concentration at a specific particle size to the total particle concentration (1.41×10^{13} particles/ml). As the positive displacement pump generated highly localized shear stresses near the wall during the pump stroke, the tail distribution increased significantly compared to the maglev centrifugal pump.

Subsequently, we used as-received particle concentrations (ranging in size from 0.51 to 1 μm) to simulate the change in tail distribution at 5000 seconds. We used Equation 4 to simulate agglomeration concentrations (e.g., singlet, doublet, triplet, etc.) at their correlated particle sizes. We were able to obtain the change in tail distribution by cumulating the simulated agglomerates.

Consequently, we determined the agglomeration index of CMP slurries by fitting both experimental and modeled tail distributions, as shown in Figure 7-3. Circulated slurries had *AI* values of 2.48 and 4.48 in the maglev centrifugal and positive displacement pumps, respectively. As *AI* can be defined as Log (*G/W*), the relative shear stress between pumping devices can be determined using identical slurry stability (*W*). As a result, the shear stress in the maglev centrifugal pump system was 100 times lower than that in the positive displacement pump system.

To investigate how slurry chemistry affected the agglomeration index, we circulated typical CMP slurries with varying chemicals (e.g., pH, salt, and surfactant) and abrasive particles (e.g., size and type) in the slurry distribution using the positive displacement pump. We used the as-received slurries to simulate changes in tail distributions. Table 7-1 lists the *AI* values of those slurries; values ranged from 0.6 to 5. Slurries with lower *AI* values had more stable abrasive particles. The *AI* values for silica slurry (80 nm) were 1.76 at pH 9 and 2.46 at pH 3. Circulated slurries at pH 9 had less oversize tail distribution compared to circulated slurry at pH 3, as shown in Figure 7-4.

To assess how the agglomeration index affected polishing performance, we used these slurries (80 nm silica) to polish Cu wafers; the goal was to investigate particle-induced defectivity. Figure 7-5 shows typical AFM images of polished Cu wafers using as-received and circulated slurries. Figure 7-5 (a) shows the corresponding surface roughness (RMS). A Cu wafer that was not subjected to the polishing process had an uneven surface and high surface roughness (RMS = 6.14 nm), as shown in Figure 7-5(b). In contrast, a Cu wafer that was polished by as-received slurries had a flat surface and lower surface roughness (RMS = 2.64 nm), as shown in Figure 7-5(c). As circulated slurries at pH 3 had more agglomerated particles,

they resulted in high surface roughness (RMS = 7.98 nm) and large micro-scratches on polished Cu wafers, as shown in Figure 7-5(e); however, circulated slurries at pH 9 resulted in less surface roughness (RMS = 2.99 nm) on polished Cu wafers, as shown in Figure 7-5(d).

Our numerous polishing tests (e.g., using Cu, low k, and silica CMP) revealed that slurries with higher agglomeration index values (*AI* > 1.8) tended to contain more agglomerated particles during the handling process and to cause more surface defectivity (e.g., pits and micro-scratches) during CMP, as shown in Figure 7-6. Consequently, the agglomeration index can be used to quantify the degree of agglomeration in highly stable CMP slurries, and the use of low *AI* slurries during polishing can further minimize particle-induced defectivity.

Summary

The presence of agglomerated particles in a CMP slurry is one of the main causes of defects during polishing, particularly as the manufacturing nodes continue to scale down. The degree of agglomeration depends on external (shear stress) and internal (slurry chemistry) forces. Therefore, we developed the agglomeration index (AI) to quantify the agglomeration phenomena caused by both external and internal forces. In typical CMP slurries, AI values range from 0.6 to 5; slurries with a lower agglomeration index have more stable abrasive particles. Our modeled and experimental results revealed that the shear stress in a positive displacement pump was 100 times greater than that in a magnetically levitated centrifugal pump. In addition, our numerous polishing experiments revealed that slurries with higher agglomeration index values (AI > 1.8) contained more agglomerated particles during the handling process and caused more surface defectivity during polishing. Our novel method can be applied to determine slurry stability, and thus further minimize particle-induced defectivity during CMP of metals and dielectrics.

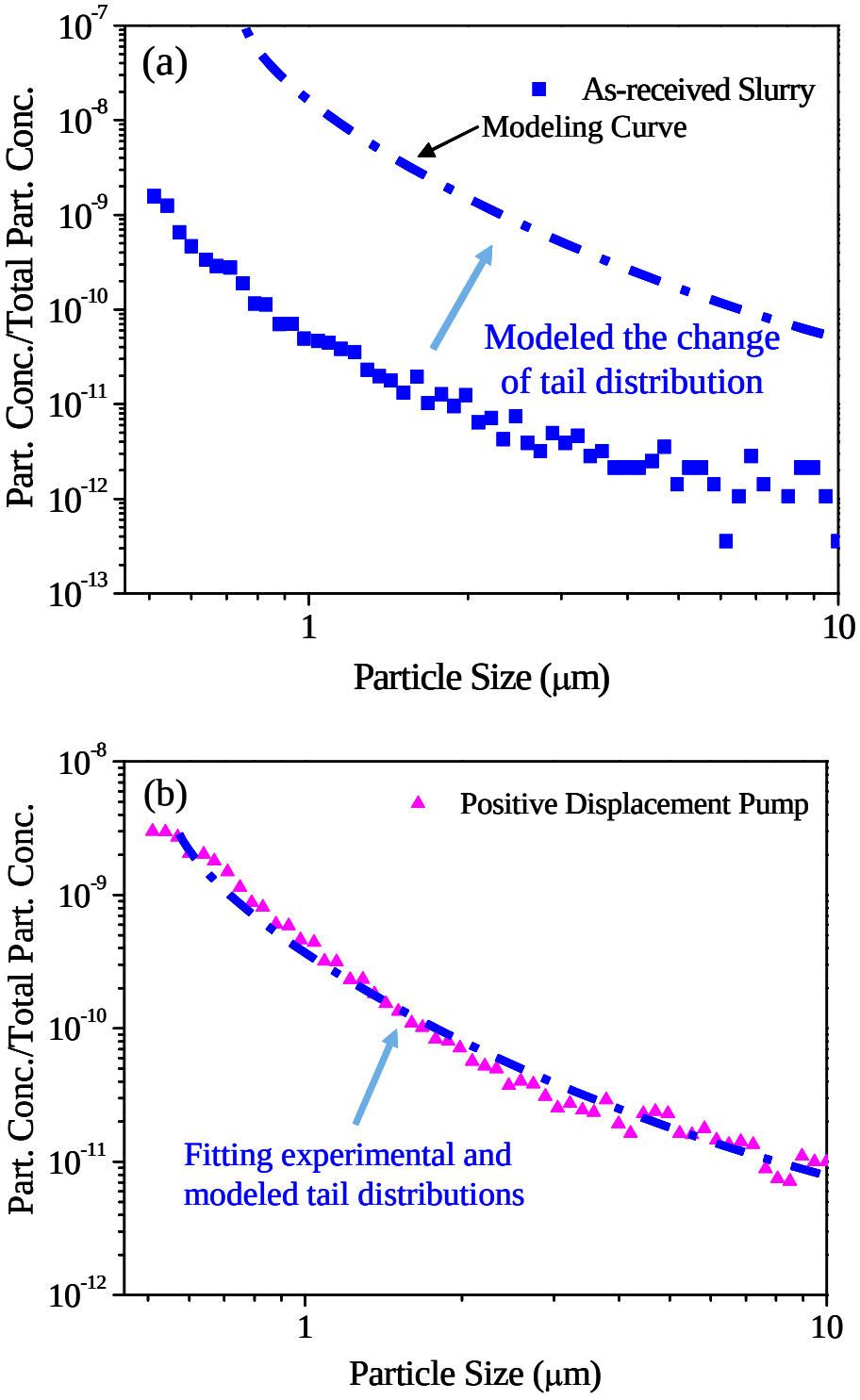

Figure 7-1. Schematic illustration of how the agglomeration index is determined: (a) modeling the change in tail distribution of oversize particles; and (b) fitting experimental and modeled tail distributions to obtain the agglomeration index.

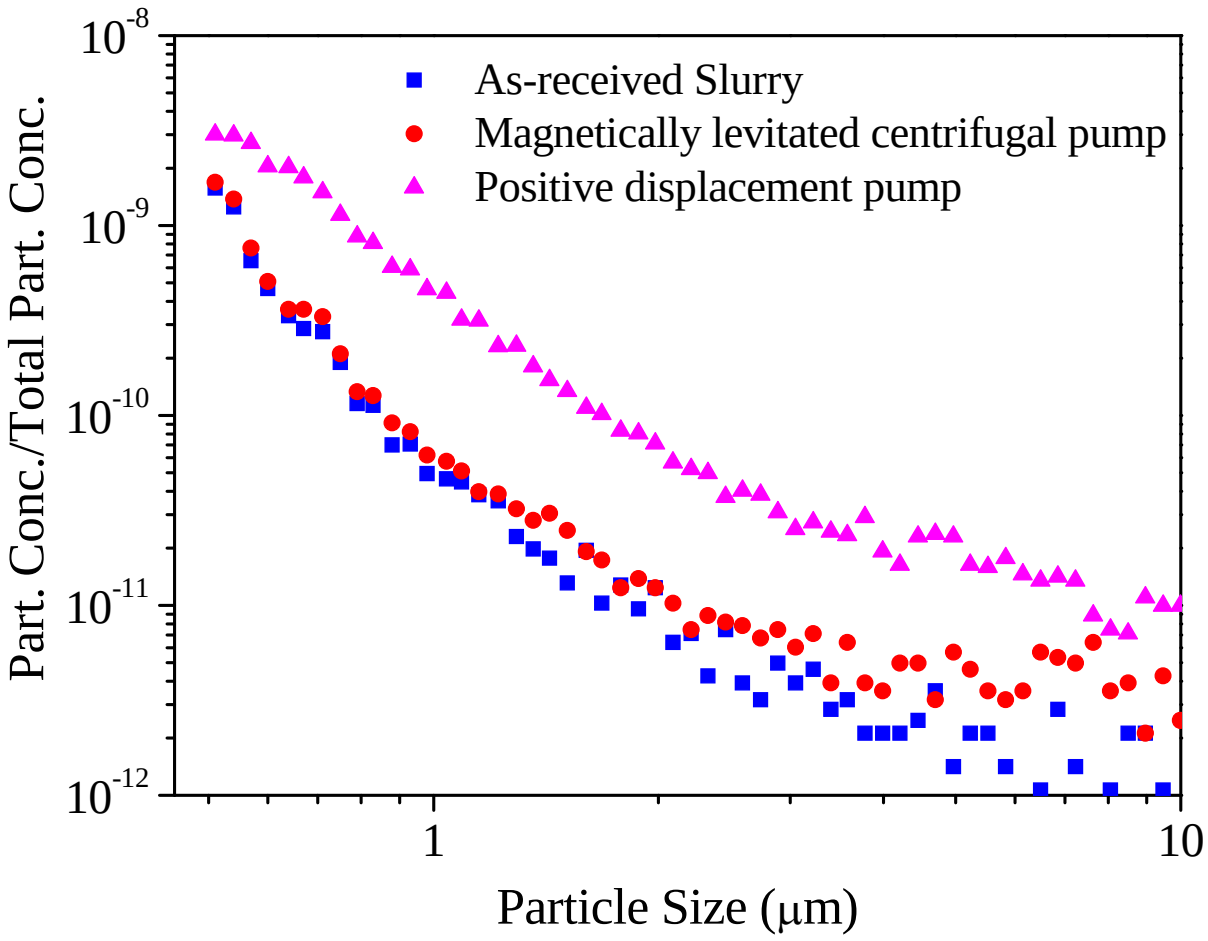

Figure 7-2. Tail distributions of as-received slurry and circulated slurries by positive displacement and maglev centrifugal pumps.

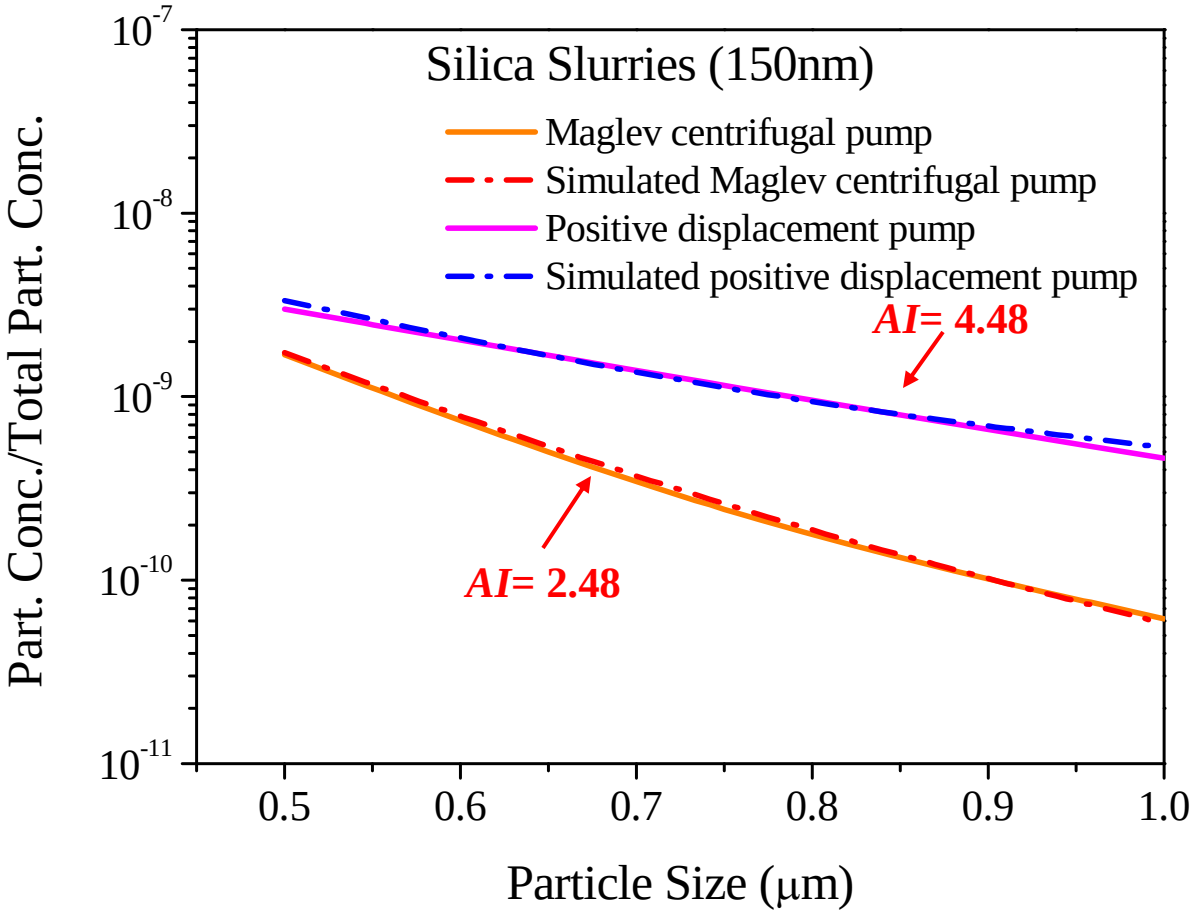

Figure 7-3. Effect of external shear stress on the agglomeration index: experimental and modeled tail distributions in positive displacement and maglev centrifugal pumps.

Table 7-1. Agglomeration indexes of typical chemical mechanical polishing (CMP) slurries.

	Slurry	Agglomeration Index (*AI*)
A	150nm Silica: pH 10	4.48
B	80nm Silica: pH 9	1.76
C	80nm Silica: pH 9+Anionic	0.66
D	80nm Silica: pH 3	2.46
E	30nm Silica: pH 11	1.36
F	30nm Silica: pH 11+Salt	1.66
G	30nm Silica: pH 7	3.92
H	30nm Silica: pH 7+Salt	4.26
I	30nm Silica: pH 2	4.36
J	30nm Silica: pH 2+Salt	4.96
K	70nm Ceria: pH 5+Cationic 1	2.36
L	70nm Ceria: pH 5+Cationic 2	1.96

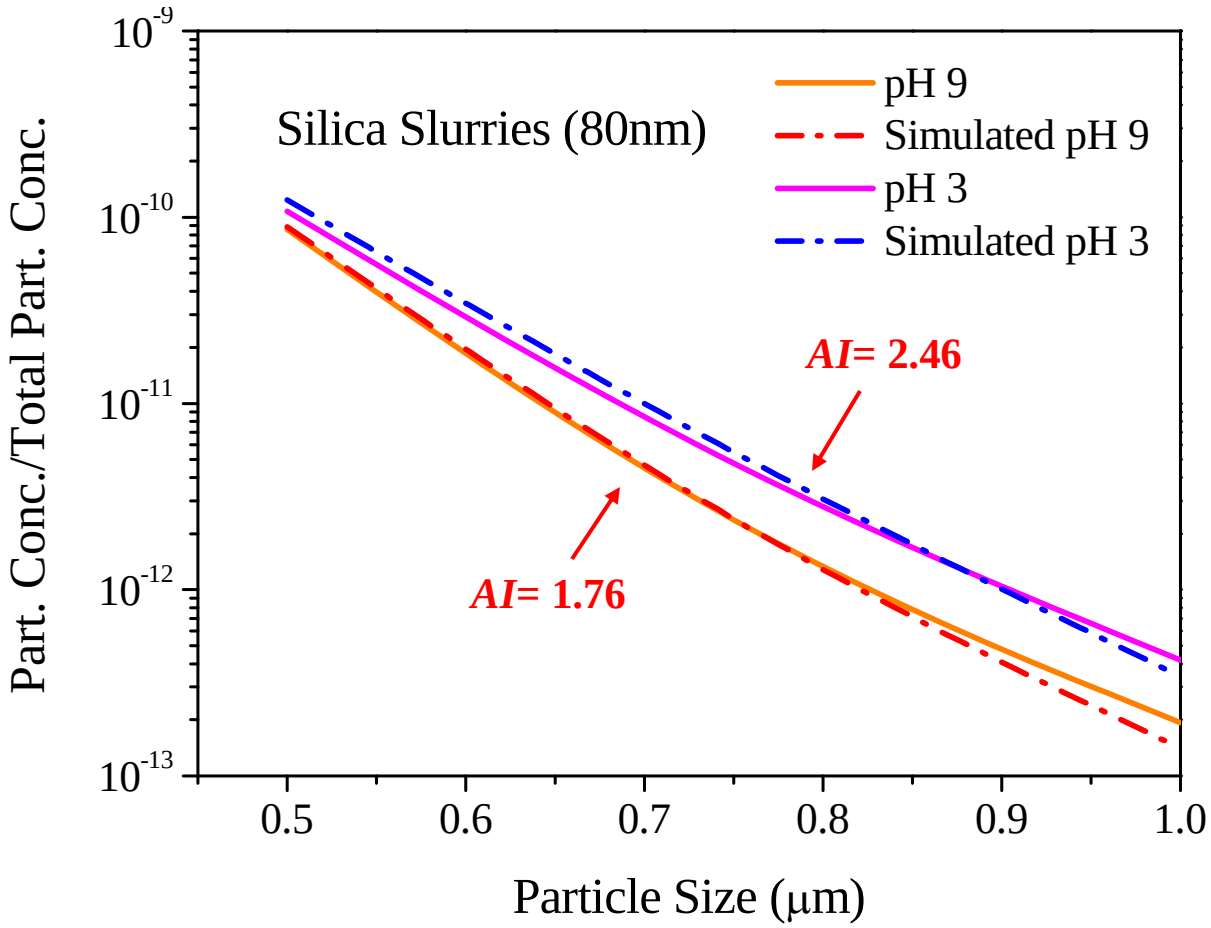

Figure 7-4. Effect of internal slurry chemistry on the agglomeration index: experimental and modeled tail distributions in circulated slurries (80 nm silica) at pH 9 and 3.

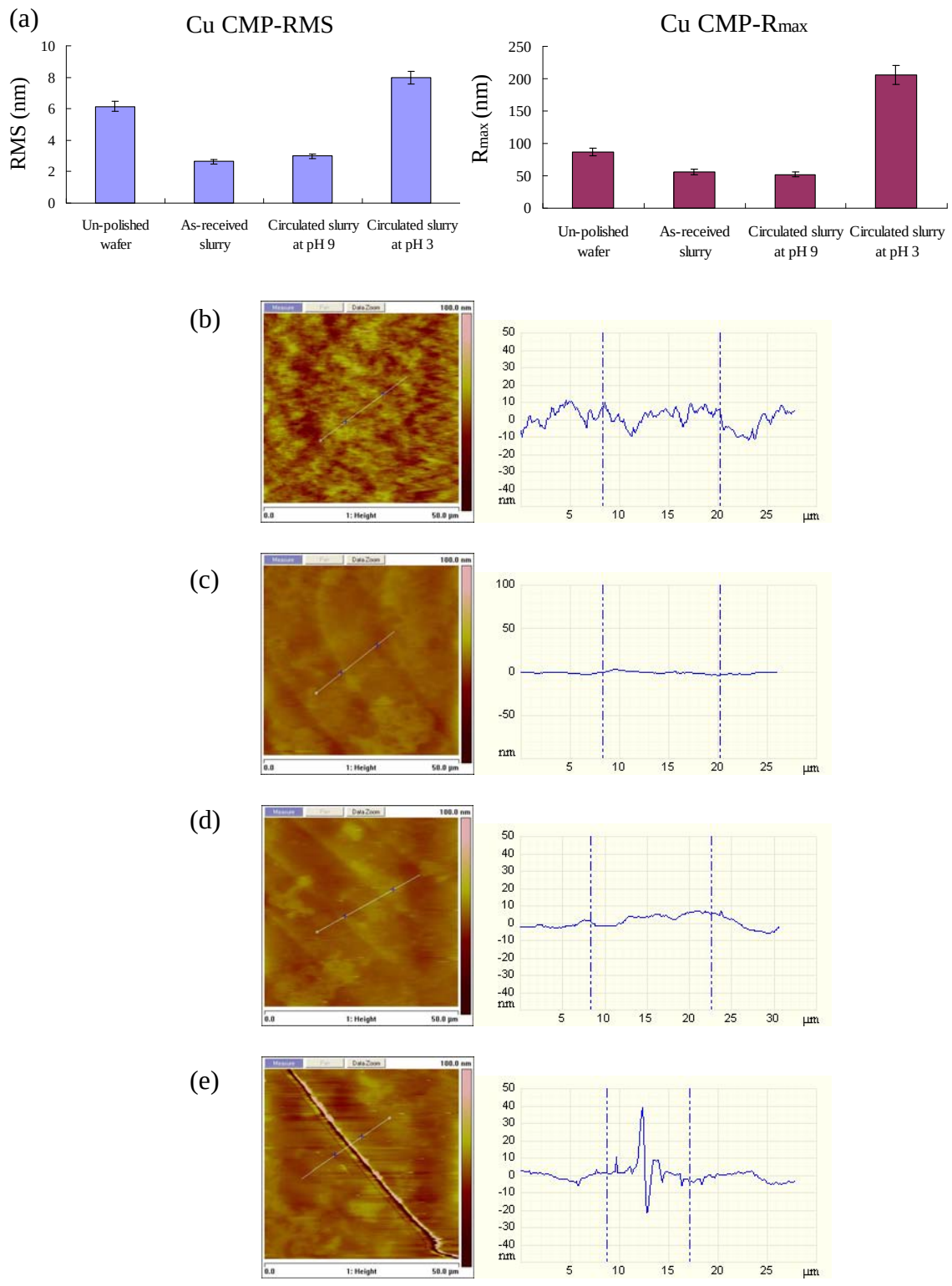

Figure 7-5. Cu chemical mechanical polishing (CMP): (a) surface roughness (RMS and R_{max}); and AFM images of Cu wafers (b) un-polished, (c) polished by as-received slurry, (d) polished by circulated slurry at pH 9, and (e) polished by circulated slurry at pH 3.

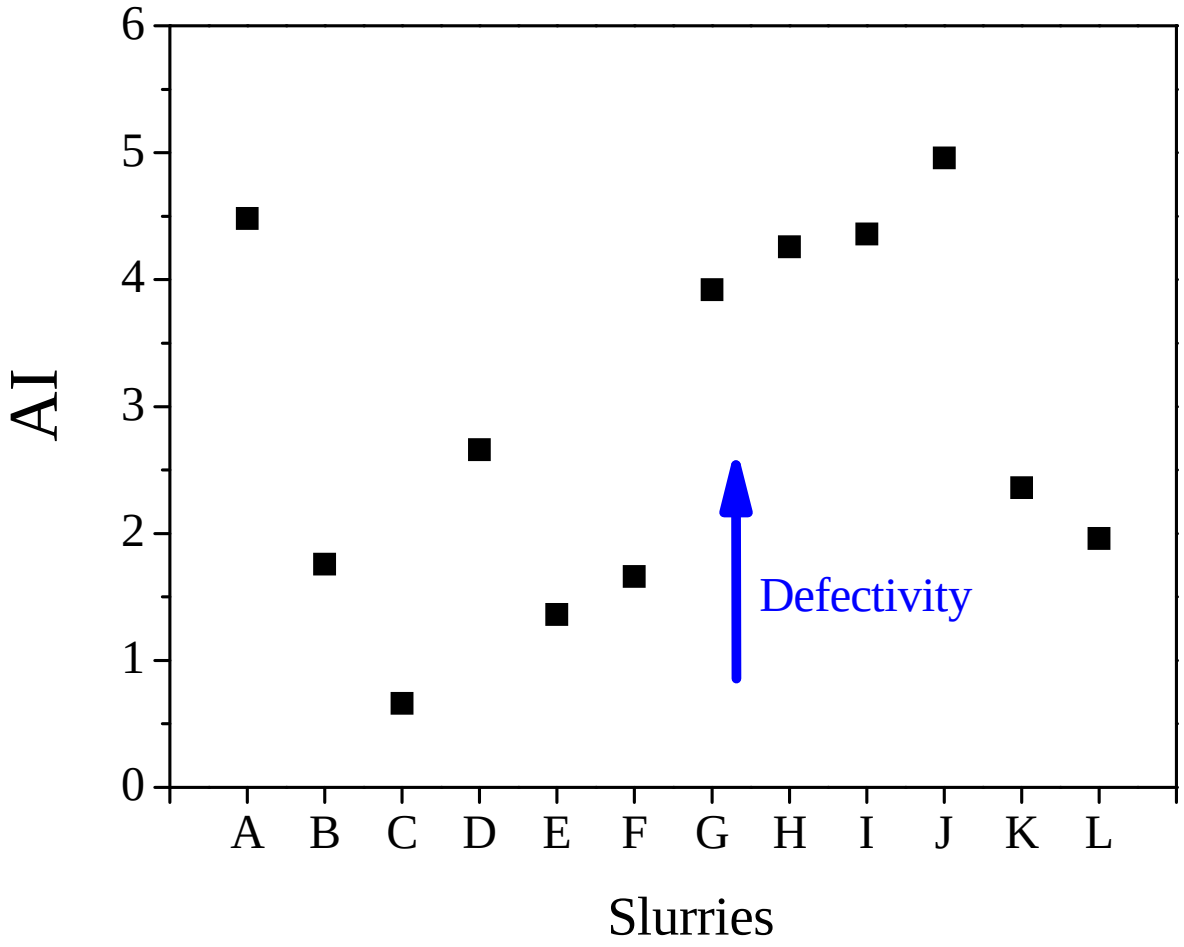

Figure 7-6. Plot of the agglomeration index (*AI*) versus typical chemical mechanical polishing (CMP) slurries in determining particle-induced defectivity.

CHAPTER 8
CONCLUSIONS AND SUGGESTIONS FOR FUTURE WORK

Conclusions

In the chemical mechanical planarization of dielectrics and metals, the presence of oversize particles in the slurry is one of the main causes of defectivity. Pumps within the slurry distribution system play a significant role in increasing both the number and distribution of oversize particles. Therefore, the effect of stress induced by different types of pump on particle agglomeration was investigated. We found the mean value of normalized oversize concentrations in the positive displacement pump system at 500 turnovers to be 6 times higher than that of a magnetically levitated centrifugal pump system. The magnetically levitated centrifugal pump was a low shear pump and did not increase the concentration of oversize particles significantly with slurry turnovers. A positive correlation was established between the roughness/defect density and the degree of agglomeration.

Thus, a stable suspension in chemical mechanical polishing (CMP) slurry is an essential requirement to ensure superior polishing performance. The agglomeration of the slurries was found to depend both on the external shear stress and the interparticle forces acting on the slurries. Our results indicate that alkaline silica slurries exhibited larger repulsive interparticle forces that successfully defended against shear flow and resulted in less agglomerated particles during the handling process. The least particle-induced defectivity was observed on polished low k wafers that utilized highly alkali slurries. Thus, alkaline silica slurries are the best condition for robust slurries to minimize the process-induced particle agglomeration and surface defectivity during CMP of metals and dielectrics.

Furthermore, the stability of slurry can be obtained by adding surfactants (e.g., anionic and cationic surfactants) to provide the polymer stabilization between particles. Typically, to

obtain high removal rates of dielectric substrates, the ceria slurry is taken near its isoelectric point (IEP) (e.g., pH 6~7), and the silica slurry is alkaline (e.g., pH 9~11). The addition of anionic and cationic surfactants into ceria slurries at pH 6 and anionic surfactants into silica slurries at pH 9 can provide a stronger potential barrier to defend against the stress-induced particle agglomeration, resulting in the minimization of surface defectivity during CMP of dielectric materials.

Highly stable slurry plays an important role in chemical mechanical polishing (CMP) as it decreases particle-induced defectivity. Typically the stability of the slurry is measured by light scattering measurements. However, such measurements are inadequate in determining the degree of agglomeration. We have a novel experimental/theoretical approach to determine the degree of agglomeration in typical CMP slurries. This method is based on subjecting the slurry to high shear forces and measuring the particle agglomeration characteristic of their tail distribution. By modeling the change in the tail distribution, the degree of agglomeration can be determined. Consequently, the agglomeration index (*AI*) was established by this approach, and distributed in the range of 0.6 to 5; the lower agglomeration index of the slurry, the more stability of colloidal suspensions. Based on numerous polishing results, slurries with a high agglomeration index (*AI* > 1.8) were unstable and tended to agglomerate more oversize particles during the handling process that caused a significant increase in surface defectivity (e.g., micro-scratches) during CMP. This novel method can be applied to determine the slurry stability for minimizing particle-induced defectivity during CMP of metals and dielectrics.

Suggestions for Future Work

As manufacturing nodes continually scale down, new challenges emerge from both the front and back end processes. For example, shrinking the transistor feature size is expected to apply atomic scale polishing to polysilicon polishing. Thus, the trend in CMP slurries is to

reduce particle sizes with tunable chemicals in order to ensure slurry stability and protect a device from damages. To minimize particle-induced defectivity, slurry stability/robustness is essential. Achieving robustness is made possible by introducing polymer surfactants (ionic and nonionic surfactants) into colloidal suspensions.

The mechanism of surfactant adsorption onto metal oxide surfaces (e.g., silica, ceria, and alumina) is the key factor in achieving polymer stabilization. Thus, fourier transform infrared spectroscopy (FTIR) can be employed for studying the surfactant adsorption due to its sensitivity in detecting chemical bonding.

Furthermore, the effect of surfactant concentrations on the magnitude of surface charges of colloidal particles should also be studied. The addition of ionic surfactants into reverse charge particles could worsen the slurry stability due to screening the surface charges, but then improve the slurry stability because more surfactants adsorb onto particle surfaces. Thus, the quantity of surfactant concentration could be determined.

Finally, the agglomeration index can be employed for determining the degree of agglomeration in commercial CMP slurries. More extensive slurry studies will be needed to be conducted as a function of particle types (e.g., alumina, silica, and ceria), particle sizes, and chemicals to build up the agglomeration index. The slurry stability will be confirmed by the polishing performance.

LIST OF REFERENCES

Abi05 J. T. Abiade, W. Choi, R. K. Singh, *J. Mater. Res*., **20**, 1139 (2005).

Asa95 A. H. Perera, J.-H. Lid, Y.-C. Ku, M. Azrak, B. Taylor, J. Hayden, M. Thompson, M. Blackwell, *EDM Tech. Dig.*, 679 (1995).

Bal04 S. Balakumar, X. T. Chen, Y. W. Chen, T. Selvaraj, B. F. Lin, R. Kumar, T. Hara, M. Fujimoto, and Y. Shimura, *Thin Solid Films*, **462–463**, 161 (2004).

Bar99 J. Bare, B. Johl, T. Lemke, *Semiconductor International*, January (1999).

Bas00 G. B. Basim, J. J. Adler, U. Mahajan, R. K. Singh, B. M. Moudgil, *J. Electrochem. Soc*., **147**, 3523 (2000).

Bas02 G. B. Basim and B. M. Moudgil, *J. Colloid Interface Sci.*, **256**, 137 (2002).

Bas03 G. B. Basim, I. U. Vakarelski, and B. M. Moudgil, *J. Colloid Interface Sci.*, **263**, 506 (2003).

Ber08 P. Bernard, S. Valette, S. Daveau, J.C. Abry, P. Tabary, Ph. Kapsa, *Tribology International*, **41**, 416 (2008).

Bib98 T. Bibby and K. Holland, *J. Electron. Mater*., **27**, 1073 (1998).

Bie99 M. Bielmann, U. Mahajan, R. K. Singh, D. O. Shah, and B. J. Pallab, *Electrochem.and Solid-StateLetters*, **2**, 148 (1999).

Bor02 C. L. Borst, W. N. Gill, R. J. Gutmann, *Chemical–Mechanical Polishing of Low Dielectric Constant Polymers and Organosilicate Glasses: Fundamental Mechanisms and Application to IC Interconnect Technology*, Kluwer Academic Publishers, Boston (2002).

Bow02 P. Bowen, *J. Dispers. Sci. Technol*., **23**, 631 (2002).

Bu05 K. H Bu and B. M. Moudgil, *Mater. Res. Soc. Symp. Proc*., **867**, W8.5.1 (2005).

Bu07 K. H. Bu and B. M. Moudgil, *J. Electrochem. Soc.*, **154**, H631 (2007).

But91 H.-J. Butt, *Biophysical Journal*, **60**, 1438 (1991).

But95 H.-J. Butt, M. Jaschke, and W. Ducker, *Bioelectrochemistry and Bioenergetics*, **38**, 191 (1995).

Cha96 A. Chatterjee, D. Rogers, J. McKee, I. Ali, S. Nag, and I.-C. Chen, *IEDM Tech. Dig*., 829 (1996).

Cha04a B. Chandran, R. Mahajan, M. Bohr, C.-H. Jan, and Q. T. Vu, *Future Fab International*, 17 (2004).

Cha04b N. Chandrasekaran, S. Ramarajan, W. Lee, G. M. Sabde, S. Meikle, *J. Electrochem. Soc*., **151**, G882 (2004).

Cha08 F. C. Chang, S. Tanawade and R. Singh, *Semiconductor International*, **31**, 46 (2008).

Cha09 F.-C. Chang, S. Tanawade, and R. K. Singh, *J. Electrochem. Soc*., **156**, H39 (2009).

Cho04a W. Choi, S.-M. Lee, and R. K. Singh, *Electrochem. Solid-State Lett.*, **7**, G141 (2004).

Cho04b W. Choi, U. Mahajan, S.-M. Lee, J. Abiade, and R. K. Singh, *J. Electrochem. Soc*., **151**, G185 (2004).

Coo90 L.M. Cook, *J. Non-Crystall. Solids*, **120**, 152 (1990).

Cum95 M. J. Cumbo, D. Fairhurst, S. D. Jacobs, and B. E. Puchebner, *Applied Optics*, **34**, 3743 (1995).

Den06 D. Denardis, D. Rosaled-Yeomans, L. Borucki, and A. Philipossian, *Thin Solid Films*, **513**, 311 (2006).

Doe08 R. Doering and Y. Nishi, *Handbook of semiconductor manufacturing technology*, CRC Press, Boca Raton, (2008).

Duc91 W. A. Ducker, T. J. Senden, and R. M. Pashley, *Nature*, **353**, 239 (1991).

Duc92 W. A. Ducker, T. J. Senden, and R. M. Pashley, *Langmuir*, **8** , 1831 (1992).

Ein07 Y. Ein-Eli and D. Starosvetsky, *Electrochim. Acta*, **52**, 1825 (2007).

Eli98 M. Elimelech, J. Gregory, X. Jia, R. A. Williams, *Particle Deposition and Aggregation*, Butterworth-Heinemann, Oxford, (1998).

Eom02 D.-H. Eom, J.-G. Park, and E.-S. Lee, *Jpn. J. Appl. Phys.*, **41**, 1305 (2002).

Eom07 D. H. Eom, I. K. Kim, J. H. Han, and J. G. Park, *J. Electrochem. Soc.*, **154**, d38 (2007).

Eva92 C. Evans, R. Brundle, and S. Wilson, *Encyclopedia of Materials Characterization Encyclopedia of Materials Characterization*, Elsevier Butterworth-Heinemann, Boston, (1992).

Fran00 G. V.Franks, Z. Zhou, N. J. Duin, and D. V. Boger, *J. Rheol*. **44**, 759 (2000).

Gop06 T. Gopal and J. B. Talbot, *J. Electrochem. Soc*., **153**, G622 (2006).

Hac97 V. A. Hackley, *J. Am. Ceram. Soc.*, **80**, 2315 (1997).

Hay95 Y. Hayashi, M. Sakurai, T. Nakajima, K. Hayashi, *Jpn. J. Appl. Phys.*, **34**, 1037 (1995).

Hig82 K. Higashitani, R. Ogawa, G. Hosokawa, and Y. Matsuno, *J. Chem. Eng. Jpn.*, **15,** 299 (1982).

Hij04 K.-I. Hijioka, F. Ito, M. Tagami, H. Ohtake, Y. Harada, T. Takeuchi, S. Saito and Y. Hayashi, *Jpn. J. Appl. Phys.*, **43**, 1807 (2004).

Hun01 R. J. Hunter, *Foundations of colloid science*, Oxford University Press, (2001).

Ile79 R. Iler, *The Chemistry of Silica*, Wiley, New York (1979).

Isr91 J. Israelachvili, *Intermolecular and Surface Forces*, Academic Press, London, (1991).

ITRS07 International Technology Roadmap for Semiconductors, *interconnect*, (2007).

Joh03 B. Johl and R.K. Singh, *Solid State Technology*, **46**, 63 (2003).

Len08 Y. Leng, *Materials Characterization: Introduction to Microscopic and Spectroscopic Methods*, John Wiley & Sons, Singapore, (2008)

Li08 Y. Li, *Microelectronic Applications of Chemical Mechanical Planarization*, John Wiley & Sons, New Jersey, (2008)

Lin08 J.-Y. Lin, A. C. West, and C.-C. Wan, *J. Electrochem. Soc.*, **155**, H396 (2008).

Lit04 M. Litchy and R. Schoeb, *Semiconductor International*, **27**, 87 (2004).

Lit05 M. Litchy and R. Schoeb, *MRS Symp. Proc.*, **867**, W2.8.1 (2005).

Kah08 A.B. Kahng, *IEEE Transactions on Computer-Aided Design of Integrated Circuits and Systems*, 27, 3 (2008).

Kap02 M. Kappl, H.-J. Butt, *Part. Part. Syst. Charact.*, **19**, 129 (2002).

Kim08a I.-K. Kim, Y.-J. Kang, T.-G. Kim, and J.-G. Park, *Jpn. J. Appl. Phys.*, **47**, 108 (2008).

Kim08b S. Kim, J. H. So, D. J. Lee, and S. M. Yang, *J. Colloid Interface Sci.*, **319**, 48 (2008).

Klo02 S. G. Kloster, T. Xu, G. Blaine, J. Sun, Y. Zhou, *Interconnect Technology Conference, Proc. IEEE*, 242 (2002).

Kub67 O. Kubaschewski, E. Evans, and C. Alcock, *Metallurgical Thermochemistry*, Pergamon Press, Oxford (1967).

Mae03 K. Maex, M. R. Baklanov, D. Shamiryan, F. Iacopi, S. H. Brongersma, and Z. S. Yanovitskaya, *J. Appl. Phys.*, **93**, 8793 (2003).

Mah00 U. Mahajan, M. Bielman, and R. K. Singh, *Mater. Res. Soc. Proc.*, **566**, 27 (2000).

Mis07 K. Mistry, C. Allen, C. Auth, B. Beattie, and D. Bergstrom, *Proceedings of International Electron Devices Meeting*, 247 (2007).

Mor02 I. D. Morrison and S. Ross, *Colloidal suspensions: Suspensions, Emulsions, and Foams*, John Wiley and Sins, New York, (2002).

Mur93 S. P. Murarka, *Metallization: Theory and Practice for VLSI and ULSI*, Butterworth Heinemann, Boston, MA, (1993).

Nai02 R. Nair, *IBM J. Res. Develop.*, 223 (2002).

Nic01 K. Nicholes, R. K. Singh, D. Grant, and M. R. Litchy, *Semiconductor International*, July, 201 (2001).

Ois00 T. Oishi, K. Shiozawa, A. Furukawa, Y. Abe, and Y. Tokuda, *IEEE Transactions on Electron Devices*, **47**, 822 (2000).

Oss02 K. Osseo-Asare, *J. Electrochem. Soc.*, **149**, G651 (2002).

Pal99 B. J. Palla and D. O. Shah, *IEEE/CPMT Int. Electron. Manufact. Tech. Symp.*, 362 (1999).

Pal00 B. J. Palla and D. O. Shah, *J. Colloid Interface Sci.*, **223**, 102 (2000).

Pal02 B. J. Palla and D. O. Shah, *J. Colloid Interface Sci.*, **256**, 143 (2002).

Pan07 S. Pandija, D. Roy, and S. V. Babu, *Mater. Chem. Phys.*, **102**, 144 (2007).

Ram00 S. Ramarajan, Y. Li, M. Hariharaputhiran, Y. S. Her, and S. V. Babu, *Electrochem. Solid-State Lett.*, **3**, 232 (2000).

Par65 G. A. Parks, *Chem. Rev.*, **65**, 177 (1965).

Pro98 T. Provder, *Particle Size Distribution III: Assessment and Characterization, Chapter 6*, American Chemical Society (ACS) Symposium Series, Orlando, FL.

Ram00 S. Ramarajan, Y. Li, M. Hariharaputhiran, Y.-S. Her, and S. V. Babua, *Electrochem. Solid-State Lett.*, **3**, 232 (2000).

Rem06 E. E. Remsen, S. Anjur, D. Boldridge, M. Kamiti, S. Li, T. Johns, C. Dowell, J. Kasthurirangan, and P. Feeney, *J. Electrochem. Soc.*, **153**, G453 (2006).

Ros04 M. J. Rosen, *Surfactants and Interfacial Phenomena*, Wiley, New York, NY, (2004).

Rus89 W. B. Russel, D. A. Saville, and W. R. Schowalter, *Colloidal Dispersions*, Cambridge University, United Kingdom, (1989).

Sak93 T. Sakurai, *IEEE Transactions on Electron Devices*, **40**, 118 (1993).

Sez01 S. M. Sze, *Semiconductor Devices: Physics and Technology*, Wiley, New York, NY, (2001).

Sha04 D. Shamiryan, T. Abell, F. Lacopi, K. Maex, *Mater. Today*, **7**, 34 (2004).

Smo17 M. von Smoluchowski, *Z. Phys. Chem.*, **92**, 129 (1917).

Sin01 R. K. Singh and B. R. Roberts, *IEEE/SEMI Adv. Semiconduct.Manufact. Conf.*, p. 107 (2001).

Sin02a R. K. Singh, R. Bajaj, *MRS Bull*., **27**, 743 (2002).

Sin02b R. K. Singh, S.-M. Lee, K.-S. Choi, G.. B. Basim, W. S. Choi, Z. Chen, and B. M. Moudgil, *MRS Bull.*, **27**, 752 (2002).

Sin04 R. K. Singh, G. Conner, and B. R. Roberts, *Solid State Technol*., **47**, 61 (2004).

Sta02 M. Staiger, P. Bowen, J. Ketterer, and J. Bohonek, *J. Dispers. Sci. Technol*., **23**, 619 (2002).

Ste96 J. M. Steigerwald, S.P. Murarka, R.J. Gutmann, *Chemical Mechanical Planarization of Microelectric Materials*, New York (1996).

Ste05 H. Stechemesser and B. Dobiáš, *Coagulation and flocculation*, Taylor & Francis, Boca Raton (2005).

Sup04 P. Suphantharida and K. Osseo-Asare, *J Electrochem Soc.*, **151**, G658 (2004).

Tam02 S. Tamilmani, W. Huang, S. Raghavan, and R. Small, *J. Electrochem. Soc.*, **149**, G638 (2002).

Teo04 T. Y. Teo, W. L. Goh, V. S. K. Lim, L. S. Leong, T. Y. Tse, and L. Chan, *J. Vac. Sci. Tech.*, **B 22**, 65 (2004).

Tse97 W.-T. Tseng, Y.-T. Hsieh, C.-F. Lin, M.-S. Tsai, and M.-S. Feng, *J. Electrochem. Soc.*, **144**, 1100 (1997).

Vid05 G. Vidrich, J.-F. Castagnet, and H. Ferkelz, *J. Electrochem. Soc*.,**152**, C294 (2005).

Xu02 G. Xu, E. Andideh, J. Bielefeld, and T. Scherban, *Interconnect Technology Conference, Proc. IEEE*, 57 (2002).

Zan04 P. B. Zantye, A. Kumar, and A. K. Sikder, *Mater. Sci. Eng. R*, **45**, 89 (2004).

Zen05 T. F. Zeng, and T. Sun, *IEEE Trans. Trans. Semiconduct. Manufact.*, **18**, 655 (2005).

BIOGRAPHICAL SKETCH

Feng-Chi Chang was born in 1976, in Taiwan. He received his B.S. in materials science from Tatung University, Taipei, Taiwan, in 1999. Feng-Chi pursued further studies at National Cheng Kung University, Tainan, Taiwan, and obtained his M.S. in 2001. In January 2004, he was a process engineer at the chemical mechanical polishing (CMP) department in Taiwan Semiconductor Manufacturing Company (TSMC), where he worked in oxide and tungsten CMP and process development.

In fall 2004, Feng-Chi began his Ph.D. studies at the University of Florida. In August 2005, he joined Dr. Singh's group for CMP studies. His dissertation research focused on the effects of external forces on particle agglomeration during CMP of metals and dielectrics. In May 2007, he interned at Sinmat Inc., an R&D company in CMP slurry, where he studied slurry formulation for material removal, slurry stability, and polishing uniformity. In December 2008, he graduated from the University of Florida with a doctorate in the Department of Materials Science and Engineering.